

HUMAN-LIKE ROBOT HEAD DESIGN

A THESIS SUBMITTED TO
THE GRADUATE SCHOOL OF NATURAL AND APPLIED SCIENCES
OF
MIDDLE EAST TECHNICAL UNIVERSITY

BY

ORHAN ÖLÇÜCÜOĞLU

IN PARTIAL FULFILLMENT OF THE REQUIREMENTS
FOR
THE DEGREE OF MASTER OF SCIENCE
IN
MECHANICAL ENGINEERING

SEPTEMBER 2007

Approval of the thesis:

HUMAN-LIKE ROBOT HEAD DESIGN

submitted by ORHAN ÖLÇÜCÜOĞLU in partial fulfillment of the requirements for the degree of **Master of Science in Mechanical Engineering, Middle East Technical University** by,

Prof. Dr. Canan ÖZGEN
Dean, Graduate School of **Natural and Applied Sciences** _____

Prof. Dr. S. Kemal İDER
Head of Department, **Mechanical Engineering** _____

Assist. Prof. Dr. A. Buğra KOKU
Supervisor, **Mechanical Engineering Dept., METU** _____

Assist. Prof. Dr. E. İlhan KONUKSEVEN
Co-Supervisor, **Mechanical Engineering Dept., METU** _____

Examining Committee Members

Prof. Dr. M. Eres SÖYLEMEZ
Mechanical Engineering Dept., METU _____

Assist. Prof. Dr. A. Buğra KOKU
Mechanical Engineering Dept., METU _____

Prof. Dr. Kemal İDER
Mechanical Engineering Dept., METU _____

Assist. Prof. Dr. E. İlhan KONUKSEVEN
Mechanical Engineering Dept., METU _____

Assist. Prof. Dr. Erkan Ü. MUMCUOĞLU
Informatics Institute, METU _____

Date: _____ 06.09.2007 _____

I hereby declare that all information in this document has been obtained and presented in accordance with academic rules and ethical conduct. I also declare that, as required by these rules and conduct, I have fully cited and referenced all material and results that are not original to this work.

Name, Last Name : Orhan ÖLÇÜCÜOĞLU

Signature :

ABSTRACT

HUMAN-LIKE ROBOT HEAD DESIGN

ÖLÇÜCÜOĞLU, Orhan

M. Sc., Department of Mechanical Engineering

Supervisor: Assist. Prof. Dr. A. Buğra KOKU

Co-Supervisor: Assist. Prof. Dr. E. İlhan KONUKSEVEN

September 2007, 133 pages

In the thesis study, it is intended to design and manufacture an anthropomorphic robot head that can resemble human head/neck and eye movements. The designed robot head consists of a 4-DOF neck and a 4-DOF head. The head is composed of 3-DOF eyes and 1-DOF jaw. This work focuses on the head/neck and eyes therefore; the other free to move parts such as eyebrows, eyelids, ears etc. are not implemented.

The general kinematic human modeling technique can be applied to facilitate the humanoid robotics design process since human anatomy can be represented as a sequence of rigid bodies connected by joints. In this study, we refer to the anthropometric data in determining the dimensions of all parts in order to have a robot head as human-like as possible. In addition, motion types, motion ranges and their velocities are considered. These factors are of great importance in imitating the human head movements as close as possible.

It is intended that the developed humanoid robot head will be used as a research platform in studying fields such as; social interaction between human and robots, artificial intelligence and virtual reality. It will also be an experimental setup to conduct experiments for studying active vision systems.

Keywords: Humanoid Robot, Anthropomorphic, Robotic Head, Robot Design

ÖZ

HUMAN-LIKE ROBOT HEAD DESIGN

ÖLÇÜCÜOĞLU, Orhan

Yüksek Lisans, Makine Mühendisliği Bölümü

Tez Yöneticisi: Yrd. Doç. Dr. A. Buğra KOKU

Ortak Tez Yöneticisi: Yrd. Doç. Dr. E. İlhan KONUKSEVEN

Eylül 2007, 133 sayfa

Bu tez çalışmasında, insanın baş/boyun ve göz hareketlerini yapabilen bir antropomorfik robot kafanın tasarımı ve üretimi amaçlanmıştır. Tasarlanan robot kafa 4 serbestlik dereceli bir boyundan ve 4 serbestlik dereceli bir baştan oluşmaktadır. Baş 3 serbestlik dereceli gözlerden ve 1 serbestlik dereceli çeneden meydana gelmektedir. Bu çalışma baş/boyun ve gözlere odaklandığından, kafada yer alan göz kapakları, kaşlar, kulaklar vb. diğer hareketli parçalar tamamlanmamıştır.

Genel kinematik insan modelleme tekniği, insan anatomisinin eklemlerle bağlanmış bir dizi katı parçalarla ifade edilebilmesinden dolayı, insansı robotiğin tasarım sürecini kolaylaştırmak için uygulanabilir. Bu çalışmada, robot kafanın mümkün olabildiğince insana benzemesi için tüm parçaların ölçülerinin belirlenmesinde antropomorfik verilere başvurulmuştur. Ayrıca, hareket tipleri, hareket aralıkları ve bu hareketlerin hızları göz önünde bulundurulmuştur. Bu etkenler insan kafa hareketlerinin taklit edilmesinde büyük öneme sahiptir.

Geliştirilen robot kafanın; insanlar ve robotlar arasında sosyal etkileşim, yapay zekâ ve sanal gerçeklik gibi çalışma alanlarında bir araştırma platformu olarak kullanılması hedeflenmektedir. Ayrıca robot, etkin görme sistemleri çalışmaları için de bir deney düzeneği olacaktır.

Anahtar Kelimeler: İnsansı Robot, Antropomorfik, Robotik Kafa, Robot Tasarımı

To My Parents

ACKNOWLEDGMENTS

I would like to thank my thesis supervisor Assist. Prof. Dr. Buğra Koku and co-supervisor Assist. Prof. Dr. E. İlhan Konukseven for providing me this research opportunity.

I would like to express my gratitude to Res. Assist. Özgür Başer and Atilla Bayram for their valuable recommendations in the design period, encouragement and continuous help.

I am deeply grateful to my family for their support and love.

This study was partly supported by the State Planning Organization (DPT) Grant No: BAP-18-11-DPT-2002-K120510.

TABLE OF CONTENTS

ABSTRACT	iv
ÖZ.....	vi
DEDICATION	viii
ACKNOWLEDGMENTS.....	ix
TABLE OF CONTENTS	x
LIST OF TABLES	xiii
LIST OF FIGURES.....	xiv
LIST OF SYMBOLS.....	xvi
CHAPTERS	1
1. INTRODUCTION	1
1.1 Background.....	1
1.2 Objectives of the Thesis.....	14
1.3 Outline of the Thesis.....	14
2. PRINCIPLES OF HUMANOID ROBOTICS.....	16
2.1 Introduction.....	16
2.2 Purpose.....	18
2.3 Components	18
2.3.1 Sensors	19
2.3.1.1 Proprioceptive Sensors	19
2.3.1.2 Exteroceptive Sensors.....	19
2.3.2 Actuators	20
2.3.3 Planning and Control.....	20
2.4 Parts of Humanoid Robots.....	20
2.5 Selected Previous Robotic Head Projects	22
2.5.1 COG	22
2.5.2 Kismet	23
2.5.3 MAVERic.....	24
2.5.4 UCSD	25

2.5.5 WE-4R.....	25
2.5.6 Comparison	26
3. DESIGN CONSIDERATIONS	28
3.1 Introduction.....	28
3.2 Anthropomorphic Data	29
3.2.1 Major Dimensions	29
3.2.2 Weight.....	30
3.3 Eye Movements	31
3.3.1 Saccades	32
3.3.2 Smooth Pursuit	33
3.3.3 Vergence Movement	33
3.3.4 Vestibulo-Ocular Reflex.....	35
3.3.5 Opto-kinetic Reflex	35
3.3.6 Angular Velocities and Ranges	35
3.4 Head Movements	36
3.4.1 Stabilization of the Head	36
3.4.2 Angle of Ranges	38
3.5 Jaw	38
3.6 Summary	40
4. MODELING AND ANALYSING	41
4.1 General Human Modeling.....	41
4.2 Kinematic Model of Head/Neck	43
4.3 Kinematic Model of Eyes	44
4.4 Kinematic Model of Jaw	45
4.5 Kinematic Analysis.....	45
4.5.1 Forward Kinematics	47
4.5.2 Inverse Kinematics.....	50
4.6 Verification of the Analyses	58
4.7 Summary	62
5. MECHANICAL CONFIGURATION	63
5.1 Overall Design	63
5.2 Joint Mechanisms	64
5.2.1 Neck	64
5.2.2 Head	68
5.2.3 Jaw.....	68

5.2.4 Eyes	70
5.3 Balancing	70
5.4 Summary	71
6. ELECTRICAL DESIGN	72
6.1 Power Supply	73
6.2 Robot Sensors	73
6.3 Custom Circuit Boards.....	74
6.4 Programming Using the Robot Head	76
7. RESULTS AND CONCLUSION.....	77
7.1 Results.....	77
7.2 Conclusion and Future Work	83
REFERENCES.....	85
APPENDICES.....	92
Appendix A: Technical Drawings	92
Appendix B: Circuit Schematics.....	117
Appendix C: Actuator Specifications	122
Appendix D: Specifications of Rapid Prototyping Machine	129
Appendix E: CMOS Camera Specifications.....	131
Appendix F: Communication Protocol.....	132

LIST OF TABLES

Table 2.1 Robot Heads are compared based on the number of mechanical DOF	27
Table 3.1 Average Values of the Major Head Dimensions [58].....	30
Table 3.2 Average Male Head Mass [59].....	30
Table 3.3 Average Mass Moments of Inertia* of the Male Head [$\text{kg.m}^2 \times 10^{-3}$] [59].....	31
Table 3.4 Motion Ranges and Velocities [62].....	36
Table 3.5 Ranges of Motion of Head [67].....	39
Table 4.1 Kinematic Parameters for the Model.....	46
Table 6.1 Circuit Boards on the Robot.....	73
Table 7.1 Major Head Dimensions with Results.....	79
Table 7.2 DOF Configuration.....	79
Table 7.3 Range of Movements of Each Joint.....	80
Table C.1 Technical Specifications of RC1 – SANWA HYPER ERG-VB.....	120
Table C.2 Technical Specifications of RC2 – SANWA SX 091.....	121
Table C.3 Technical Specifications of DunkerMotoren G 30.2.....	122
Table C.4 Technical Specifications of DunkerMotoren PLG 30 Planetary Gearbox.....	123
Table C.5 Data Used in the Calculations for Each Joint Axis.....	124
Table D.1 Technical Specifications of the Machine.....	127
Table D.2 Material Properties of PA2200.....	128
Table D.3 Mechanical Properties of PA2200.....	128
Table E.1 JMK JK-007A Micro Wired Pinhole Color Audio Camera.....	129
Table E.2 JMK WS-309AS Micro Wired Pinhole Color Audio Wireless Camera.....	129
Table F.1 Motor ID Numbers and Microcontroller Pin Connections.....	133

LIST OF FIGURES

Figure 1.1 Infanoid With A Four-Year-Old Boy [6]	3
Figure 1.2 The ROBOTA dolls are a family of mini humanoid robots	3
Figure 1.3 Pearl The Nurse Robot	4
Figure 1.4 HERMES: A Versatile Service Robot [14]	5
Figure 1.5 Honda’s ASIMO [17]	5
Figure 1.6 Robonaut Working with an Astronaut in Test Field [20]	6
Figure 1.7 HRP-2, a humanoid, helps assembling a panel [21]	6
Figure 1.8 HRP-1S is remotely controlled to drive an industrial vehicle	7
Figure 1.9 a) MAVERic [23] b) A 30-DOF Humanoid Test Bed [24]	8
Figure 1.10 The HR-2 Robot [25]	8
Figure 1.11 ETL Humanoid [27]	9
Figure 1.12 a) Dav: Mental Deveopment Robot [29] b) H6: As A Research Platform [31]	10
Figure 1.13 The projected installations of service robots in 2005-2008 [32]	11
Figure 1.14 Face Robots are very challenging to develop a) K-Bot [39] b) SAYA [40]	12
Figure 2.1 How human should a humanoid (robot) be?	17
Figure 2.2 Parts of Humanoid Robot HRP-2P [50]	21
Figure 2.3 COG with its one the creators [47]	22
Figure 2.4 The mechanical DOF arrangement of COG’s neck and eyes [50]	23
Figure 2.5 Kismet, The Emotion Exhibiting Robot Head	23
Figure 2.6 MAVERic is used for studying oculo-motor coordination [23]	24
Figure 2.7 The Robotic Head Developed at UC San Diego [54]	25
Figure 2.8 WE-4R, Emotion Expressions Robot by Waseda University [57]	26
Figure 3.1 The Major Head Dimensions [58]	29
Figure 3.2 The Metrics of a Saccadic Eye Movement [62]	33
Figure 3.3 The relationship of saccadic amplitude to peak velocity (V) and duration (D)	34
Figure 3.4 The Metrics of a Smooth Pursuit Eye Movement [62]	34
Figure 3.5 Rotation Axes of the Eye Movements	36
Figure 3.6 Body Planes [65]	38

Figure 3.7 Various Ranges of Motion for Different Joints [67]	39
Figure 4.1 Human Skeletal System and Its Anatomy [70]	42
Figure 4.2 The Human Spine [72]	42
Figure 4.3 a) Cervical Region of the Spine, b) Cervical Vertebrae [73], c) Kinematic Model	43
Figure 4.4 Possible Eye Movements and Muscle Groups [60].....	44
Figure 4.5 Kinematic Model of Eyes.....	44
Figure 4.6 Kinematic Model of the Robot.....	46
Figure 4.7 Verification of the Forward and Inverse Kinematics Solutions Based on θ_3	58
Figure 4.8 Verification of the Forward and Inverse Kinematics Solutions Based on θ_1	59
Figure 4.9 Verification of the Forward and Inverse Kinematics Solutions Based on θ_2	60
Figure 4.10 Verification of the Forward Solutions of the Focal Points	61
Figure 5.1 An External View of the CAD Model of the Robot.....	64
Figure 5.2 1 st DOF of the Neck Mechanism.....	65
Figure 5.3 Assembly of the 2 nd DOF of the Neck Mechanism	66
Figure 5.4 Assembly of the 3 rd DOF of the Neck Mechanism	67
Figure 5.5 4 DOF Neck Joint Mechanism.....	68
Figure 5.6 The Head Structure	69
Figure 5.7 The 1-DOF Jaw Mechanism	69
Figure 5.8 3-DOF Eye Mechanism with Two Cameras	71
Figure 6.1 Block diagram of the basic electronic system	72
Figure 6.2 Power transfer system	73
Figure 6.3 Assembly of the Modified Rotary Potentiometers, a)First Axis, b) Second Axis.....	74
Figure 6.4 PIC Based Control Board.....	75
Figure 7.1 An Overview of the Developed Robotic Head.....	77
Figure 7.2 A Photo of the Designed Robotic Head	78
Figure 7.3 Major Dimensions of the Manufactured Robotic Head.....	78
Figure 7.4 Average time elapsed vs. amplitude of motion for all movements of the right eye	81
Figure 7.5 Average time elapsed vs. amplitude of motion for all movements of the neck.....	83

LIST OF SYMBOLS

θ_i	Joint variables of the robot
d_i	Joint offsets of the robot
a_i	Effective link lengths of the robot
α_i	Twist angles of the robot
\hat{C}	Transformation matrix
a, b	Right-Sided coordinate frames
R	Frame origin of the fifth joint
\bar{r}	The fifth joint origin location in matrix form
$\bar{u}_1, \bar{u}_2, \bar{u}_3$	Unit vectors of Cartesian coordinates
$e^{\bar{u}_k \theta_k}$	Exponential rotation matrix with k^{th} joint variable around \bar{u}_k
x, y, z or r_1, r_2, r_3	Base frame components of the fifth joint origin location
\bar{f}_L, \bar{f}_R	The column representations of the eyes' center positions
σ	Uncertainty coefficient
J_{L_i}	Mass moments of inertia of the i^{th} joint
$c\theta_i$	$\cos \theta_i$
$s\theta_i$	$\sin \theta_i$
DC_i, RC_i	Actuator type
T	Torque at the shaft of the gearbox
$M_{\max.cont}$	Maximum continuous torque of the motor
M_{α_i}	Minimum torque required to move the joint
$\alpha_{i,\max}$	Maximum angular velocity
i	Reduction ratio of the gearbox
η	Efficiency of the gearbox

CHAPTER 1

INTRODUCTION

1.1 Background

Can rapidly growing technology success to create an artificial man? If yes, will the society accept these new kinds of artificial creatures as a part of it? The answers to these questions are debatable. Although we are far away from creating such a machine in the near future, the existence of a great expectations and effort towards realizing this goal cannot be ignored. When or whether this dream will come true is unknown; however, it is certain that the development of robots that are very handy will be continued.

The great improvements in technology allowed us to operate mechanical systems automatically. These automatic machines improved product quality considerably. By using electronic instruments, industrial machines were reached high level of precision. In fact, high precision in manufacturing resulted in good quality products as well as precise machinery giving opportunities to produce components in very small sizes. One important outcome of these developments was the powerful computers. They allowed development of programs consisting of very complicated algorithms.

While all these developments take place, robots became very common in manufacturing lines as “industrial robots”. The majority of industrial robots employed in industry were working according to prerecorded sequence of movements. They performed a variety of tasks such as spray painting, arc welding, palletizing, cutting and assembling etc. In these tasks, the movement sequence was always replayed, without any change. However, many potential “new” tasks which require some form of sensing appeared. Hence, modifying the robot’s motions based on the sensory information with computer control became essential [1].

The robots enriched with sensors and empowered with high-speed computers brought another opportunity to interrogate the capability of realizing autonomous machines. The combination of the robots, computers and sensors opened the gate of the world to the intelligent machines.

In order to facilitate the human life, scientists put their utmost efforts. The common goal of all these efforts is to design and realize machines very close to human in form and functionality in order to perform similar tasks. This trend can easily be observed when looking at the pioneers of industrial robots. There, one can see manipulators, having degrees of freedom in different numbers, fixed on a base. They perform certain tasks according to their end-effectors located at the last degree of freedom. These manipulators seem to be inspired from the human arm. Since being fixed has limited applicability, another type of industrial robots, mobile robots have been developed. They are used to carry loads from one place to another. May they resemble human locomotion and ability to take something to somewhere? It can be seen from the evolution stages of robots that the intention is to imitate human abilities. This eventually leads to the robots to be designed in human form. As a result of these, a new class of robotics which is referred to as *humanoid robotics* is born.

Recent advances in technology especially in electronics and computer engineering have opened the door to a new robotic age and encouraged us to picture a future with more intelligent, socially accepted robots acting as our companions.

In general, humanoid robotics is an application area of robotics in which robots are designed in human form and can perform human-like behaviors. The humanoids will have important applications in the areas of servicing elderly, assisting co-workers, working in hazardous environment etc. They are also used to explore issues of developmental structure, physical embodiment, integration of multiple sensory and motor systems, and social interaction [2].

Humanoid robots are designed and evaluated to help people with some disabilities (handicapped) such as autism. People with autism are marked by impaired social interaction, communication, and restricted and repetitive behavior [3]. Infanoid is one of the humanoid robots being able to interact emotionally with such humans (Figure 1.1). Its

capability of attentive and emotional interaction with humans comes through gaze, pointing and facial expressions, etc. [4]. Robot, a commercial doll, is another humanoid robot which is intended to be used in experiments with autistic children (Figure 1.2). To carry out the experiments, it is equipped with sensory systems such as speech and vision. Since, measuring the child's ability to social interaction with others needs these basic sensing capabilities [5]. Researches showed that the autistic children interacting with the humanoid robots naturally get into a social loop keeping them relaxed [4].

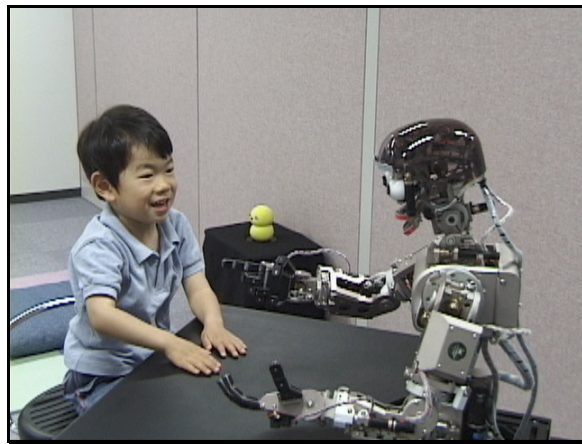


Figure 1.1 Infanoid With A Four-Year-Old Boy [6].



Figure 1.2 The ROBOTA dolls are a family of mini humanoid robots. They are educational toys [7].

Service robots are used to serve elderly. Mataric [8] states that “As robots increasingly become part of our everyday lives, they will serve as caretakers for the elderly and disabled”. Pearl (Personal Robotic Assistant for the Elderly) project is aimed to develop a mobile, personal service robot assisting elderly people who suffer from chronic disorders in their everyday life (Figure 1.3.a) [9]. Pearl serves the patients by reminding to take medicine, for instance (Figure 1.3.b). It is a platform for tele-presence that allows establishing connection between patients and care-givers. It also assists by collecting the data about the patient’s systematic progress [10]. Flo is another service robot design which is very similar to Pearl [11].

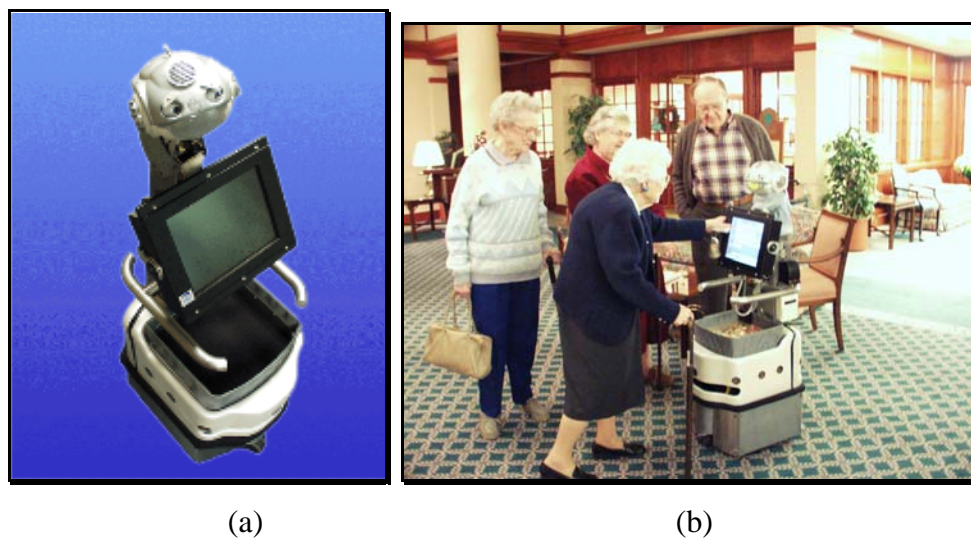


Figure 1.3 a) Pearl The Nurse Robot b) Pearl's First Steps in an Elderly Care Facility (Longwood, Oakmont) [12].

High degree robustness, adaptability and advanced communications skills are expected from service robots as well as flexibility, modularity and extendability. HERMES is such a robot having the variety of abilities (Figure 1.4). It has been demonstrated in a museum to test its interaction and communication skills [13].



Figure 1.4 HERMES: A Versatile Service Robot [14].

ASIMO is an autonomous service robot developed to function in indoor environments. It is designed to assist humans in their daily tasks. HONDA, developer of the humanoid, announced that ASIMO can autonomously act as a receptionist, or even deliver drinks on a tray (Figure 1.5). ASIMO, the most popular humanoid robot in the world, is the predecessor of humanoids P1, P2 and P3 all from Honda, who invests in R&D on humanoid robotics since 1986 [15] [16].

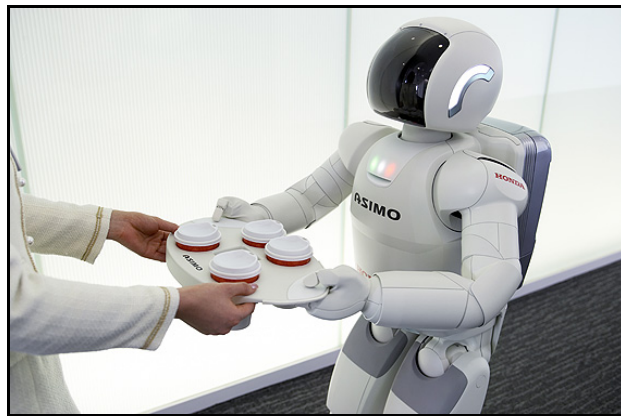


Figure 1.5 In recent years, there has been a growing awareness of the importance of humanoid robotics after Honda's ASIMO [17].

Researchers are studying to develop humanoids to assist their co-workers in an environment with different working conditions they work with humans. Robonaut is a mobile autonomous upper torso humanoid developed for assisting human co-workers at the Johnson Space Center, Houston, USA. It is a human scale robot that is able to work with the tools designed and used for space missions (Figure 1.6). In Figure 1.7, HRP-2, developed by Kawada Industries to use in actual environments, is seen when helping his colleague to assemble a panel [18]. Humanoids offer great potential for assisting humans with a wide range of tasks [19].



Figure 1.6 Robonaut Working with an Astronaut in Test Field [20].



Figure 1.7 HRP-2, a humanoid, helps assembling a panel [21].

Humanoids can be used in hazardous environments. Beyond being the means of research, entertainment and advertisement, humanoids can be utilized in dangerous domains. Remotely controlled humanoids can use industrial vehicles for restoration purposes (Figure 1.8). As an example, they can be used to drive a backhoe (the most frequently used industrial vehicle in the construction environments) to help rescue after an

earthquake, which will be very dangerous both for the rescue team and the people wounded under the subsidence. Another example to a dangerous zone might be a field contaminated by chemical leakage. Purifying such zones is too risky therefore machines equipped with humanoids can be preferred instead of a human operator.



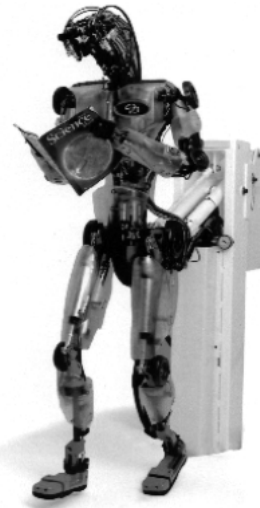
Figure 1.8 HRP-1S is remotely controlled to drive an industrial vehicle. It has been developed to operate the vehicle with tele-operation [22].

Neurobiological studies can be performed on a humanoid robot. In human body there are many different control systems and their working principles have to be addressed. For this reason, humanoids are being developed throughout the world. MAVERic is a robotic head developed for oculomotor research at the Laboratory of RIKEN Brain Science Institute (Figure 1.9.a). With two cameras in each eye and multiple degrees of freedom in the neck and eyes, oculomotor coordination is investigated [23]. Vijakumar et al. [24] used a 30-DOF humanoid robot as a test bed to investigate the interplay between oculomotor control, visual processing and limb control in humans (Figure 1.9.b).

Humanoid robots can also be used for educational purposes, for example, software development. HR-2 is an example to such a humanoid (Figure 1.10). Heralic [25] stated the goal of the project as “creating a low-cost miniature humanoid system with vision and speech capabilities to obtain an educational platform for software development in the field of complex adaptive systems.”



(a)



(b)

Figure 1.9 a) MAVERic [23] b) A 30-DOF Humanoid Test Bed [24].



Figure 1.10 The HR-2 Robot [25].

Redundancy in degrees of freedom in human body can be investigated using a humanoid robot. Nagakubo et al. [26] developed ETL, an upper torso humanoid, to explore new methodologies of controlling complex systems (Figure 1.11). In designing the robot one of the objectives was that how to exploit redundant degrees of freedom in task situations of humanoids.

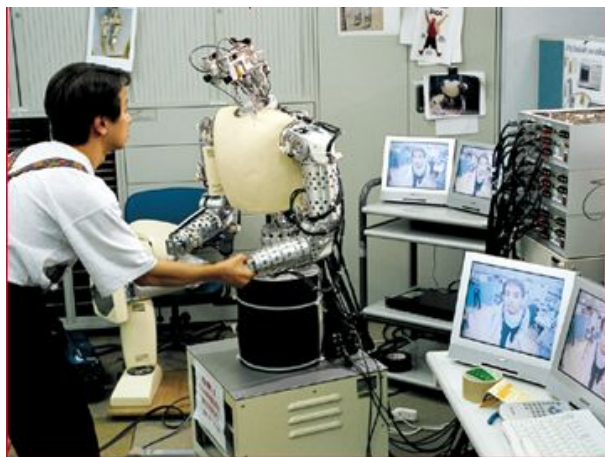


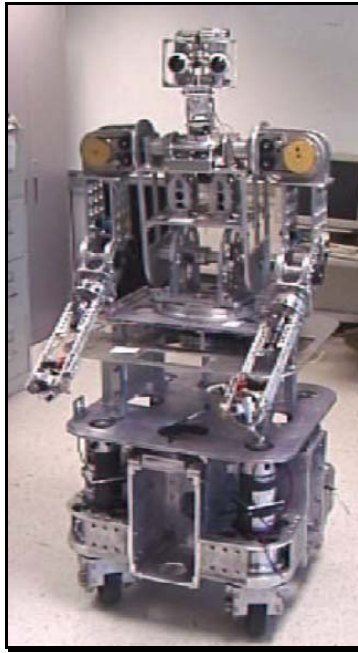
Figure 1.11 ETL Humanoid [27].

Humanoids are the best platforms to be used in artificial intelligence applications. Since it is expected from humanoids to move autonomously they have to have a certain level of intelligence. This needs an iterative code development procedure as well as a robust experimental set-up. Humanoids, therefore, are suitable to practice the existence theories and to develop new ones. For example, one of the major goals of designing humanoid robot KHR-2 is to have a reliable platform to implement artificial intelligence theories (Park et al. [28]). As another example, Han et al. [29] are using DAV: Mental Development Robot as a sensory system basis to increase machine intelligent (Figure 1.12.a). Nishikawi et al. [30] developed a robot “H6” as a test bed to experiment various aspects of intelligent humanoid robotics (Figure 1.12.b).

It is worth noting that although the above mentioned application fields seem specific to the robots; it might be possible to change the subject of research because humanoids provide the researcher with several modalities already implemented on them.

Although humanoid robotics is a new field of robotics, it is growing rapidly worldwide. When the application areas such as maintenance tasks of industrial plants, human care, tele-operations of construction machines, security services and so on, are taken into consideration it can easily be seen that humanoids can be important in the near future.

A robot that is in human form and similar to a human by means of abilities may perform different tasks that humans cannot do or are not willing to do. Such a humanoid robot will be a big contribution towards increasing the quality of human life.



(a)



(b)

Figure 1.12 a) Dav: Mental Developmental Robot [29] b) H6: As A Research Platform [31].

It is now predictable that they will be of great worth to invest. According to the results of the study conducted and published by The International Federation of Robotics (IFR) in cooperation with the United Nations Economic Commission for Europe (UNECE) in 2005, humanoid installations will start to rise very strongly in near future (Figure 1.13) [32]. This statistical estimation reveals that humanoid robotics will be the most popular robotic field in the next decade.

Humanoid robots are very complicated systems therefore many research laboratories divide the whole body into relatively small portions to focus on specific research issues.

There are many researches focused on development of a humanoid biped robot. In these studies it can be seen that human locomotion is taken as the starting point in the design process of a full humanoid robot. Wisse designed and manufactured prototypes of two legged robots to investigate human walking [33]. Today's Honda R&D's humanoids [15] [16], WABIAN series of Waseda University [34], H6 & H7 [30], KHR-2 [28] and HRP (HRP-2L) [18], the other well known biped robots, were all developed as having two legs without upper body. After achieving stable locomotion, developers continued to complete their humanoids' other portions.

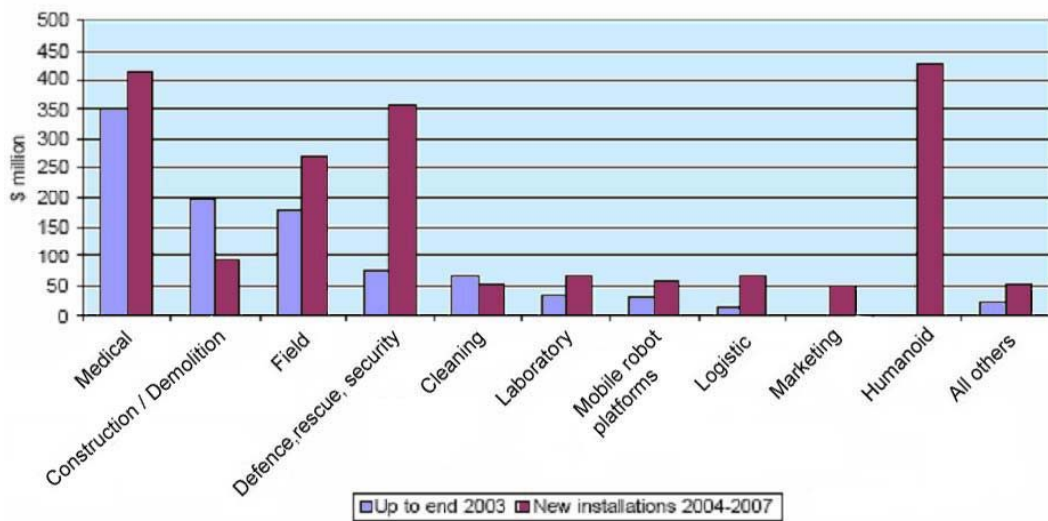


Figure 1.13 The chart shows stock at the end of 2004 and the projected installations of service robots in 2005-2008 [32].

The great majority of the researches concerned the upper torso of human. Medusa, anthropomorphic robot torso, having an arm, a head and a binocular head is designed for research in vision coordination and learning by imitation [35]. COG is another upper torso humanoid robot. To study human intelligence, the creators of COG thought that building a robot in human form is essential [36]. ETL Humanoid is also designed as an upper torso humanoid to conduct human interaction experiments. It has the upper portion of human body (head, eyes, arms and torso) [26]. Infanoid, designed for assisting handicapped and disabled people, is another upper torso humanoid. Wendy which is designed to work with humans has arms, a head and torso with wheels instead of legs [37]. In Robonaut project, the upper body is combined with a robotic mobility platform to yield a dexterous humanoid.

Robotic hands and face robots were always attractive. There are specific works on robot hands. For instance, Weiss and Woern [38] developed a servo-hydraulically actuated anthropomorphic robot hand to meet the requirements of service robots. Face robots are very challenging to develop. In Figure 1.14, two popular face robots, K-Bot and SAYA are shown.

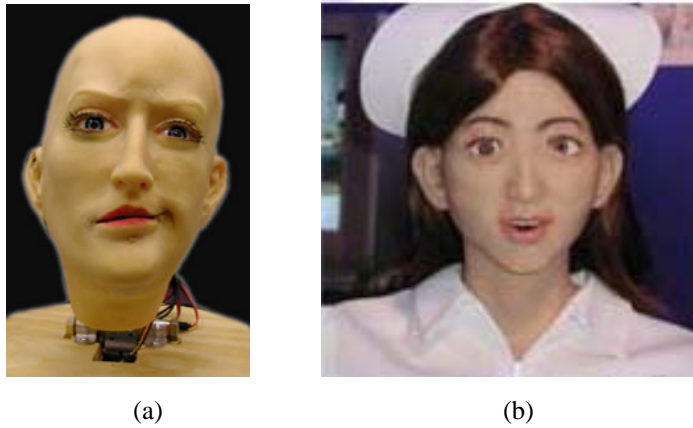


Figure 1.14 Two Popular Face Robots a) K-Bot [39] b) SAYA [40].

Another portion in human body which is largely studied is the head and neck. Human-like robotic heads are also good platforms to investigate many issues. Although there are projects that are only interested in head, most of the above mentioned projects have quite complex head structures. In Chapter 2, a detailed description about the previous studies of humanoid head robots will be given. In what follows, we will focus on the importance of the head in humanoid robots.

Interaction of human with humanoid robots which are developed to serve people in a social setting is inevitable. Humans interacting with an individual use various ways such as talking (verbal communication) and performing gestures to convey their social message to the observer. On the other hand, it is possible to transmit the psychological (or emotional) state by using facial expressions (or mimics) and eye movements. Facial expressions, a form of nonverbal communication, result from motions of face muscles. Obviously, facial expressions are very important in conveying social information among humans.

Sakagami et al. [15] clearly state that “Interaction is important for any kind of robot to perform tasks in human society like carrying luggage, pushing a cart, serving drinks, taking tools from the table and so on. The robot has to understand human’s high-level task requirements by using its low-level sensory modules such as eyes, ears and tactile sensors.”

Di Salvo et al. [41] express the importance of existence of features in human-robot interaction as “In human-robot interaction; presence of certain features, the dimensions of the head and the total number of facial feature heavily influence the perception of humanness in robot’s heads.”

Bischoff and Graefe [42] explain the human conversation as “Human conversation is usually multimodal. Multimodality enhances the richness of the communication and interaction and allows more complex information to be conveyed than is possible with a single or two modalities. Consequently, implementing most of the human senses and communication channels is a prime prerequisite for cooperative, user-friendly and versatile personal robotic assistants”. They continue in this issue by claiming that; “Ideally, they should, in addition to communication via spoken language, generate and understand gestures, body and facial expressions and touch events, to fully support a truly natural and, thus, human-friendly interaction” .

In addition, Kozima et al. [4] describe that “Communication is the key activity in the social interaction where one sees invisible mental states in the visible posture and movement of others”.

Since humanoid robots are intended to be employed in unstructured environments that are cohabited by humans, their physical appearance requires human shape and size. Infanoid is able to manage eye-contact which is also very important to establish a social interaction. Kismet is a humanoid robotic head designed for research in social interaction of humans with robots [43]. Humanoids like Pearl can help elderly people who are forced to live alone, deprived of social contacts [10].

The goal in humanoid robotics is to develop an intelligent agent in human form that can imitate human behaviors, whereas the ultimate goal is to design and manufacture a humanoid robot which is practically indistinguishable from a human being. This implies designing a full body humanoid consisting of two legs, two arms, a torso, a head and eyes. The common point in the application areas of humanoids is interaction with humans since they are developed to contribute to human daily life. Therefore, with the above reasoning, the head, the eyes and the mimics are the most important components of a humanoid for interaction with others.

1.2 Objectives of the Thesis

In the thesis study, it is intended to design and manufacture an anthropomorphic robotic head that can perform human head/neck and eye movements. The designed robotic head consists of a 4-DOF neck and a 4-DOF head. The head is composed of 3-DOF eyes and 1-DOF jaw. This work focuses on the head/neck and eyes, therefore, the other free to move parts such as eyebrows, eyelids, ears etc. are not implemented.

The general kinematic human modeling technique can be applied to facilitate the humanoid robotics design process since human anatomy can be represented as a sequence of rigid bodies connected by joints. In this process, we refer to the anthropometric data in determining the dimensions of all parts in order to have a robotic head as human-like as possible. In addition, motion types, motion ranges and their velocities are considered. These factors are of great importance in imitating the human head movements as close as possible.

It is intended that the developed humanoid robotic head will be used as a research platform in studying fields such as; social interaction between human and robots, artificial intelligence and virtual reality. It will also be an experimental setup to conduct experiments for studying active vision systems. In order to facilitate the usage of this robotic head, a software library containing a high-level programming interface is provided as well.

1.3 Outline of the Thesis

In this manuscript, design steps of an anthropomorphic robotic head/neck system are given. As well as the steps, the humanoid robotics as a new field of robotics is briefly introduced. The thesis manuscript is organized in the following manner.

Chapter 2 presents an introduction to humanoid robotics and provides the related work on previous head projects with a comparison between them. Chapter 3 gives the design considerations and determines the design constraints on the thesis. Chapter 4 describes how modeling is done for the robot and gives the details of its kinematic analysis.

Chapter 5 presents the details of the robot's mechanical design and Chapter 6 gives the details of the electronics design. Finally, Chapter 7 concludes and discusses the experiences for future research.

Appendices are organized as follows:

Appendix A includes all the technical drawings of the designed and manufactured parts. Appendix B contains all the schematics for the custom circuit boards on the robot. Appendix C contains the actuator specifications and actuator selection calculations. Appendix D gives the technical specifications of Rapid Prototyping Machine used in manufacturing the robot. It also includes material and mechanical properties of polyamide material. Appendix E provides the technical specifications of camera modules.

CHAPTER 2

PRINCIPLES OF HUMANOID ROBOTICS

This chapter gives the preliminary concepts of humanoid robotics starting from the definition of it. Then, previous robotic head projects, which are used to guide our design process, are considered.

2.1 Introduction

Humanoid Robotics is an application area in which robots are designed according to an anthropomorphic model. Here, humanoid means a machine or creature that looks and moves like a human being [44] or having human characteristics or form; resembling human beings. Anthropomorphic, on the other hand, (*anthropos*: human + *morphe*: form) refers resembling or made to resemble a human form [45].

Scientists and specialists from many different fields such as mechanical, electrical and computer engineers, roboticists, computer scientists, artificial intelligence researchers, psychologists, physicists, biologists, cognitive scientists, neurobiologists, philosophers, linguists and artists combine their efforts to design and manufacture a robot as human-like as possible [46] [47]. Since they are complicated mechatronic systems, designing a human-like robot needs a lot of labor and facility as well as knowledge in various fields of engineering and science.

Humanoid robots are created to be used in some of the same physical and mental tasks that humans do. To accomplish those tasks, they are formed similar to human body. Hirukawa says that “human-shaped robots have the advantage of being able to work in the same space as people and use the same tools and vehicles.” [48]. Therefore, a

humanoid robot can be defined as a robot with its overall appearance based on that of the human body [46].

A humanoid robot has to be autonomous because it should respond to changes in its environment or itself while it tries to reach its goal. In this, humanoids and other kinds of robots like industrial robots are separated from each other [46].

However, it is not possible to say that a robot is humanoid by only considering its outward appearance. Expression, communication and behavior are also the key aspects for a robot to be perceived as human-like [41]. Although the form of the robot is very crucial, ability to imitate humans in a social environment is necessary for them to be accepted as a member of the society. In order to have a basis to criticize how human a humanoid should be, the perception of human to non-human entities has to be addressed.

For that, we will outline a controversial theory, put forward by Japanese roboticist Mashiro Mori in 1970, called “The Uncanny Valley”. It claims that to explain the emotional response of humans to robots (or non-human entities) a non-linear relationship like the one shown in Figure 2.1 can be foreseen.

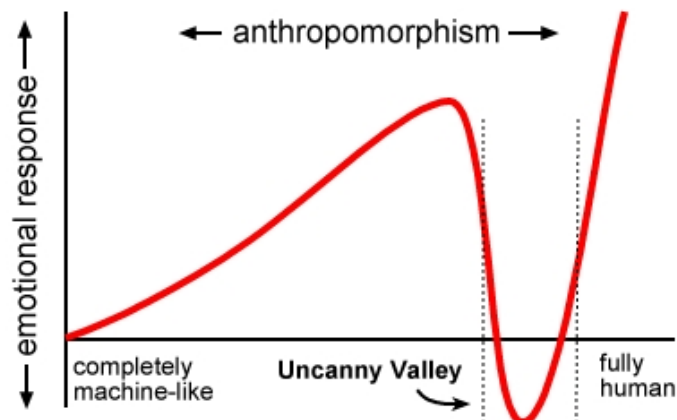


Figure 2.1 How Human should a humanoid (robot) be? The answer lies in the graphic. Mori’s The Uncanny Valley [49].

According to Mori, emotional response of humans to robots, in general, can have three major stages. In the first stage, making a robot as human-like as possible will be

attractive. As a consequence, the emotional response of humans to that robot will become positive and emphatic. This positive-ness has been reflected as the first peak in the graphic. As for the second stage, when a point at which it is difficult to distinguish the robot from a human being is reached, that response suddenly becomes strongly repulsive because in a way it is surprisingly understood that the entity looks like a human but it is actually not a human. This is the region where the emotional response is negative. The argument about the theory comes through the belief that humans show the same reaction to all entities that are suddenly found strange after a while the interaction starts with them. Finally, as the appearance and motion are indistinguishable to that of human being (in this stage the two are accepted almost the same), the emotional response is again positive and approaches to human-human empathy level [49].

2.2 Purpose

Humanoids offers a unique research tool in several scientific areas. Besides, they can facilitate our everyday lives as being personal assistants. Currently, humanoid robots are being specifically developed:

- to help sick and elderly [4] [5] [9] [11] [13] [15].
- to assist their co-workers in the field to extend capabilities of them [18] [20].
- to employ as a servant
- to provide entertainment
- to be used in hazardous environments [22].
- to be used as an educational experimental setup [25] .
- to perform neurobiological studies on them [23] [24].
- to understand the human body's biological and mental processes [29].
- to investigate redundancy in degrees of freedom in human body [26].
- to be used in artificial intelligence applications [28] [30].
- to understand and simulate human cognition [2].

2.3 Components

The major components of a humanoid robot are its structural parts and mechanisms. Humanoids are also composed of sensors, actuators and a control architecture which handles planning and control.

2.3.1 Sensors

Sensors are devices used to capture information about the physical environment. The importance of such devices in robotics is not negligible. They play a fundamental role in the performance of a robotic system.

According to the type of measurement information that they give us as output, they can be classified as proprioceptive and exteroceptive sensors.

2.3.1.1 Proprioceptive Sensors

The proprioceptive system is one of the two sensory systems in the human body. It measures internal quantities such as the velocity of a limb joint, muscle extension and muscle tension etc. The proprioceptive sensors that are used in humanoid robots can be listed as follows:

- Position sensors that indicate the actual position of the robot.
- Velocity sensors to measure the speed of the robot
- Accelerometers to measure the acceleration.
- Tilt sensors to measure inclination.
- Force sensors to measure contact force with environment. They are usually placed in robot's hands and feet.

2.3.1.2 Exteroceptive Sensors

The other sensory system in the human body is the exteroceptive system. It reacts to the changes which result in physical contact of the environment and the human body. Temperature fluctuations in the ambient and deformation of the skin surface can be given as examples to such changes. The information taken by means of the exteroceptive sensory system is critical for the robot to establish interaction with the physical world.

In humanoid robotics the following exteroceptive sensors are utilized.

- Proximity sensors to measure the relative distance (range) between the sensor and objects. Sonars, infrared sensors or tactile sensors, capacitive or piezoresistive sensors.

- Vision sensors to recognize objects and determine their properties. CCD cameras commonly.
- Sound sensors to hear what is spoken (e.g. microphones).

2.3.2 Actuators

Actuators are servomechanisms used to transmit energy for the operation of a system or mechanism [45]. Since the motion of each joint in a humanoid robot should mimic its counterparts in human body, actuators must be selected properly among the below types.

- Electric actuators
- Hydraulic actuators
- Piezoelectric actuators
- Ultrasonic actuators
- Pneumatic actuators

2.3.3 Planning and Control

The bottom line in planning and control of a humanoid is that the movement of the robot has to be human-like. In addition to that, these movements should consume minimum energy. In order to perform a good control, the controller needs to be fed from the sensory systems in a logical manner. Information about the internal and external parameters must precisely be known by the robot. The robot should be able to accomplish its decision making process by using those parameters. Its problem solving skills should also be considered in planning and control phases of the humanoid. It is needed to implement artificial intelligence techniques in order to obtain an autonomously behaving robot. The other major issues in planning and control can be given as self-collision detection, path planning and obstacle avoidance.

2.4 Parts of Humanoid Robots

The parts of a humanoid are obviously the parts of a human body. They should be considered as the subdivisions of a huge system. A system like a human body is not easy to handle at once. That is why many humanoid robotics project teams choose to spend

their efforts on a portion of the body. Based on the functionality, those portions are investigated separately and then they are combined to complete the full system.

In general, humanoid robots have a torso with a head, two arms, two legs and two feet. In Figure 2.2 the major parts of the humanoid robot HRP2-2P are shown.

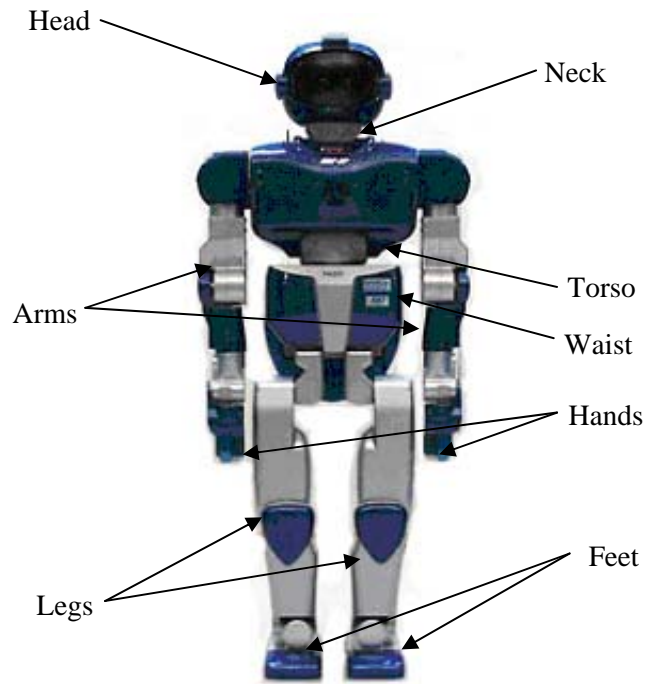


Figure 2.2 Parts of Humanoid Robot HRP-2P [50].

Within these parts the head/neck system has been chosen for design and manufacture. As mentioned in Chapter 1, the human head plays a very important role in social interaction. Since the head, the eyes and the mimics are the most important components of a humanoid for interaction with others we selected designing and manufacturing a robotic head. Hence, in the next section we will examine the previously developed robotic heads which were used as references in a more detailed fashion.

2.5 Selected Previous Robotic Head Projects

2.5.1 COG

COG is an upper torso robot developed at MIT AI Laboratory. Its development process goes back to the early 1990's. COG's developers believe that if a robot with human-like intelligence is wanted to be built it has to have a human-like body [51]. This belief is supported by the necessity of interaction of the robot with humans to reach human level intelligent. Jung et al. [52] provide an excellent experiment of anthropomorphic robot evaluation and suggest that physical embodiment improves the perception of robots.



Figure 2.3 COG With Its One of the Creators [47].

COG has 22 mechanical DOF, in total. They are organized as follows: two 6-DOF arms, a 3-DOF torso, a 4-DOF neck, and 3-DOF combined in its eyes. In this design we will focus on the neck and eyes' DOF. COG, as having 3-DOF eyes and 4-DOF neck mechanisms, can mimic the range and speed of the human eyes and head. Two neck axes are directly driven to perform yaw and lower pitch motions. A two-axis differential allows performing the upper pitch and roll motions. The eyes have 3 DOF; each eye has an independent pan/yaw axis (which allows the robot to look right and left and accommodates vergence movements) and the two eyes share a single tilt axis (which allows the robot to look up and down). Each of the mechanical degrees of freedom in the head is equipped with a high-resolution optical encoder for determining position.

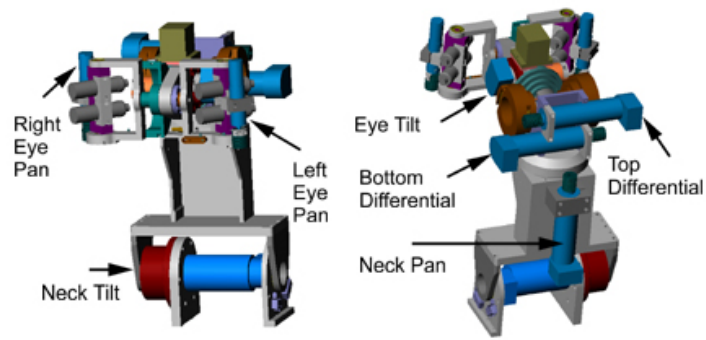


Figure 2.4 The mechanical DOF arrangement of COG's neck and eyes [50].

In COG's head each eye has two cameras as exteroceptive (vision) sensors. They are placed to mimic the human retina. In each eye, one camera provides a wide 120 degree field-of-view for peripheral vision and the other camera provides a narrow 20 degree field-of-view at high resolution for foveal vision. The head also contains proprioceptive sensors such as a 3-axis inertial sensor which acts much like the human inner-ear.

COG is a sophisticated research platform so that it can be used for many of the above mentioned purposes.

2.5.2 Kismet

Kismet is an autonomous robot developed also at MIT AI Laboratory to interact and cooperate with people in their daily lives. Kismet is able to perceive a wide range of natural social cues from its visual and auditory channels. It can respond to those cues through gaze direction, facial expression, body posture, and vocal babbles.

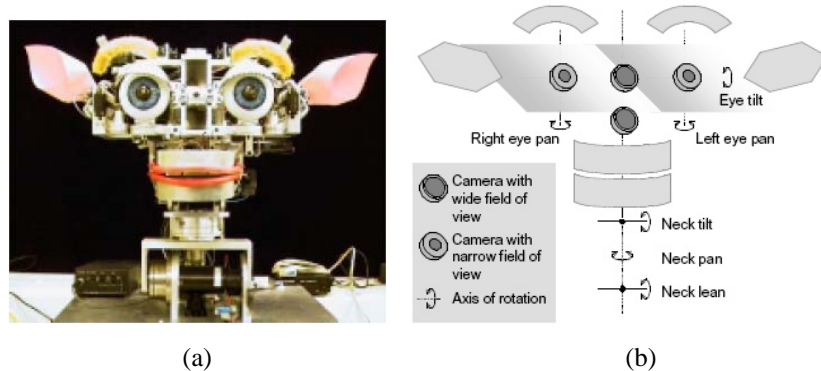


Figure 2.5 a) Kismet, The Emotion Exhibiting Robotic Head, b) The Major Axes and Camera Places [43].

Kismet has 3-DOF eyes to control gaze direction and a 3-DOF neck. In addition to these degrees of freedom, it has a 15-DOF face so in total there are 21 DOF. The distribution of the face DOF are as follows: 2 DOF for each ear (total 4 DOF), 2 DOF for each eyebrow (total 4 DOF), 1 DOF for each eyelid (total 2 DOF), 4 DOF for the lips and 1 DOF for the mouth. By using its 15 actuators Kismet can display its emotional state and deliver social signals. The expressions that Kismet can show are anger, fatigue, fear, disgust, excitement, happiness, interest, sadness and surprise.

The robot is also equipped with exteroceptive (visual and auditory), and proprioceptive sensory inputs. The robot's vision system consists of four color CCD cameras mounted on a stereo active vision head. Two wide field of view cameras are mounted centrally and move with respect to the head. There is also a camera mounted within the pupil of each eye are used for higher resolution post-attentional processing, such as eye detection [53].

2.5.3 MAVERic

MAVERic is a versatile robotic vision head developed for oculo-motor research at the RIKEN Brain Science Institute's Laboratory for Mathematical Neuroscience. It has 7 DOF. They are pan and tilt in each eye and head rotate, nod and tilt. MAVERic is equipped with multiple sensory modalities including position sensing (7 DOF), load sensing (3 DOF), stereo microphones, foveal and peripheral vision in each eye and a 6-axes gyroscope in addition to laser range finders in each eye. Research with MAVERic investigates visuomotor coordination using multiple degrees of freedom camera systems [23].

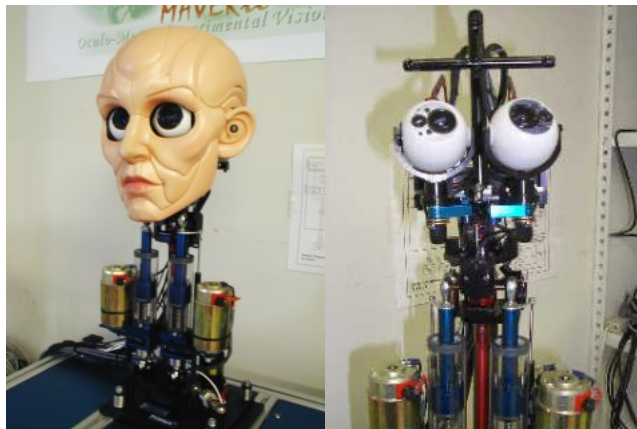


Figure 2.6 MAVERic is used for studying oculo-motor coordination [23].

2.5.4 UCSD

University of California at San Diego has also developed an anthropomorphic robotic head for studying autonomous development and learning. The head is designed as a research platform to investigate active vision systems. It is able to mimic the major degrees of freedom of the human neck and eyes at similar velocities. It has also additional degrees of freedom to imitate a few of facial expressions.

In the head there are 9 mechanical degrees of freedom in total. The neck can pan left-right and tilt up-down using 2 DOF. Each eyeball can independently pan and tilt (4 DOF). Remaining degrees of freedom are used to open and close the mouth (1 DOF), raise and lower the corners of the mouth (1 DOF) and move up and down the eyebrows (1 DOF). With these additional degrees of freedom, the robotic head can show some of the facial expressions such as smiling, frowning and surprised [54] [55].

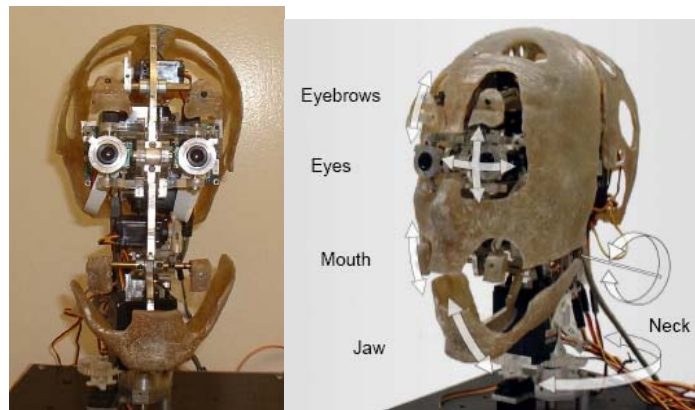


Figure 2.7 The Robotic Head Developed at UC San Diego [54].

2.5.5 WE-4R

WE-4R (Waseda Eye No.4 Refined), is another highly developed upper torso humanoid robot. It is the last version of the humanoids designed at Waseda University since 1995. The main goal of the study is to develop an emotion expression humanoid robot. The robot is expected to be able to communicate with humans in a natural way by exhibiting human-like emotion. In this last version there are 47 mechanical degrees of freedom. The

distribution of those are: Arms: 18, Waist: 2, Neck: 4, Eyeballs: 3, Eyelids: 6, Eyebrows: 8, Lips: 4, Jaw: 1, Lungs:1.

The sensory systems of WE-4R are rather improved. It is equipped with visual, auditory, cutaneous and olfactory sensation systems. Two color CCD cameras are placed as eyes. In the auditory system which can determine the direction of sound source microphones are used. Tactile and temperature sensors are utilized in the cutaneous system. There are four semiconductor gas sensors to form the olfactory sensory system [56] [57].

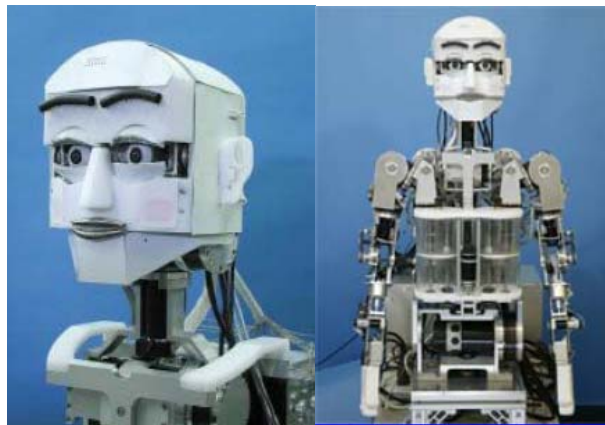


Figure 2.8 WE-4R, Emotion Expression Robot by Waseda University [57].

2.5.6 Comparison

We would like to compare the five humanoid robotic heads with respect to their degrees of freedom in the neck and eyes. As can be seen in Table 2.1, COG, Kismet and UCSD have equal degrees of freedom as 6 DOF whereas WE4R and MAVERic have 7 DOF. Here, WE4R and MAVERic are superior ones but WE4R has the most human-like head. Its neck is more realistic as having one additional DOF. Although MAVERic has 4 DOF in its eyes mechanism, it shows redundancy. 3 DOF, as in WE4R, will suffice to perform human eyes movements. Therefore, WE4R has the most developed robotic head as far as the number of degrees of freedom of the neck and eyes are concerned.

Table 2.1 Robotic Heads are compared based on the number of mechanical DOF.

	Eyes' DOF	Neck's DOF	Mimics' DOF	Total DOF (Neck+Eyes)
COG	3	3	none	6
KISMET	3	3	11	6
WE4R	3	4	19	7
UCSD	4	2	3	6
MAVERic	4	3	none	7

CHAPTER 3

DESIGN CONSIDERATIONS

In this chapter, design issues and constraints will be discussed. The fundamental features that are present in the design of the robot will be introduced. The design criteria about the robot head/neck will be given.

3.1 Introduction

An anthropomorphic robot head should have similar features with a human head. First of all; the outside view of the robot should resemble human face to a certain degree. Next, it should accommodate the features such as eyes, eyelids, nose, ears, chin, mouth etc. as much as possible. To define the degrees of freedom of a robotic head, the motions performed by the head must be determined considering the mechanical constraints on the design. The structural components, their materials, electronic equipment and actuators should be selected in order to satisfy the dynamic behaviors of a human head. In order to do this, the motion types, ranges and velocities of a human head should be closely examined focusing on the dimensions, weight and movements.

The application area that the robot is intended to be used influences the design parameters heavily. The designed robotic head will mainly be used to explore human-robot interaction in a social setting. Since human partner would like to perceive the robot as human-like. This is very important to interact with the robot in a social context. Therefore, mechanical design of the components has to be done accordingly.

3.2 Anthropomorphic Data

Anthropometric measurements should be a guide for the design. We refer to the following anthropometric data in determining the dimensions of major parts present in the designed robotic head.

3.2.1 Major Dimensions

In order to design a robot head, the shape and the size of a human head are considered. Since it is going to be an anthropomorphic robotic head, its appearance should be similar to a human. The general dimensions of the head with respect to the statistical studies are obtained and evaluated.

We regard the five principle anthropometric measurements for human head. They are illustrated in Figure 3.1. Their mean values and standard deviations are tabulated in Table 3.1. This data is taken from a research conducted aiming to provide the necessary anthropomorphic data of the Turkish Male Population for the manufacturers, engineers etc. [58].

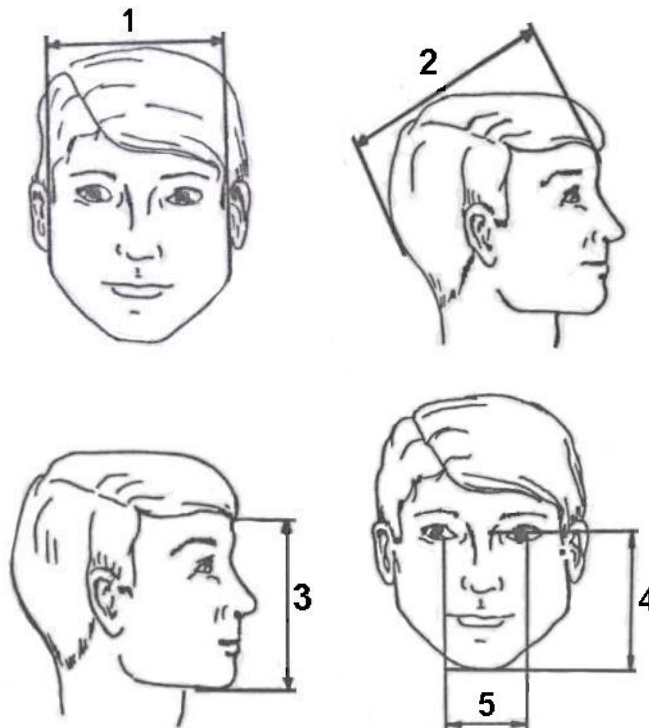


Figure 3.1 Major Head Dimensions [58].

Table 3.1 Average Values of the Major Head Dimensions [58]

	Anthropometric Measure	Mean [cm]	Standard Deviation
1	Head Width	15.1	1.63
2	Head Length	18.71	1.01
3	Head Height	18.72	1.12
4	Distance Between Eyes and Jaw	11.63	0.8
5	Distance Between Eyes	6.12	0.45

3.2.2 Weight

During the design we definitely need to consider the components' weights. We give the following statistical results showing the Average Male Head Mass in Table 3.2 and the Average Mass Moments of Inertia of the Male Head in Table 3.3. Due to the restrictions in actuator selection, the remaining parts in the head have to be designed as light as possible. Power consumption is another problem for robots operated by batteries. Although it is not planned to run our setup with batteries, as a future projection, we decided to reduce the robot's weight as much as we can. Thus, we refer to the below data given as the upper limit of the weight for the developed head robot.

Table 3.2 Average Male Head Mass [59]

Reference	No. of subjects	Average Body Mass [kg]	Average Head Mass [kg]
Walker et al., 1973	16	67.1	4.49
Hubbard and McLeod, 1974	11		4.54
Reynolds et al., 1975	6	65.2	3.98
Adjusted per HMRTF*	6	76.9	4.69
Beier et al., 1980	19	74.7	4.32
McConville et al., 1980	31	77.5	4.55**
Robbins, 1983	25	76.7	4.54***

* The Human Mechanical Response Task Force (HMRTF) of the Society of Automotive Engineers (SAE).

** Based on adjusted head volume of 95% of the reported head volume (4396 cm^3) and a head specific gravity of 1.097.

*** Based on an estimated head volume of 4137 cm^3 and a head specific gravity of 1.097.

Table 3.3 Average Mass Moments of Inertia* of the Male Head [$\text{kg}\cdot\text{m}^2 \times 10^{-3}$] [59].

Reference	I _{xx}	I _{yy}	I _{zz}
Walker et al., 1973		23.3	
Hubbard and McLeod, 1974	17.4	16.4	20.3
Adjusted per HMRTF	22.6	21.3	26.3
Beier et al., 1980 (16 male subjects only)	20.7	22.6	14.9
McConville et al., 1980	20.4	23.2	15.1
Adjusted by sp. gr. 1.097	22.4	25.5	16.6
Robbins, 1983	20.0	22.2	14.5
Adjusted by sp. gr. 1.097	22.0	24.2	15.9

* The mass moments of inertia given are about the x, y, or z anatomic axes through the center of gravity of the head.

**The origin of the coordinate axes is at the center of gravity (cg) of the head, and the x axis is in the posteroanterior direction (roll axis), while the z axis is in the inferosuperior direction (yaw axis) and the y axis is in the lateral direction (tilt axis).

3.3 Eye Movements

The human senses provide us with important sources of information about our surroundings. The majority of the information is gathered from environment by the eyes [60]. We also perform essential tasks with our eyes, such as finding objects of interest, directing the eyes towards these objects, pursuing and identifying these objects. In this respect, existence of functional eyes in a robotic head is essential. Therefore, in the design process, features of the human eyes should be investigated. In this subsection, general information about the eye movements is given.

In addition, eye movements should be well studied and understood because the movements of eyeballs determine the information gathered from the environment so eye movements are important to understand vision. They can be considered in two ways: as a motor system whose output is the position of the eyes relative to the head, and as a part of a sensory system where what matters is where the eyes are pointing in space, which technically called gaze [61].

There are five basic categories of eye movements: saccades, smooth pursuit, vergence, vestibulo-ocular and opto-kinetic movements. The first three eye movements are

voluntary whereas the last two are involuntary. In what follows, the functions of each type of eye movement will briefly be introduced.

3.3.1 Saccades

Saccades are very fast, refocussing (ballistic) movements of the eyes. During a saccade the point of fixation is suddenly changed. In order to see an object clearly, its image has to be projected onto the center of the fovea. To examine different objects, the eye should be brought onto the target deliberately. This action will consequently disrupt vision. To obtain a clear vision again, the eyes are moved as fast as they can be. These movements of eyes are called saccades. Saccades range in amplitude from the small movements to the larger movements. For example, while reading the small movements are made. While gazing around a room the much larger movements are needed [62]. During a saccade, little or no visual perception occurs [60].

Saccades, in humans, can be very fast. The speed of a saccade changes according to the amplitude of the saccadic movement. While for large saccades (80 degrees) the peak velocity may be over 500 [deg/sec], for small saccades (20 degrees) it may be about 150 [deg/sec] (This is the unique feature of the saccades.) However, in the literature, one can find the value 1000 [deg/sec] for the eyes to move during a saccade. The time period of a saccadic eye movement is shown in Figure 3.2. There is a 200 [ms] delay between the decision of a move and the beginning of the eye movement. In this delay, the position of the target with respect to the fovea is calculated. Since the saccade-generating system cannot respond to subsequent changes in the position of the target during the delay time, saccadic eye movements are said to be ballistic. In this period, if the target changes its position, the saccade will miss the target, and another saccade will be generated to find the correct position of it [62]. Thus, in saccadic performance, the saccade's generation can not directly be influenced by any errors [63].

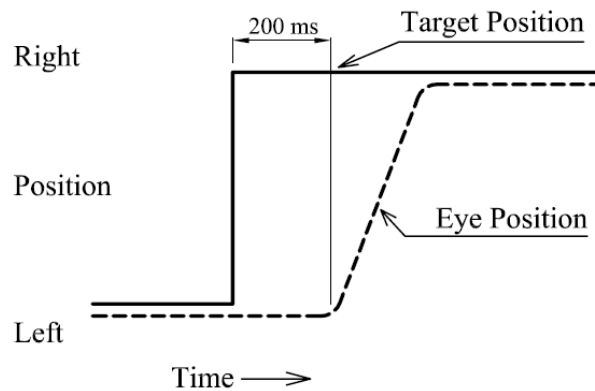


Figure 3.2 The metrics of a saccadic eye movement. The full line indicates the position of a fixation target and the dashed line the position of the fovea. When the target moves suddenly to the right, there is a delay about 200 [ms] before the eye begins to move to the new target position.

(After Fuchs, 1967) [62].

3.3.2 Smooth Pursuit

The second voluntary eye movement is smooth pursuit. It is the oculomotor behavior of tracking moving stimulus on the fovea. In other words, the image of a moving object is maintained on the high-resolution central area of the visual field. Therefore, they enable continuous vision of objects moving within the environment [62]. Smooth pursuit eye movements last very long when compared to saccades. In smooth pursuit, the eyes can move at up to 100 [deg/sec].

3.3.3 Vergence Movement

The last voluntary eye movement is vergence. Vergence movements adjust each eye for viewing targets at different distances. By rotating the eyes in opposite directions, a single object is fixed on both foveas. Since there is a constant distance between the two eyeballs, each eye receives a slightly different image of the object. For this reason, this type of movements are disconjugate (move separately) unlike other types are conjugate that is two eyes move in the same direction [60]. This feature will allow the perception of third dimension. It is important to succeed vergence movements to estimate the depth of an object. Similar to the saccadic movement, the peak velocity of vergence movement can be related to its amplitude.

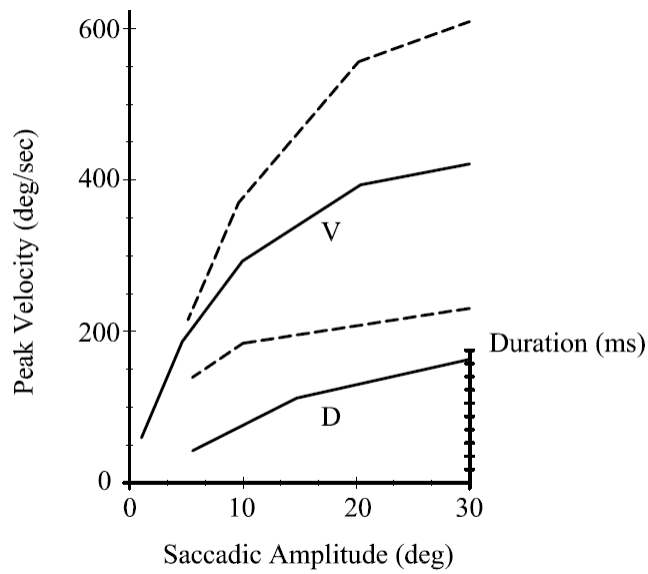


Figure 3.3 The relationship of saccadic amplitude to peak velocity (V) and duration (D) is illustrated. Dashed lines indicate standard deviation of velocity. (Adapted from Zee DS, Robinson DA. Velocity characteristics of normal human saccades, In: Topics in Neuro-ophthalmology, Edited by Thompson HS, Daroff R, Glaser JS, and Sanders MD, Baltimore, Williams and Wilkins, 1979, with permission.) [62]

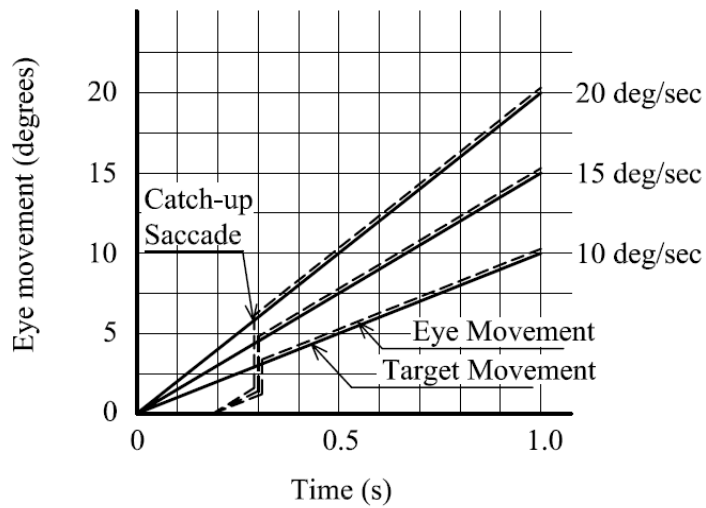


Figure 3.4 The metrics of smooth pursuit eye movement. These traces show eye movements tracking a stimulus moving at different velocities. After a quick saccade to capture the target, the eye movement attains a velocity that matches the velocity of the target. (After Fuchs, 1967) [62].

3.3.4 Vestibulo-Ocular Reflex

The vestibulo-ocular reflex is used to counterbalance the head movements. This movement occurs when one looks at a target while turning his head. During the turning period, the visual field will be automatically oriented to compensate for the head rotation so that the image of the target is kept at the same place on the fovea.

As far as the functions of the vestibulo-ocular reflex is considered, one can find three major reflexes: 1) the rotational, 2) the translational vestibulo-ocular reflexes, which respond the angular and linear components of head motion, respectively, and 3) the ocular counter-rolling response or optokinetic reflex which adapts the eye position during head tilting and rotation. In depth information about the mentioned reflexes are provided in references [62] and [64] may be seen.

3.3.5 Optokinetic Reflex

In fact, the vestibulo-ocular reflex and the optokinetic reflex operate together to maintain the image of an object on the retina. The vestibulo-ocular reflex is used to compensate for fast head motions whereas the optokinetic reflex serves to orient the visual field to stabilize the eyes during slow head movements. In order to explain the optokinetic reflex, the following well-known example is frequently used. In a moving train, one looks at a tree out of the window. The tree will be perceived as moving since the person is relatively stationary. After a certain period of time the tree will be out of the (field of) vision. At this time the optokinetic reflex will move the eyes back to their original position which is the position where they first recognize the tree.

3.3.6 Angular Velocities and Ranges

The rotation axes of the eye movements are shown in Figure 3.5. The motion ranges and velocities are tabulated in Table 3.4.

Table 3.4 Motion Ranges and Velocities [62]

		Angular Velocity	
Motion	Range [deg]	Smooth Pursuit [deg/sec]	Saccade [deg/sec]
Turning along the horizontal (Yaw)	± 25	100	500
Turning along the vertical (Tilt)	± 20		

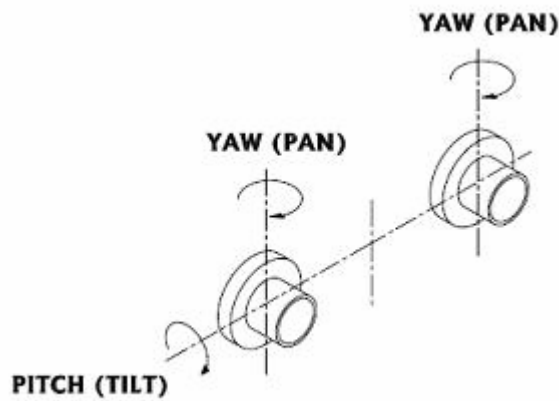


Figure 3.5 Rotation Axes of the Eye Movements.

3.4 Head Movements

Rotations of the head are generally explained as having components in one or more of the three planes: horizontal (yaw, rotation about Z or vertical axis), sagittal (pitch, rotation about the Y or interaural axis), and torsional or frontal (roll, rotation about X or nasaloccipital axis) [62]. Yaw, pitch and roll terms will be referred throughout this manuscript as the name of the rotation axes and the motion types.

3.4.1 Stabilization of the Head

After the eye movements, the head movements are investigated. It is important to remind that our robotic head will be stationary, that is, we are not implementing a torso in this

thesis study. We quote the following four paragraph information which is found very useful about head movements directly from reference [62].

“Head perturbations that occur during locomotion are a major threat to clear vision. Although the vestibulo-ocular reflex (VOR) can compensate for head rotations by producing compensatory eye rotations, its ability to do so is limited; for example, when head velocities approximately exceed 350 [deg/sec], saturation is reached and the reflex is no longer works adequately. Measurement of the rotational perturbations of the head during walking or running in place indicates that angular head velocity usually does not exceed 100 [deg/sec] even during running.

During natural behaviour, eye and head movements usually occur together. During natural activities such as locomotion, the head is held relatively steady, with velocities generally below 100 [deg/sec]. The frequency interval of rotational head perturbations that occur during locomotion ranges between 0.5 and 5.0 Hz. The stability of the head during such perturbations is mainly due to the mass of the head and the viscoelastic properties of the neck. The vestibulocollic and cervicocollic reflexes may prevent the head oscillations in pitch and roll while subjects are in motion.

During large gaze shifts to reorient the head and eyes in space the vestibulo-ocular reflex is in part disconnected. During smaller eye-head saccades in response to visual stimuli within the field of vision, a linear addition of the saccade command and the vestibulo-ocular reflex may occur.

During combined, smooth eye-head tracking, the vestibulo-ocular reflex is probably cancelled by an internal smooth pursuit signal. In addition, the VOR gain may be reduced during smooth eye-head tracking”.

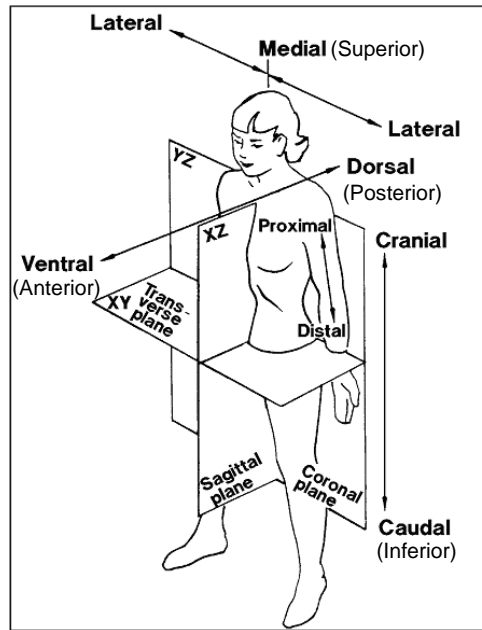


Figure 3.6 Anatomical Planes of the Body [65].

The neurological studies show that under normal conditions the angular head velocity does not exceed 100 [deg/sec]. Therefore, this value can be taken as the target velocity for the degrees of freedom of the neck.

3.4.2 Angle of Ranges

Active neck range of motion is the number of degrees through which people can move their head in various directions [66]. Range of motion is measured in three directions: (1) bending the head forward and backward (flexion-extension) (Figure 3.7.a), (2) turning the head left and right (axial rotation) (Figure 3.7.b), and (3) bending the head left and right (lateral bending) (Figure 3.7.c) [67].

3.5 Jaw

Talking, which is a human-like behavior, can increase the humanness of the robot and contribute to the establishment of a social relationship between the robot and people. A jaw allows controlling the mouth's opening and closing which can be used to imitate speech. To this end we decided to add a jaw mechanism consisting of the lower jaw (mandible) to our design. The mandible should be designed so that it can accommodate

the necessary equipment to realize the lower lip. Besides, it has to have suitable protrudes to mount the skin etc.

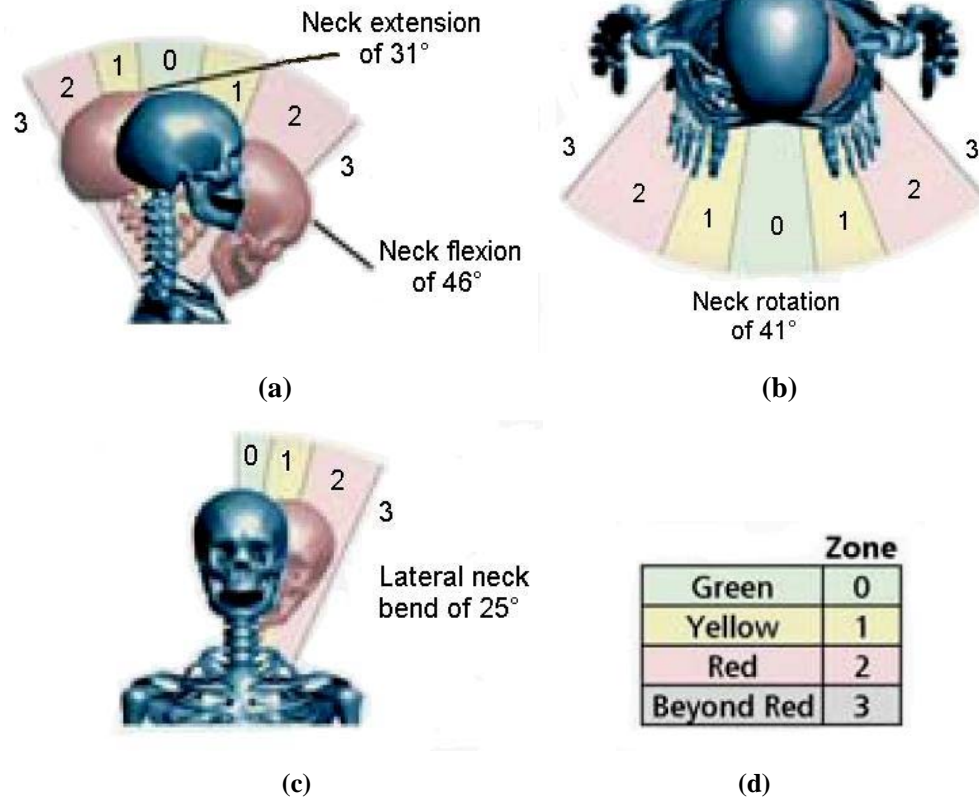


Figure 3.7 Various ranges of motion for different joints. For exact values of each Zone, see Table 3.5 below [67]

Table 3.5 Range of Motion of Head [67].

		Range of Motion Zones [deg]			
Movement		0	1	2	3
Neck	Flexion (Tilt)	0-9	10-22	23-45	46+
	Extension (Tilt)	0-6	7-15	16-30	31+
	Rotational (Yaw)	0-8	9-20	21-40	41+
	Lateral Bend (Roll)	0-5	6-12	13-24	25+

Data for this table was modified Chaffin, 1999 and Woodson, 1992. There are the actual angular measurements of body joints in each of the four Zones for range of motion.

3.6 Summary

The major concerns in designing a humanoid robot are a lightweight construction, prevention of hazards to users, and a motion space that corresponds to that of human beings. The robot must have manlike appearance and dexterity. The design of the body of a mechatronical robot, which is intended to imitate the mechanical and sensory properties of humans, can only be realized in an intensive iterative process [68].

The fundamental issues taken into consideration in designing our robotic head can be summarized as follows:

1. The overall dimensions must be as close as possible to that of humans. The five major dimensions given in Table 3.1 are the upper limits for the design.
2. The human head has several moving joints so they must properly be replaced by the mechanical ones. We developed a 4-DOF neck and 3-DOF eyes mechanisms. There is also 1 DOF jaw.
3. The ranges of motion of each joint should be similar to those of humans. Values given in Table 3.4 and 3.5 are taken as reference values to achieve.
4. The achievable joint velocities must be as close as possible to that of humans. For the neck movements, 100 [deg/sec], and for the eye movements 500 [deg/sec] are the target velocities.
5. The robot's hardware should minimize the overall weight. The maximum weight for the head should not exceed 4 [kg].
6. Actuator selection should be done by following the anthropomorphic data so that human like motion can be realized by our robot.
7. The joint torques should be enough to support the mechanical structure together with the dynamics required to simulate the human head movements.
8. The robotic head should be easy to control, easy to program, low cost, easy to maintain and easy to assembly (wiring is also an important issue).

CHAPTER 4

MODELING AND ANALYSING

This chapter describes the way how we model our human like robotic head. Its each part is specifically considered and formed according to the design considerations mentioned in Chapter 2. Kinematic analysis of the developed head and neck combination model is performed in detail. The analytical solution to the forward and the semi-analytical solution to the inverse kinematic problems are solved using the algebra based on exponential rotation matrices.

4.1 General Human Modeling

The general human modeling method is adapted from kinematics science which focuses on motion without considering forces influencing the movement. As far as the human movements are considered, kinematics concerns the positions, velocities and accelerations of the rigid body sections of human body such as foot, hand, arm and head. Position describes the location of a body segment or joint in space. Velocities and accelerations can be computed from position by differentiating with respect to time.

The human skeleton system (Figure 4.1) is assumed to be consisting of rigid (non-deforming) bodies linked consecutively in a kinematic structure. In this structure, the bodies are connected to another by joints. A joint is positioned at the intersection of two bodies. The joint arrangement between these bodies is of great importance since it determines the motion freedom. In general, the joints allow rotational motions making three kinds of position angles as flexing, pivot and twisting. Each is given by degrees of freedom (DOF) where one DOF is represented by one rotational axis [69]. Therefore, most of the portions of the human body can be considered as the collection of serially connected revolute joints.

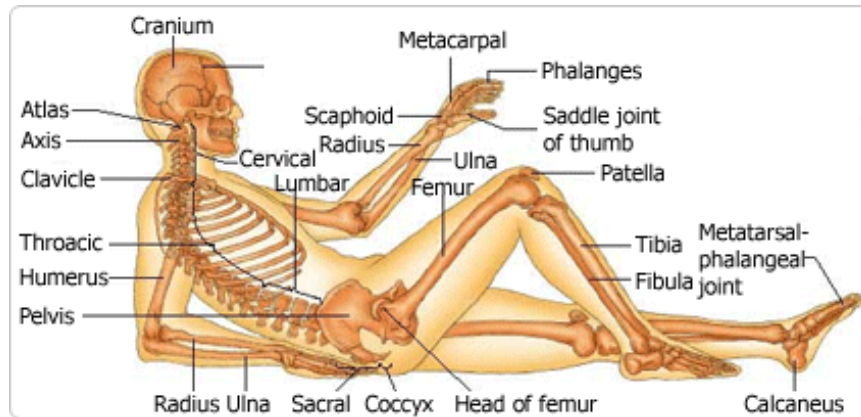


Figure 4.1 Human Skeletal System and Its Anatomy [70].

Since it is aimed to design and manufacture a robotic head, in this study, the anatomy of spine should be examined. In Figure 4.2, sections of the spine are shown. It consists of several vertebrae connected by ligaments, small muscles, vertebral joints, and intervertebral disks.

The spinal column consists of 33 vertebrae organized into five regions: 1) Cervical, 2) Thoracic, 3) Lumbar, 4) Sacral, 5) Coccyx. Flexion, extension, lateral movement, circumduction and rotation are the movements permitted in the vertebral column.



Figure 4.2 The Human Spine [72].

Therefore, we consider modeling the cervical region of the spine as a kinematic chain to obtain the movements of human head and neck. Since each part in this model is assumed to be a rigid body, at any given time, it is possible to find the location and orientation of a specific point in this kinematic chain.

4.2 Kinematic Model of Head/Neck

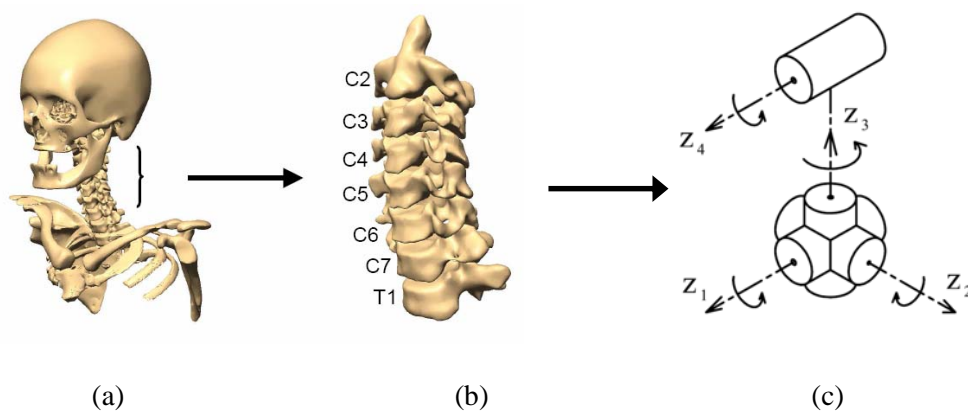


Figure 4.3 a) Cervical Region of the Spine, b) Cervical Vertebrae [73], c) The Kinematic Model.

The head and neck system is a complex and overcomplete biomechanical linkage with multiple degrees of freedom of movement about each of its eight joints. Yaw motion is performed about C1-C2, pitch is about either C1-Skull or C6-7—T1 and roll by combined lateral flexion of C2-C5. The simplifications are introduced after these kinematic examinations [74].

Since we try to construct a robotic neck, we should investigate the cervical region of the spine. In Figure 4.3, the cervical region of the spine is shown. The cervical vertebrae constitute the neck in other words the cervical spine lies within the neck [71]. Extension, or movement backward, and the extent of lateral movement are freest in the cervical region comparing to the other parts of the spine [72].

Although each vertebra has 3 DOF in the cervical part of the spine, we implemented a 4-DOF mechanism (in total) for simplicity in our model. A simple sketch of this model is given in Figure 4.3.c.

4.3 Kinematic Model of Eyes

The eyes mechanism should be designed so that movements similar to human eyes' can successfully be achieved. As can be seen in Figure 4.4, the human anatomy permits three different rotations: 1) both eyes can independently rotate about vertical axes passing through their centers (pan), 2) they can be oriented about a horizontal axis for performing tilt motion, 3) each eyeball can turn about an axis which is in the direction of sight. The last one is usually ignored in designing vision systems because the range of motion is so limited and moreover, it can be simulated by image processing. Thus, the first and second rotations are taken into consideration in our design resulting in a 3-DOF mechanism.

We modeled the mechanism as shown in Figure 4.5.

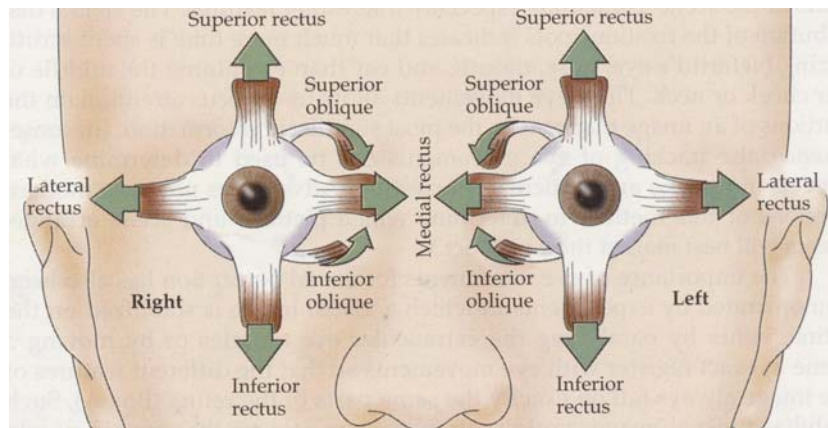


Figure 4.4 Possible Eye Movements and Muscle Groups [60].

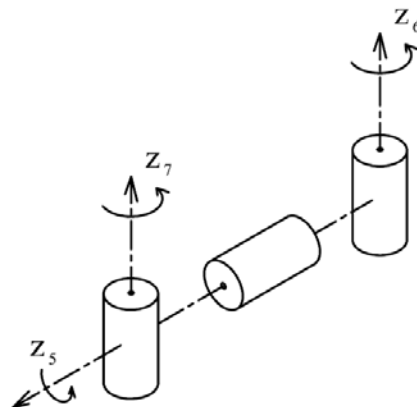


Figure 4.5 Kinematic Model of Eyes

4.4 Kinematic Model of Jaw

The mandible (lower jaw bone) holding the lower teeth in place is the largest and strongest bone of the face. This thesis work does not aim to implement a realistic jaw. For the sake of completeness, a one degree of freedom jaw mechanism is added to the design, hence, it will only show opening and closing the mouth.

4.5 Kinematic Analysis

Kinematics is a science of movement and it is divided forward (direct) and inverse (indirect) kinematics. Forward kinematics gets position and orientation of last segment in a kinematic chain by defining angles for every joint. On the other hand, inverse kinematics computes joint angles of a kinematics chain based on the position and orientation of last kinematics segment.

If most of the portions of human body are connected successively they can be treated as a serial type robotic manipulator. In the analysis the method presented in [75] is used. The kinematic model of the manipulator is obtained by using the method of Denavit and Hartenberg. The exponential rotation matrices defined in [76], [77] are used instead of homogeneous transformation matrices because of their convenience in making the kinematic equations more compact and simple. A more detailed kinematic model of the manipulator is given in Figure 4.6 with frame attachments according to the D-H convention, where θ_i, d_i, a_i and α_i represent the joint variables, the joint offsets, the effective link lengths and the twist angles, respectively.

The origin of the base frame is located at the intersection of the first three joint axes, i.e. there is a spherical joint arrangement. The kinematic parameters according to this model can be obtained by simply drawing necessary auxiliary views. They are tabulated in Table 4.1.

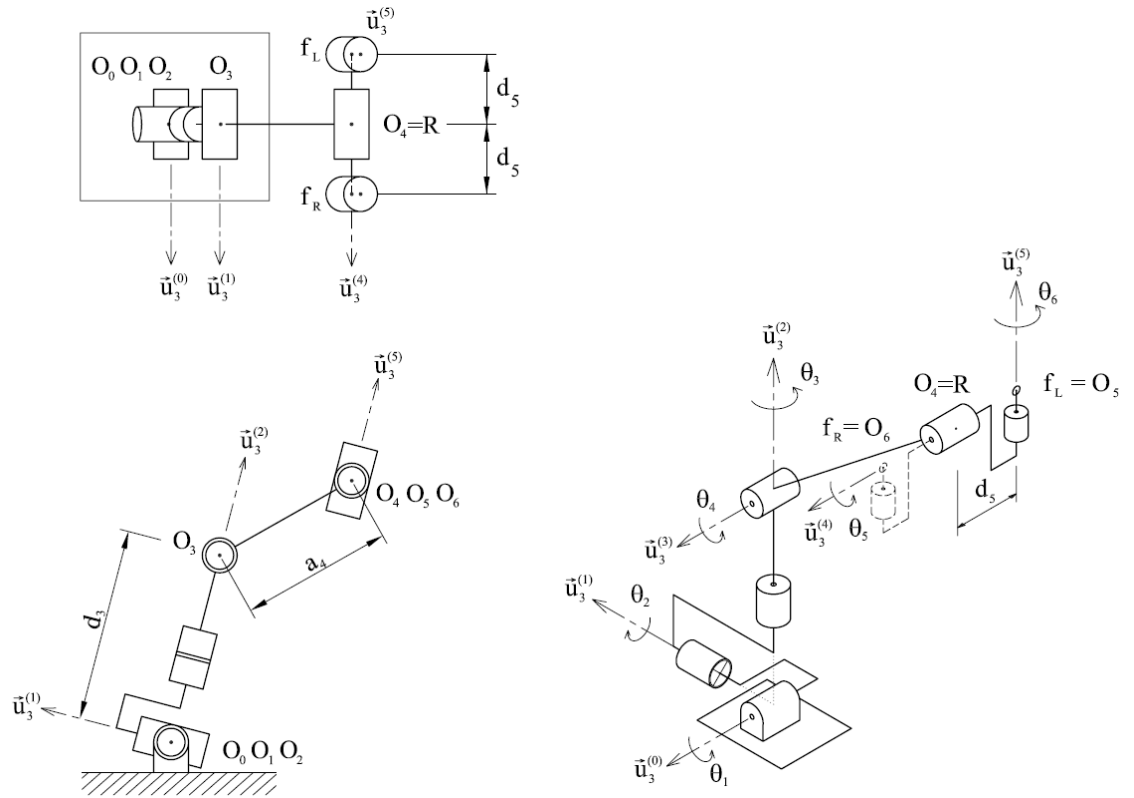


Figure 4.6 Kinematic Model of the Robot.

Table 4.1 Kinematic Parameters for the Model.

k^{th} Link	a_k	α_k	d_k	θ_k
1	0	$+\pi/2$	0	θ_1
2	0	$-\pi/2$	0	θ_2
3	0	$+\pi/2$	d_3	θ_3
4	a_4	0	0	θ_4
5	0	$-\pi/2$	d_5	θ_5
6	0	0	0	θ_6

4.5.1 Forward Kinematics

The model is a seven-revolute-joint manipulator. As can be seen in Figure 4.6, the last joint is placed for yaw motion of the left eye. The right eye is similarly placed to the other side for the same motion type. Both eyes are rotated together about $\vec{u}_3^{(4)}$. In the analysis we will ignore the right eye joint because there will be only sign change in the derived equations to obtain the position vector of it. The location equations for both eyeball centers will separately be given. Thus, the number of frames reduces to six.

A vector can be represented in two different reference frames as in the following equation.

$$\vec{r}^{(a)} = \hat{C}^{(a,b)} \vec{r}^{(b)} \quad (4.1)$$

where, $\vec{r}^{(a)}$ and $\vec{r}^{(b)}$ are the column representations of the vector \vec{r} in the frames a and b , $\hat{C}^{(a,b)}$ is the transformation matrix from the frame b to a .

Since there are six link frames in the model, there has to be six transformation matrices. They are combined to find the orientation matrix of the left eye center with respect to the base frame. It can be given as follows;

$$\hat{C}^{(0,6)} = \hat{C}^{(0,1)} \hat{C}^{(1,2)} \hat{C}^{(2,3)} \hat{C}^{(3,4)} \hat{C}^{(4,5)} \hat{C}^{(5,6)} \quad (4.2)$$

The matrix $\hat{C}^{(a,b)}$ is given as an exponential rotation matrix since the frame b is obtained by rotating frame a about an axis described by a unit vector \vec{r} through an angle θ .

$$\hat{C}^{(a,b)} = e^{\vec{r}\theta} \quad (4.3a)$$

We define the rotating axes as the k^{th} basis vector of each frame so $\vec{r} = \vec{u}_k^{(a)}$. Then Eq. (4.3a) becomes,

$$\hat{C}^{(a,b)} = e^{\vec{u}_k^{(a)}\theta} \quad (4.3b)$$

Thus, the link to link exponential rotation matrices can be written down by using the kinematic parameters given in Table 4.1.

$$\hat{C}^{(0,1)} = e^{\tilde{u}_3 \theta_1} e^{\tilde{u}_1 \pi/2} \quad (4.4a)$$

$$\hat{C}^{(1,2)} = e^{\tilde{u}_3 \theta_2} e^{-\tilde{u}_1 \pi/2} \quad (4.4b)$$

$$\hat{C}^{(2,3)} = e^{\tilde{u}_3 \theta_3} e^{\tilde{u}_1 \pi/2} \quad (4.4c)$$

$$\hat{C}^{(3,4)} = e^{\tilde{u}_3 \theta_4} \quad (4.4d)$$

$$\hat{C}^{(4,5)} = e^{\tilde{u}_3 \theta_5} e^{-\tilde{u}_1 \pi/2} \quad (4.4e)$$

$$\hat{C}^{(5,6)} = e^{\tilde{u}_3 \theta_6} \quad (4.4f)$$

Combinations of the above expressions giving the orientation matrix of the left eye center are the following (for the simplifications see [78]).

$$\hat{C}^{(0,2)} = e^{\tilde{u}_3 \theta_1} e^{\tilde{u}_1 \pi/2} e^{\tilde{u}_3 \theta_2} e^{-\tilde{u}_1 \pi/2} \quad (4.5a)$$

$$\hat{C}^{(0,3)} = e^{\tilde{u}_3 \theta_1} e^{\tilde{u}_1 \pi/2} e^{\tilde{u}_3 \theta_2} e^{-\tilde{u}_1 \pi/2} e^{\tilde{u}_3 \theta_3} e^{\tilde{u}_1 \pi/2} = e^{\tilde{u}_3 \theta_1} e^{\tilde{u}_1 \pi/2} e^{\tilde{u}_3 \theta_2} e^{\tilde{u}_2 \theta_3} \quad (4.5b)$$

$$\hat{C}^{(0,4)} = e^{\tilde{u}_3 \theta_1} e^{\tilde{u}_1 \pi/2} e^{\tilde{u}_3 \theta_2} e^{\tilde{u}_2 \theta_3} e^{\tilde{u}_3 \theta_4} \quad (4.5c)$$

$$\hat{C}^{(0,5)} = e^{\tilde{u}_3 \theta_1} e^{\tilde{u}_1 \pi/2} e^{\tilde{u}_3 \theta_2} e^{\tilde{u}_2 \theta_3} e^{\tilde{u}_3 \theta_4} e^{\tilde{u}_3 \theta_5} e^{-\tilde{u}_1 \pi/2} \quad (4.5d)$$

$$\hat{C}^{(0,6)} = e^{\tilde{u}_3 \theta_1} e^{\tilde{u}_1 \pi/2} e^{\tilde{u}_3 \theta_2} e^{\tilde{u}_2 \theta_3} e^{\tilde{u}_3 \theta_4} e^{\tilde{u}_3 \theta_5} e^{-\tilde{u}_1 \pi/2} e^{\tilde{u}_3 \theta_6} \quad (4.5e)$$

In Eq. (4.5e) θ_4 and θ_5 can be added because they are rotations about successive parallel joint axes. So the equation can be simplified as,

$$\hat{C}^{(0,6)} = e^{\tilde{u}_3 \theta_1} e^{\tilde{u}_1 \pi/2} e^{\tilde{u}_3 \theta_2} e^{\tilde{u}_2 \theta_3} e^{\tilde{u}_3 \theta_{45}} e^{-\tilde{u}_1 \pi/2} e^{\tilde{u}_3 \theta_6} \quad (4.6)$$

$$\text{where } \theta_{45} = \theta_4 + \theta_5. \quad (4.6a)$$

R is the frame origin of the fifth joint. It is the midpoint between the two eyeballs. Its location can be expressed in vector form with the transformation matrices defined above as follows,

$$\bar{r} = d_3 \bar{u}_3^{(2)} + a_4 \bar{u}_1^{(4)} \quad (4.7)$$

Using the column representation of the vectors in the base frame, Eq. (4.7) becomes,

$$\bar{r} = d_3 \bar{u}_3^{(2/0)} + a_4 \bar{u}_1^{(4/0)} \quad (4.7a)$$

$$\bar{r} = d_3 \hat{C}^{(0,2)} \bar{u}_3 + a_4 \hat{C}^{(0,4)} \bar{u}_1 \quad (4.7b)$$

where,

$$\bar{u}_1 = \begin{bmatrix} 1 \\ 0 \\ 0 \end{bmatrix} \quad \bar{u}_2 = \begin{bmatrix} 0 \\ 1 \\ 0 \end{bmatrix} \quad \bar{u}_3 = \begin{bmatrix} 0 \\ 0 \\ 1 \end{bmatrix} \quad (4.8),(4.9), (4.10)$$

$$\bar{r} = d_3 e^{\tilde{u}_3 \theta_1} e^{\tilde{u}_1 \pi/2} e^{\tilde{u}_3 \theta_2} e^{-\tilde{u}_1 \pi/2} \bar{u}_3 + a_4 e^{\tilde{u}_3 \theta_1} e^{\tilde{u}_1 \pi/2} e^{\tilde{u}_3 \theta_2} e^{\tilde{u}_2 \theta_3} e^{\tilde{u}_3 \theta_4} \bar{u}_1 \quad (4.11)$$

After expanding the rotation matrices and performing the simplifications the base frame components of point R location vector can be obtained as given below.

$$r_1 = a_4 c \theta_4 c \theta_3 c \theta_2 c \theta_1 - (d_3 + a_4 s \theta_4) s \theta_2 c \theta_1 - a_4 c \theta_4 s \theta_3 s \theta_1 \quad (4.12)$$

$$r_2 = a_4 c \theta_4 c \theta_3 c \theta_2 s \theta_1 - (d_3 + a_4 s \theta_4) s \theta_2 s \theta_1 + a_4 c \theta_4 s \theta_3 s \theta_1 \quad (4.13)$$

$$r_3 = a_4 c \theta_4 c \theta_3 s \theta_2 + (d_3 + a_4 s \theta_4) c \theta_2 \quad (4.14)$$

The column representation of the left eye center point location vector \bar{f}_L can be expressed in the base frame in the following form.

$$\bar{f}_L = \bar{r} - F_L \quad (4.15)$$

$$\text{where,} \quad \bar{F}_L = d_5 \hat{C}^{(0,6)} \bar{u}_3 \quad (4.16)$$

$$\text{or} \quad \bar{F}_L = d_5 e^{\tilde{u}_3 \theta_1} e^{\tilde{u}_1 \pi/2} e^{\tilde{u}_3 \theta_2} e^{\tilde{u}_2 \theta_3} e^{\tilde{u}_3 \theta_4} e^{\tilde{u}_3 \theta_5} e^{-\tilde{u}_1 \pi/2} e^{\tilde{u}_3 \theta_6} \bar{u}_3 \quad (4.16a)$$

After performing the simplifications the base frame components of point f_L location vector can be obtained as given below.

$$f_{L1} = a_4 c \theta_4 c \theta_3 c \theta_2 c \theta_1 - (d_3 + a_4 s \theta_4) s \theta_2 c \theta_1 - a_4 c \theta_4 s \theta_3 s \theta_1 - d_5 c \theta_3 s \theta_1 - d_5 c \theta_2 c \theta_1 s \theta_3 \quad (4.17)$$

$$f_{L2} = a_4 c \theta_4 c \theta_3 c \theta_2 s \theta_1 - (d_3 + a_4 s \theta_4) s \theta_2 s \theta_1 + a_4 c \theta_4 s \theta_3 s \theta_1 + d_5 c \theta_3 c \theta_1 - d_5 c \theta_2 s \theta_3 s \theta_1 \quad (4.18)$$

$$f_{L3} = a_4 c \theta_4 c \theta_3 s \theta_2 + (d_3 + a_4 s \theta_4) c \theta_2 - d_5 s \theta_3 s \theta_2 \quad (4.19)$$

Similarly, f_R location vector can be defined as,

$$\bar{f}_R = \bar{r} + F_L \quad (4.20)$$

$$f_{R1} = a_4 c \theta_4 c \theta_3 c \theta_2 c \theta_1 - (d_3 + a_4 s \theta_4) s \theta_2 c \theta_1 - a_4 c \theta_4 s \theta_3 s \theta_1 + d_5 c \theta_3 s \theta_1 + d_5 c \theta_2 c \theta_1 s \theta_3 \quad (4.21)$$

$$f_{R2} = a_4 c \theta_4 c \theta_3 c \theta_2 s \theta_1 - (d_3 + a_4 s \theta_4) s \theta_2 s \theta_1 + a_4 c \theta_4 s \theta_3 s \theta_1 - d_5 c \theta_3 c \theta_1 + d_5 c \theta_2 s \theta_3 s \theta_1 \quad (4.22)$$

$$f_{R3} = a_4 c \theta_4 c \theta_3 s \theta_2 + (d_3 + a_4 s \theta_4) c \theta_2 + d_5 s \theta_3 s \theta_2 \quad (4.23)$$

4.5.2 Inverse Kinematics

The inverse kinematic analysis will be carried out to determine the joint variables for a given set of coordinates and orientation.

Noting that, Eqs. (4.12), (4.13) and (4.14) are three equations with four unknowns. This happens when the wrist point equation of a manipulator contains four joint variables. Since all the joints of the model are revolute and the last three axes do not intersect at the same point, it has no closed form solution to the inverse kinematics problem [75]. Although this configuration tells us that there should not be a closed-form solution, a little effort may result useful consequences. That is, one can find an analytical solution for θ_4 , if the squares of the Eqs. (4.12), (4.13) and (4.14) are taken and summed side by side.

$$r_1^2 + r_2^2 + r_3^2 - d_3^2 - a_4^2 = 2a_4d_3s\theta_4 \quad (4.24)$$

$$\theta_4 = \sigma_4 \sin^{-1} \left[\frac{r_1^2 + r_2^2 + r_3^2 - d_3^2 - a_4^2}{2a_4d_3} \right] ; \quad \sigma_4 = \pm 1 \quad (4.25)$$

In the inverse kinematics problem, $\hat{C}^{(0,6)}$ and \bar{f} are given and \bar{r} is known from Eq. (4.11). The location of point R can also be expressed as

$$\begin{aligned} \bar{r} = e^{\bar{u}_3\theta_1} [(a_4c\theta_4c\theta_3c\theta_2 - a_4s\theta_4s\theta_2 - d_3s\theta_2)\bar{u}_1 + (a_4c\theta_4s\theta_3)\bar{u}_2 \\ + (a_4c\theta_4c\theta_3s\theta_2 + a_4s\theta_4c\theta_2 + d_3c\theta_2)\bar{u}_3] \end{aligned} \quad (4.26)$$

Pre-multiplying Eq. (4.26) by $\bar{u}_1^T, \bar{u}_2^T, \bar{u}_3^T$ will yield three scalar equations.

$$r_1c\theta_1 + r_2s\theta_1 = a_4c\theta_4c\theta_3c\theta_2 - a_4s\theta_4s\theta_2 - d_3s\theta_2 \quad (4.27)$$

$$r_2c\theta_1 - r_1s\theta_1 = a_4c\theta_4s\theta_3 \quad (4.28)$$

$$r_3 = a_4c\theta_4c\theta_3s\theta_2 + a_4s\theta_4c\theta_2 + d_3c\theta_2 \quad (4.29)$$

With known θ_4 , note that Eq. (4.28) is the simplest equation among the R point equations, depending on the sines and cosines of the first and third joint variables, either θ_1 or θ_3 can be solved in terms of the other, i.e. either θ_1 or θ_3 can be considered as the parameterized joint variable.

Inverse kinematics solution based on parameterized joint variable θ_3

Consider Eq. (4.28) and let,

$$r_2 = r_{12}c\gamma_1 \quad (4.30)$$

$$r_1 = r_{12}s\gamma_1 \quad (4.31)$$

with $r_{12} > 0$

This manipulation is also known as The Phase Angle Method.

$$r_{12} = \sqrt{r_1^2 + r_2^2} \quad (4.32)$$

$$\gamma_1 = a \tan_2(r_1, r_2) \quad (4.33)$$

$$r_{12} c \gamma_1 c \theta_1 - r_{12} s \gamma_1 s \theta_1 = a_4 c \theta_4 s \theta_3 = B \quad (4.34)$$

$$r_{12} c(\gamma_1 + \theta_1) = B \quad (4.35)$$

If r_{12} is positive then,

$$c(\gamma_1 + \theta_1) = \frac{B}{r_{12}}, \text{ and} \quad (4.36)$$

$$s(\gamma_1 + \theta_1) = \sigma_1 \sqrt{1 - \left(\frac{B}{r_{12}}\right)^2} \quad ; \quad \sigma_1 = \pm 1 \quad (4.37)$$

Hence,

$$\theta_1 = -\gamma_1 + a \tan_2 \left[\sigma_1 \sqrt{1 - \left(\frac{B}{r_{12}}\right)^2}, \left(\frac{B}{r_{12}}\right) \right] \quad (4.38)$$

θ_1 is found in terms of θ_3 , i.e. $\theta_1 = f_1(\theta_3)$.

The location of point R can also be expressed as;

$$e^{-\tilde{u}_3 \theta_2} e^{-\tilde{u}_1 \pi/2} e^{-\tilde{u}_3 \theta_1} \bar{r} = (a_4 c \theta_4 c \theta_3) \bar{u}_1 + (d_3 + a_4 s \theta_4) \bar{u}_2 - (a_4 c \theta_4 s \theta_3) \bar{u}_3 \quad (4.39)$$

Pre-multiplying Eq. (4.39) by $\bar{u}_1^T, \bar{u}_2^T, \bar{u}_3^T$ will yield three scalar equations.

$$c \theta_2 (r_1 c \theta_1 + r_2 s \theta_1) + r_3 s \theta_2 = a_4 c \theta_4 c \theta_3 \quad (4.40)$$

$$s \theta_2 (r_1 c \theta_1 + r_2 s \theta_1) - r_3 c \theta_2 = -(d_3 + a_4 s \theta_4) \quad (4.41)$$

$$r_2 c \theta_1 - r_1 s \theta_1 = a_4 c \theta_4 s \theta_3 \quad (4.42)$$

Eqs. (4.40) and (4.41) can be written in the form of $\hat{A} \hat{X} = \hat{B}$.

$$\begin{bmatrix} r_1 c \theta_1 + r_2 s \theta_1 & r_3 \\ -r_3 & r_1 c \theta_1 + r_2 s \theta_1 \end{bmatrix} \begin{bmatrix} c \theta_2 \\ s \theta_2 \end{bmatrix} = \begin{bmatrix} a_4 c \theta_4 c \theta_3 \\ -(d_3 + a_4 s \theta_4) \end{bmatrix} \quad (4.43)$$

$$\det(\hat{A}) = r_1^2 c^2 \theta_1 + r_2^2 s^2 \theta_1 + 2r_1 r_2 c \theta_1 s \theta_1 + r_3^2 = \Delta \quad (4.44)$$

If $\Delta \neq 0$ then $\hat{X} = \hat{A}^{-1} \hat{B}$.

$$\begin{bmatrix} c \theta_2 \\ s \theta_2 \end{bmatrix} = \frac{1}{\Delta} \begin{bmatrix} r_1 c \theta_1 + r_2 s \theta_1 & -r_3 \\ r_3 & r_1 c \theta_1 + r_2 s \theta_1 \end{bmatrix} \begin{bmatrix} a_4 c \theta_3 c \theta_4 \\ -(d_3 + a_4 s \theta_4) \end{bmatrix} \quad (4.45)$$

$$c \theta_2 = \frac{1}{\Delta} [(r_1 c \theta_1 + r_2 s \theta_1) a_4 c \theta_4 c \theta_3 + r_3 (d_3 + a_4 s \theta_4)] = \xi_2 \quad (4.46)$$

$$s \theta_2 = \frac{1}{\Delta} [r_3 a_4 c \theta_4 c \theta_3 - (r_1 c \theta_1 + r_2 s \theta_1) (d_3 + a_4 s \theta_4)] = \eta_2 \quad (4.47)$$

$$\theta_2 = a \tan_2[\eta_2, \xi_2] \quad (4.48)$$

θ_2 is determined in terms of θ_3 , i.e. $\theta_2 = g_2(\theta_3)$.

$\Delta = 0$

The determinant of matrix \hat{A} can only equal to zero if and only if r_1 , r_2 and r_3 are zero.

In this case the first singularity occurs. In this singularity point R become coincident with the base frame origin. However, it is physically not possible since d_3 is always greater than a_4 .

Inverse kinematics solution based on parameterized joint variable θ_1

Consider again Eq. (4.28) and note that the left side of this equation is known after taking θ_1 as the parameterized joint variable.

$$s \theta_3 = \frac{r_2 c \theta_1 - r_1 s \theta_1}{a_4 c \theta_4} \quad (4.49)$$

$$\text{If } c \theta_4 \neq 0 \quad (4.50)$$

$$\theta_3 = \sigma_3 \sin^{-1} \left[\frac{r_2 c \theta_1 - r_1 s \theta_1}{a_4 c \theta_4} \right] ; \quad \sigma_3 = \pm 1 \quad (4.51)$$

If $\theta_4 = \pm \frac{\pi}{2}$ then $\cos \theta_4$ is equal to zero. When this happens Eq. (F) will be unsolvable and the second singularity will occur. In this singularity, the location of point R is not changed with θ_3 . Physically, θ_4 can not be equal to $(-\frac{\pi}{2})$, however, $(+\frac{\pi}{2})$ is possible.

$\theta_4 = +\frac{\pi}{2}$ indicates the vertical head position. This position has to be considered in the control phase of the joint. That is, the joint variable should not be allowed to take this angle.

As for θ_2 , Eqs. (4.43) through (4.48) will not change when θ_1 is used as the parameterized joint variable. The singularity case will also be the same.

Inverse kinematics solution based on parameterized joint variable θ_2

We will now manipulate Eq. (4.41) by using The Half Angle Method to determine θ_1 .

$$\text{Define } t_1 = \tan\left(\frac{\theta_1}{2}\right) \text{ then,} \quad (4.52)$$

$$c \theta_1 = \frac{1 - t_1^2}{1 + t_1^2} \quad (4.53)$$

$$s \theta_1 = \frac{2t_1}{1 + t_1^2} \quad (4.54)$$

Consider Eq. (4.41) and rewrite it by substituting Eqs. (4.53) and (4.54) as

$$r_1 s \theta_2 \frac{1 - t_1^2}{1 + t_1^2} + r_2 s \theta_2 \frac{2t_1}{1 + t_1^2} = r_3 c \theta_2 - d_3 - a_4 s \theta_4 \quad (4.55)$$

Eq. (4.55) can be written as given below.

$$Et_1^2 - Ft_1 + G = 0$$

where,

$$E = r_3c\theta_2 - d_3 - a_4s\theta_4 + r_1s\theta_2 \quad (4.56)$$

$$F = -2r_2s\theta_2 \quad (4.57)$$

$$G = r_3c\theta_2 - d_3 - a_4s\theta_4 - r_1s\theta_2 \quad (4.58)$$

$$t_1 = \frac{-F + \sigma_1 \sqrt{F^2 - 4EG}}{2E}; \quad \sigma_1 = \pm 1 \quad (4.59)$$

If $E \neq 0$,

$$\theta_1 = a \tan_2(2t_1, 1 - t_1^2) \quad (4.60)$$

$E = 0$

Eq. (4.56) can only be equal to zero if and only if r_1 , r_3 , a_4 and d_3 are zero. If this condition is satisfied Eq. (4.59) cannot be solved. However, it is obvious that d_3 and a_4 can never equal to zero at least because they are the physical joint parameters.

$F = 0$

Also, in Eq. (4.59), F should not be equal to zero because, again it will be unsolvable. F is zero when r_2 is zero or $\theta_2 = 0$ or $\pm \pi$. This problem cannot be faced due to the limitation in θ_2 .

The left sides of Eqs. (4.40) and (4.42) are known at this stage so,

$$c\theta_3 = \frac{r_1c\theta_2c\theta_1 + r_2c\theta_2s\theta_1 + r_3s\theta_2}{a_4c\theta_4} = \xi_3 \quad (4.61)$$

$$s\theta_3 = \frac{r_2c\theta_1 - r_1s\theta_1}{a_4c\theta_4} = \eta_3 \quad (4.62)$$

If $c\theta_4 \neq 0$,

$$\theta_3 = a \tan_2(\eta_3, \xi_3) \quad (4.63)$$

If $\theta_4 = \pm \frac{\pi}{2}$ then $\cos \theta_4$ is equal to zero. This singularity has already been encountered and explained above. These singularity information is of importance to decide on the restrictions of the joint variables.

The remaining joint variables to be determined are the last two joint variables. Since the first four variables are determined, the rotation matrices of those variables are also known. If the orientation equation is rewritten as

$$e^{\tilde{u}_3 \theta_5} e^{-\tilde{u}_1 \pi/2} e^{\tilde{u}_3 \theta_6} = e^{-\tilde{u}_3 \theta_4} e^{-\tilde{u}_2 \theta_3} e^{-\tilde{u}_3 \theta_2} e^{-\tilde{u}_1 \pi/2} e^{-\tilde{u}_3 \theta_1} \hat{C}^{(0,6)} = \hat{c} \quad (4.64)$$

the right side of this equation, denoted by \hat{c} , becomes completely known. θ_5 and θ_6 can now be determined in terms of the parameterized joint variable.

i. Pre-multiply Eq. (4.64) by \bar{u}_1^T and pos-multiply by \bar{u}_3

$$\bar{u}_1^T e^{\tilde{u}_3 \theta_5} e^{-\tilde{u}_1 \pi/2} e^{\tilde{u}_3 \theta_6} \bar{u}_3 = \bar{u}_1^T \hat{c} \bar{u}_3 = c_{13} \quad (4.65)$$

$$-s\theta_5 = c_{13} \quad (4.66)$$

$$c\theta_5 = \sigma_5 \sqrt{1 - c_{13}^2} \quad ; \quad \sigma_5 = \pm 1 \quad (4.67)$$

$$\theta_5 = a \tan_2(-c_{13}, \sigma_5 \sqrt{1 - c_{13}^2}) \quad (4.68)$$

ii. Pre-multiply Eq. (4.64) by \bar{u}_1^T and pos-multiply by \bar{u}_2

$$\bar{u}_1^T e^{\tilde{u}_3 \theta_5} e^{-\tilde{u}_1 \pi/2} e^{\tilde{u}_3 \theta_6} \bar{u}_2 = \bar{u}_1^T \hat{c} \bar{u}_2 = c_{12} \quad (4.69)$$

$$-c\theta_5 s\theta_6 = c_{12} \quad (4.70)$$

$$s\theta_6 = -\frac{c_{12}}{c\theta_5}$$

iii. Pre-multiply Eq. (4.64) by \bar{u}_1^T and pos-multiply by \bar{u}_1

$$\bar{u}_1^T e^{\tilde{u}_3 \theta_5} e^{-\tilde{u}_1 \pi/2} e^{\tilde{u}_3 \theta_6} \bar{u}_1 = \bar{u}_1^T \hat{c} \bar{u}_1 = c_{11} \quad (4.71)$$

$$c \theta_5 c \theta_6 = c_{11} \quad (4.72)$$

$$c \theta_6 = \frac{c_{11}}{c \theta_5} \quad (4.73)$$

If $c \theta_5 \neq 0$ then,

$$\theta_6 = a \tan_2(-c_{12}, c_{11}) \quad (4.74)$$

4.6 Verification of the Analysis

In order to verify the found equations, a graphical study has been performed. In this study, one of the first three joint variables is selected as desired while the others are increased regularly over a period. Then, these are used in the forward kinematics equations to compute the x, y and z components of R and F (f_l and f_r) points and the orientation matrix \hat{C} . Finally, R and \hat{C} are substituted into the inverse kinematics equations to obtain the joint variables. The graphs show that the derived equations are valid. The last two joint variables are not changed in all three sets since they are independent of the R point equation. However, in each set they are included to the graphs. The locations of the focal points f_l and f_r were given separately in Eqs. (4.15) and (4.20). In order to verify those equations, a constant set is defined consisting of known joint variable values and another graph has been formed.

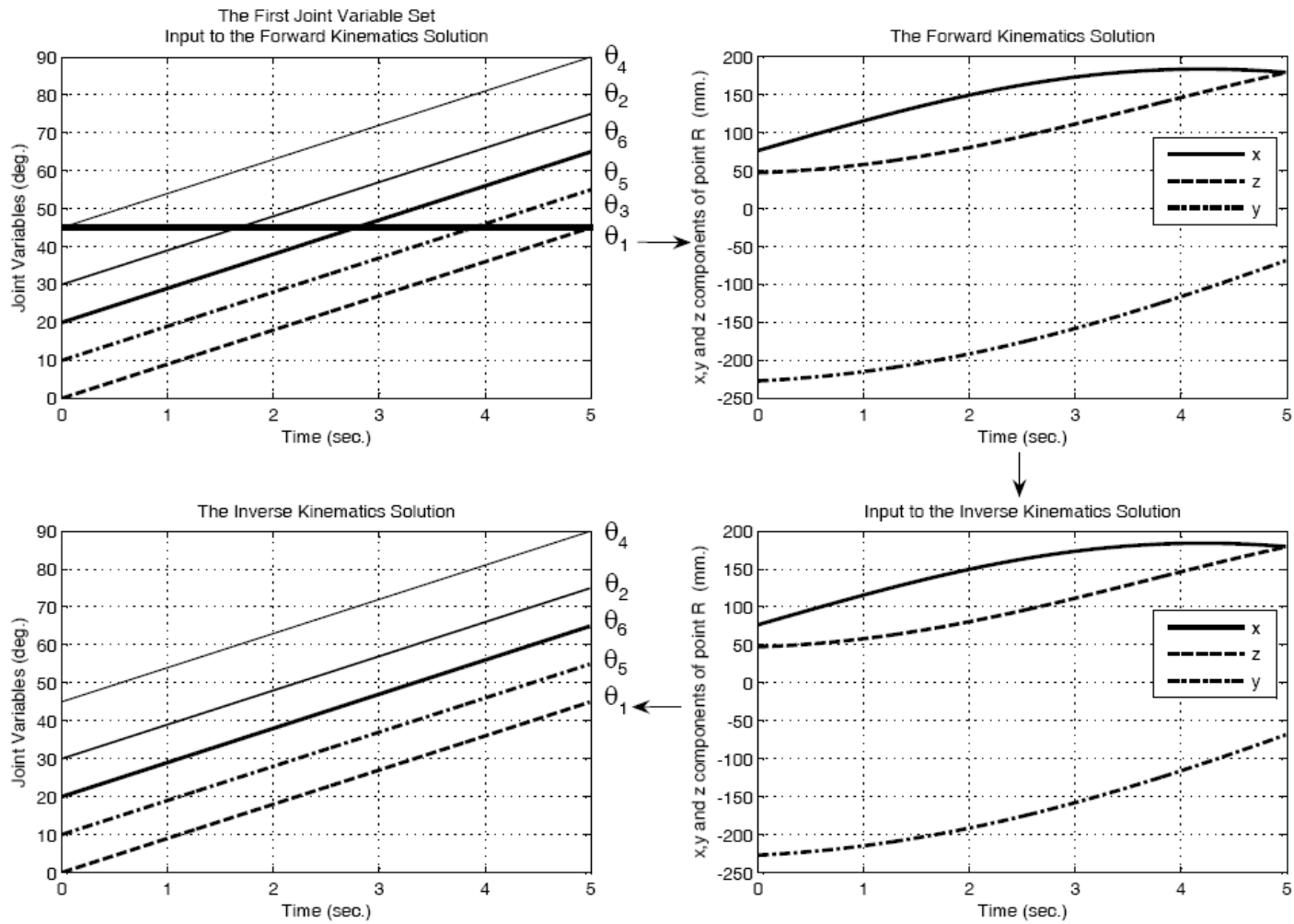


Figure 4.7 Verification of the Forward and Inverse Kinematics Solutions Based on θ_3 .

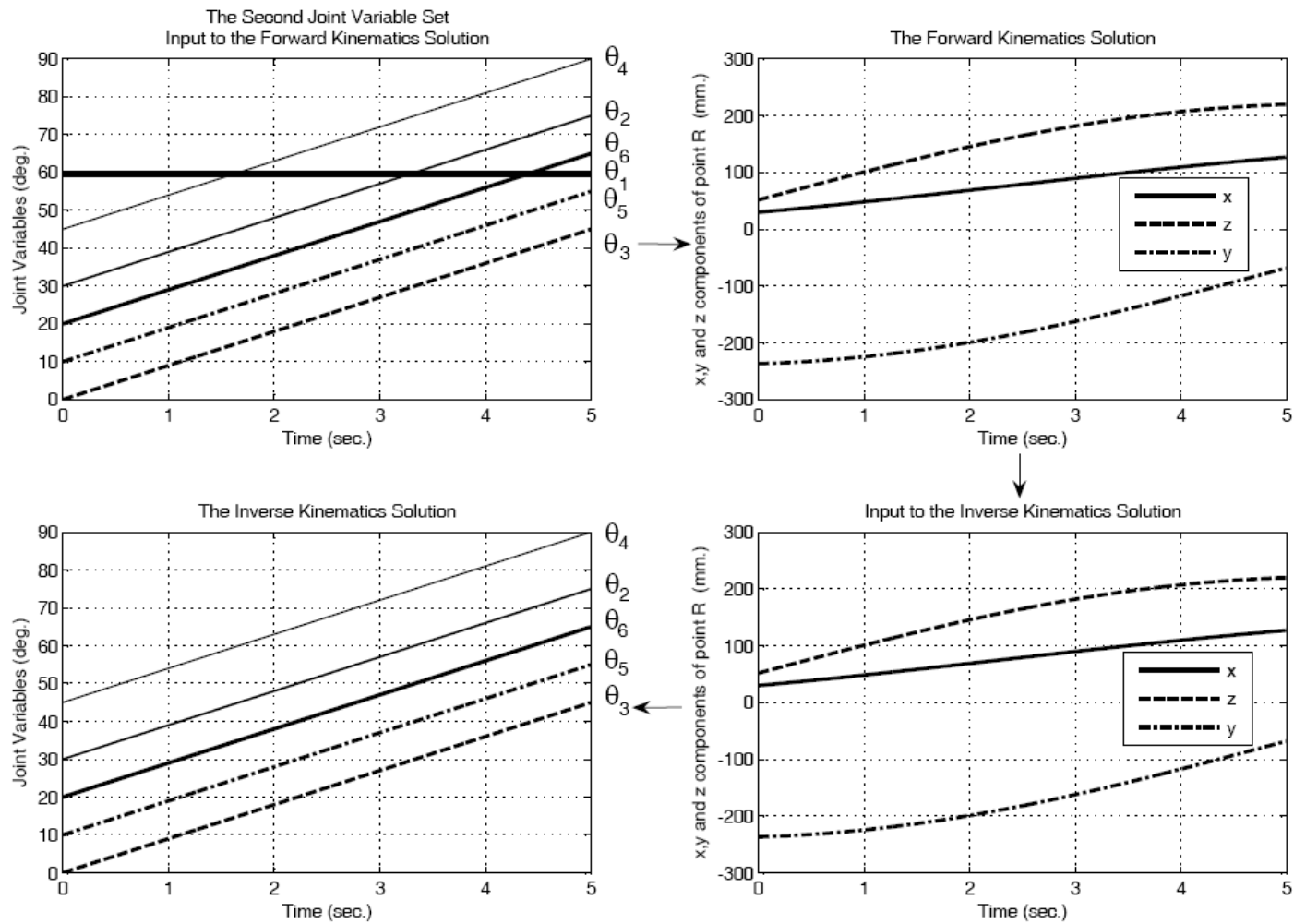


Figure 4.8 Verification of the Forward and Inverse Kinematics Solutions Based on θ_1 .

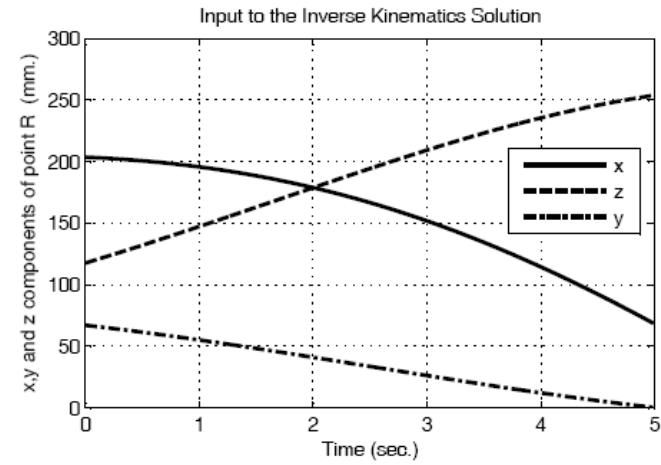
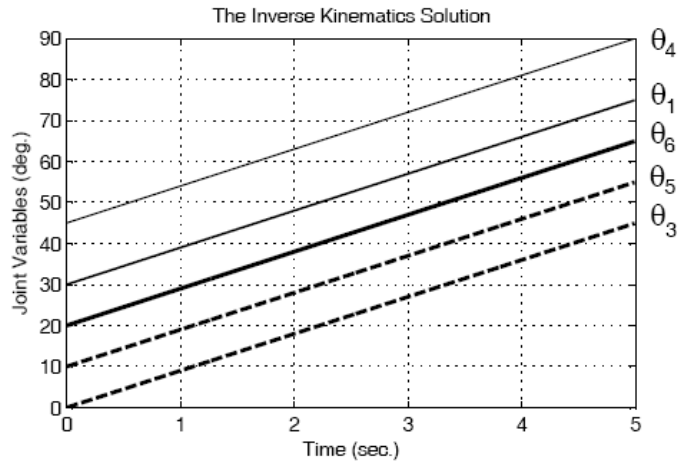
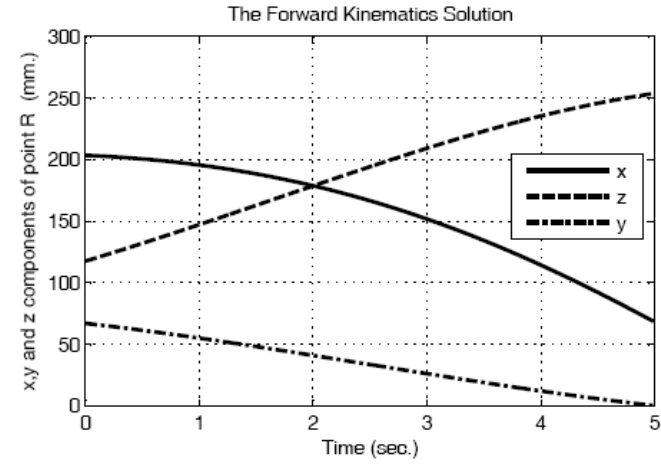
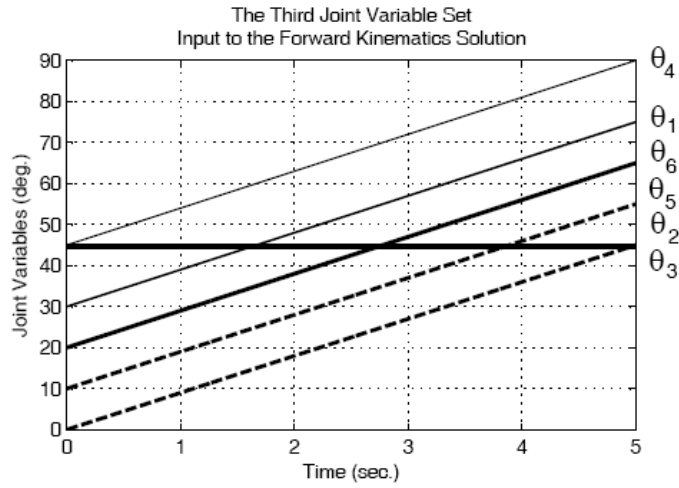


Figure 4.9 Verification of the Forward and Inverse Kinematics Solutions Based on θ_2 .

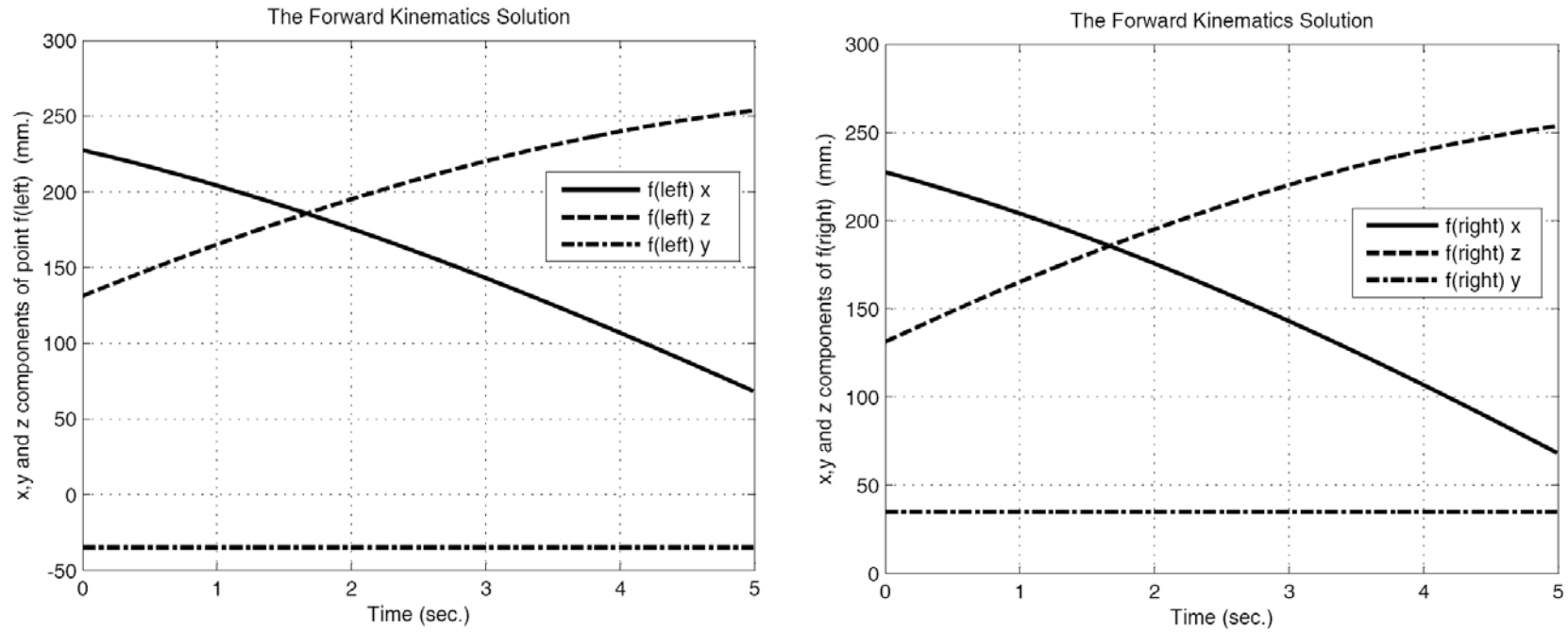


Figure 4.10 Verification of the Forward Kinematics Solutions of the Focal Points

$$\theta_1 = \left[\frac{7\pi}{6}, \frac{17\pi}{12} \right], \theta_2 = \theta_3 = \theta_4 = \frac{\pi}{2}.$$

4.7 Summary

In this study human head/neck is modeled using the general human modeling used in many developments from the field of kinematics. After deciding on the kinematic structure of the mechanism, D-H convention is used to define all the necessary parameters. For the forward and inverse kinematics problem, the method presented in [75] is facilitated. It has been seen that the method is quite convenient to apply to all of the manipulators. Since the last three joint axes do not intersect there is no closed form solution to the inverse kinematics problem. A semi analytical approach is applied to find the joint variables. The simplest equation that is the one containing least number of joint variables is used to start solving the equations for the joint variables. In addition, the joint variables in the wrist point equations are taken as the parameterized joint variables successively, in order to take a deep look at the singularities.

CHAPTER 5

MECHANICAL CONFIGURATION

This chapter describes the mechanical system design of the humanoid robotic head. The mechanical parts of the robot are designed to have human friendly appearance and moveable angle range. Rapid Prototyping technique is selected to manufacture the majority of the mechanical parts.

5.1 Overall Design

The robotic head is designed with the major degrees of freedom of the human head and neck. Range of motion of each joint and the dynamic conditions were also taken into consideration. There are two different actuator types used in the mechanisms: DC Servo motors and RC Servo motors. The first three actuators are the first type and the remaining is the second type. The robot is mounted on a platform made by aluminum sigma profiles to simplify design and construction.

Manufacturing was a big problem for majority of the construction parts. Since human head has a complex structure, its parts cannot be obtained easily with regular geometric shapes. For this reason, using traditional manufacturing processes was not a good alternative. Hence, we preferred to use rapid prototyping as the main manufacturing technique to produce the structural parts. This eased the burden on design, by allowing us to come up with parts that are almost un-manufacturable with conventional methods. The process time in this method is considerably less than the time that passes to produce the same product with the traditional methods. The material used in this process is polyamide having very low density of 0.95 g/cm^3 (The material and mechanical properties of the material can be found in Appendix D). All aspects considered, the rapid prototyping is a very advantageous means of production. On the other hand, the flanges which are used to

attach the actuators to their housings, couplings connecting the motor shafts to the housings and counterweights are manufactured from metals to obtain robust connections. In configuring the mechanical specifications we have changed the mechanisms and the construction a few times. As a result of this iterative process we obtained the existing design. An overview of the developed robotic head is shown in Figure 5.1. Obviously, it cannot be claimed that the resultant design is the best one. It will have so many aspects to reconsider before reaching a certain level of dexterity and looking.

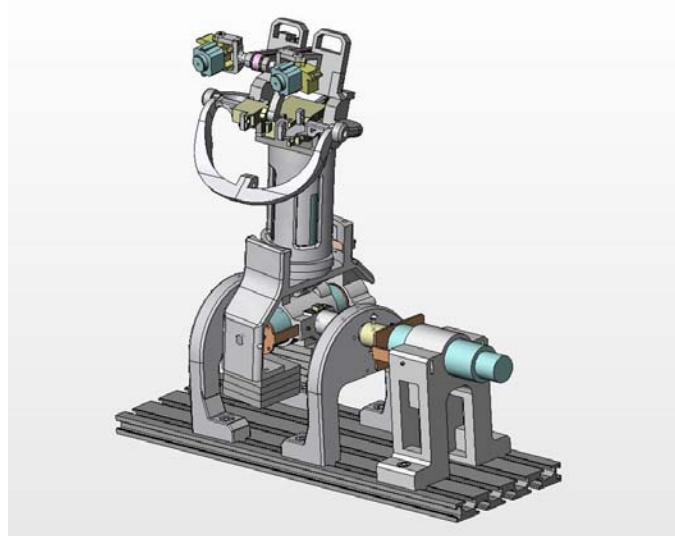


Figure 5.1 An External View of the CAD Model of the Robot.

The current design consists of 8 mechanical DOF in total. It has a 4-DOF neck mechanism. There are 3 DOF in the eye mechanism forming a vision system with two cameras placed like the eyeballs. The head also has a 1-DOF lower jaw mechanism. In what follows, each section of the mechanism will be introduced.

5.2 Joint Mechanisms

5.2.1 Neck

We implemented a 4-DOF mechanism neck according to the anthropomorphic model given in Chapter 4. The mechanism can perform bending the head forward and backward

(upper and lower pitch axes), turning the head left and right (yaw axis) and bending the head left and right (roll axis). With the developed model, bending the head forward and backward has two stages since there are two degrees of freedom for this movement. The upper pitch axis allows the head to further rotate both to look directly below and above.

The arrangement of the first degree of freedom is illustrated in Figure 5.2. The first motion is selected to lean the head as in nodding. It is directly driven by a DC Servo motor. The motor is placed in a housing to bring the shaft axis to a proper level and keep it fixed to the platform. The housing is assumed to be located to the left shoulder space of the trunk. The rotor of the motor is coupled to the next housing with a coupling. Two base parts with the spherical bearings are designed to support the rest of the mechanism. Each base part provides two types of embedded sensors. The micro limit switches are used to restrict the motion at both directions. Mechanical stops are also included into the design of the base parts. The optical sensors are located to align the mechanism (CNY70s are used as the optical sensor).

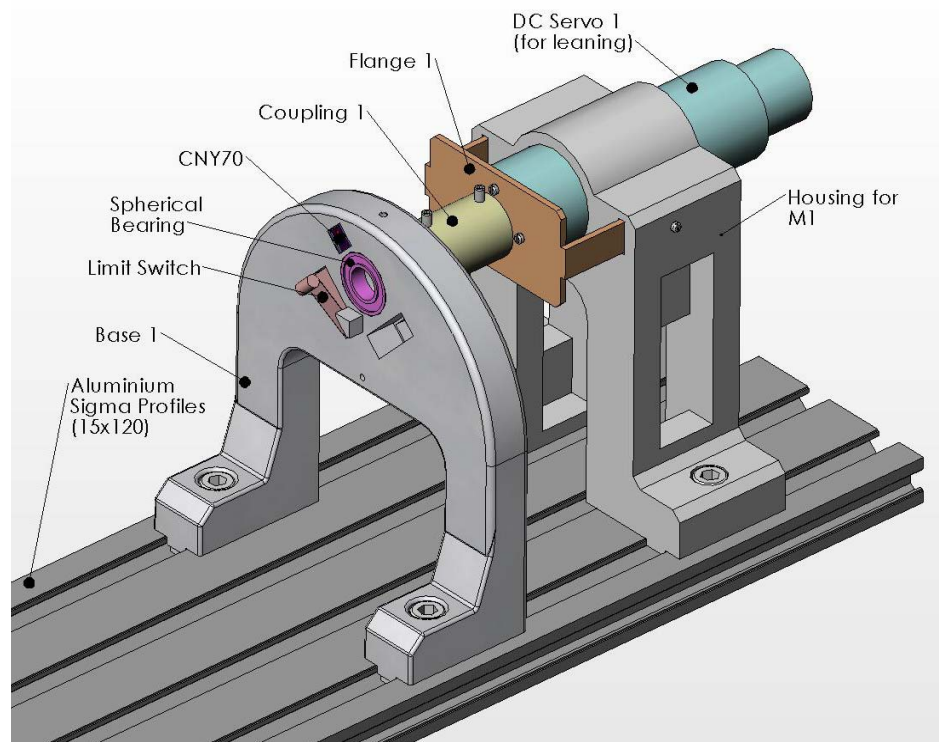


Figure 5.2 1st DOF of the Neck Mechanism.

The second motion is bending the head left and right. It is achieved by the housing shown in Figure 5.3. With this part, a universal joint is formed. The housing accommodates the sensors, the counterweights, a flange and a coupling as well as the DC Servo motor. The rotor of the motor is again coupled to the next housing with the second coupling part. At the back side of the motor, a cylindrical bearing is preferred to support the upper load. In this arrangement tactile buttons are used to limit the motion. A CNY70 is again placed for homing purpose.

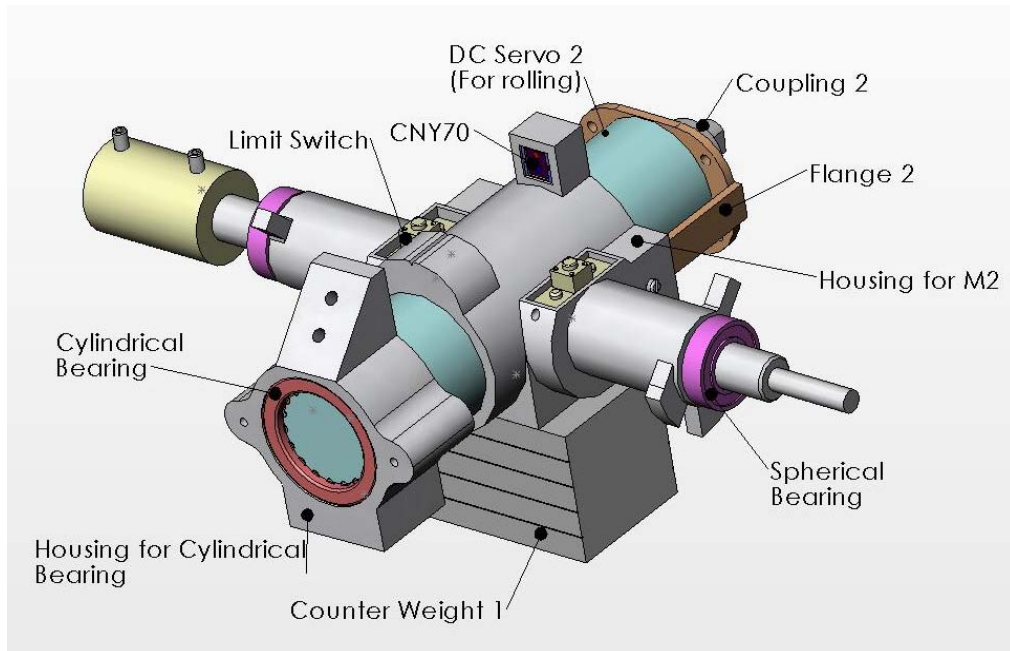


Figure 5.3 Assembly of the 2nd DOF of the Neck Mechanism

In the neck mechanism, the third DOF is selected as turning the head right and left. In designing the housing for the third DC Servo motor, balancing was a problematic issue. Like in the previous housings we had to consider the limitations and alignment together with the balancing. These complicated the part heavily. In Figure 5.4, housing can be seen. The rotary neck part is excluded from the left figure to further illustrate the inside. That part is supported by another spherical bearing as shown in the figure. By this way, the load is carried by the bearing not the actuator shaft.

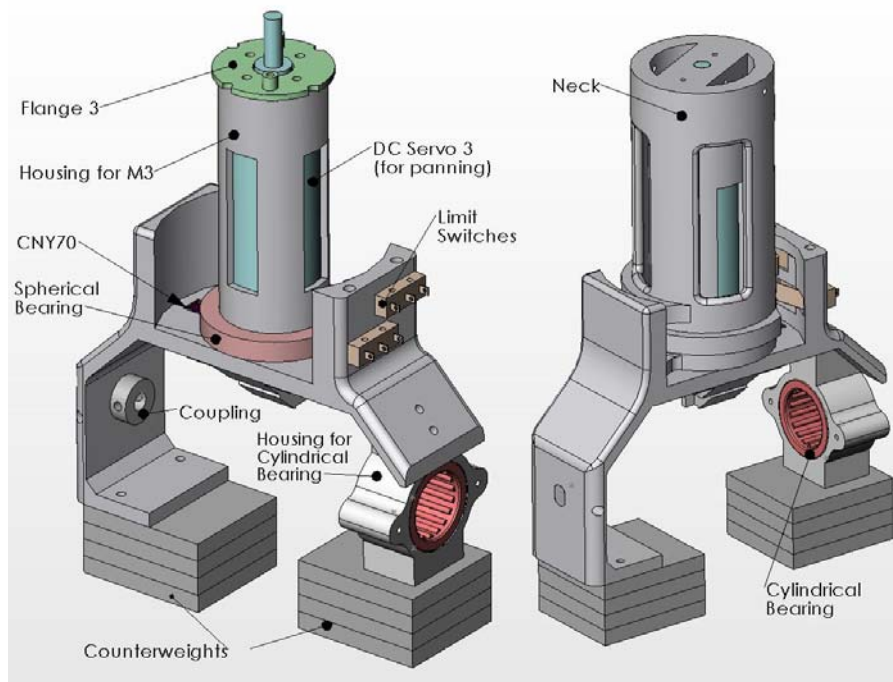


Figure 5.4 Assembly of the 3rd DOF of the Neck Mechanism

The last motion is actually completing the first one. It is again for bending the head forward and backward. Instead of a DC Servo, an RC Servo motor is preferred to drive the remaining head. The housing for the RC Servo motor is relatively simple since the motor is very small and has an easy geometry. Transmission is achieved by another coupling.

The assembled neck mechanism is illustrated in Figure 5.5. To summarize; bottom up, the first three degrees of freedom are actuated by DC servo motors. For the last degree of freedom a maxi RC servo is used. To limit each axis, tactile buttons and micro switches are embedded in the parts. Counterweights are placed in order to decrease torque requirement.

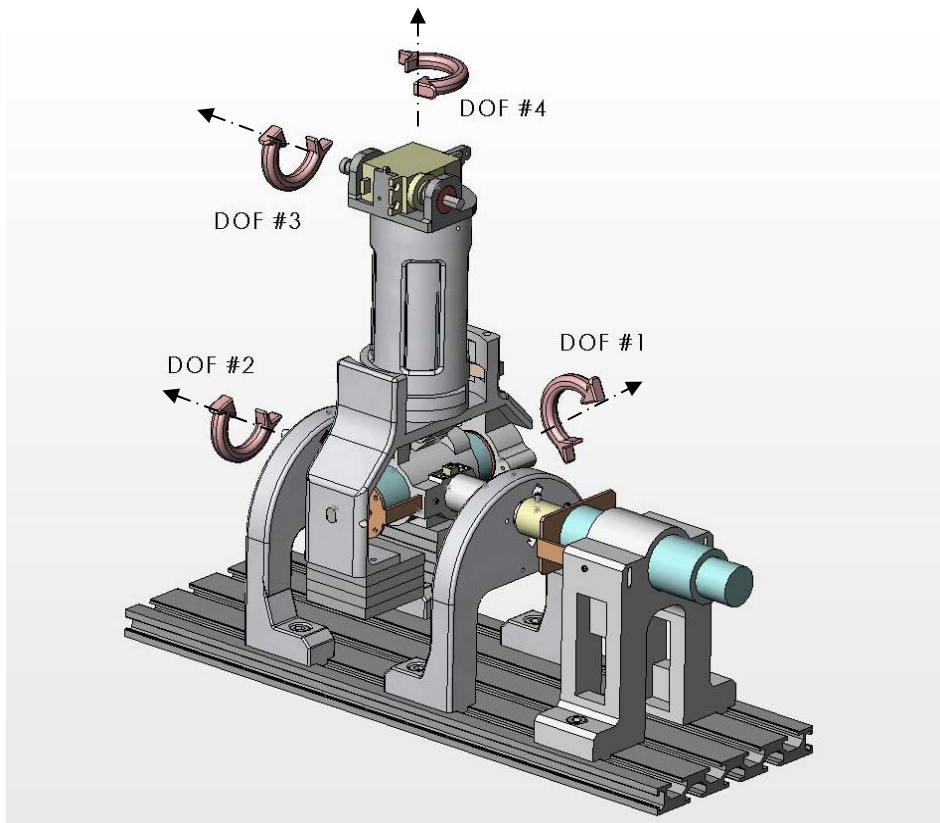


Figure 5.5 4-DOF Neck Joint Mechanism

5.2.2 Head

The head consists of two structural parts. It is divided into two parts for assembling purposes. The head is formed to accommodate the jaw and the eye mechanisms. It is designed in such a way that additional parts can easily be mounted. Its CAD model is seen in Figure 5.6.

5.2.3 Jaw

For the sake of simplicity, we developed the jaw mechanism as having one degree of freedom as in Kismet [11] and UCSD Head [12]. The lower jaw has been attached to the head structural parts with two spherical bearings. As shown in Figure 5.7, a mini RC Servo motor is used to move the jaw. We fix the motor to the jaw rather than attaching it to the head part. This proved the design to be more realistic when the mass distribution is concerned. Therefore, up-down motion of the jaw is achieved in a reverse manner.

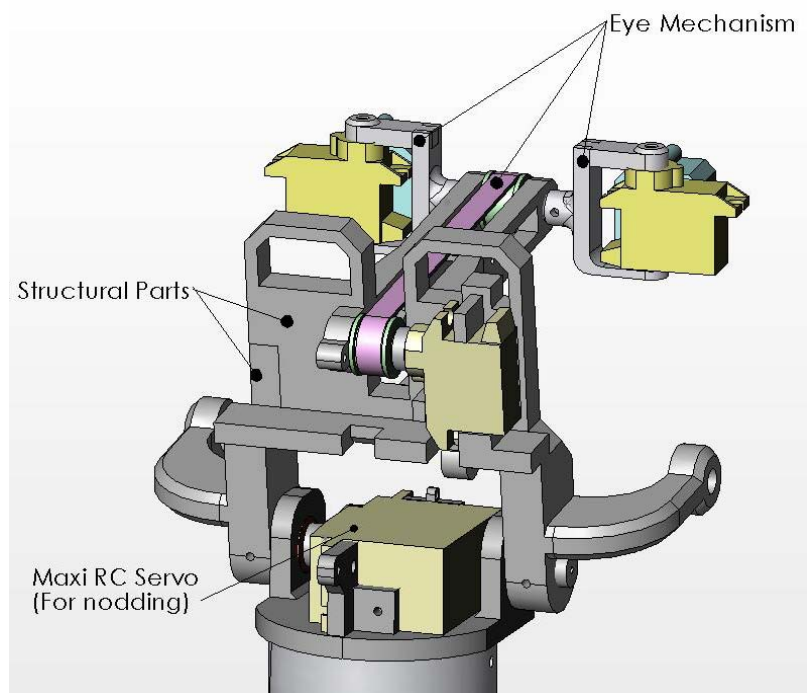


Figure 5.6 The Head Structure.

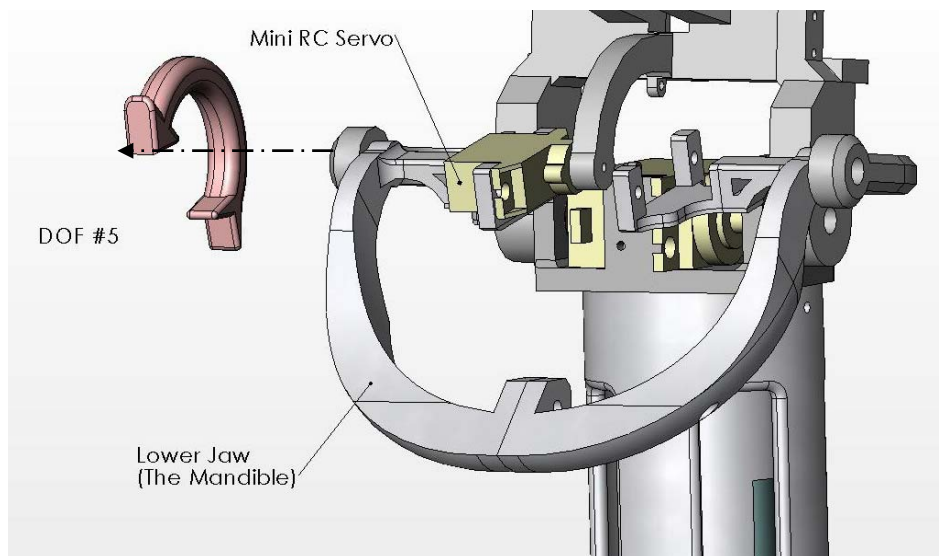


Figure 5.7 The 1-DOF Jaw Mechanism.

5.2.4 Eyes

The developed mechanism allows achieving the eye movements that the human anatomy permits. The robotic head with its 3 DOF eye mechanism can rotate the cameras in horizontal (yaw motion) and vertical (pitch motion).

We implemented the mechanism as shown in Figure 5.7. The cameras are directly attached to the mini RC servo motors to perform independent pan motion. The third servo is placed to the back of the head part and its motion is transferred by using a timing belt for tilting both eyes.

The velocity specifications are very important to satisfy. Each eye should move at the same speeds or higher than the given values. Therefore, the developed mechanisms are designed to be capable of high-speed motion.

The locations of the eyeballs (cameras) are significant, because the distance between two eyes affects both image processing and perception of the robot. The implemented mechanism allows changing the distance between the two eyeballs. By replacing the shaft connecting the two camera holder the distance can be adjusted.

5.3 Balancing

To achieve the static balance, the structural parts are designed symmetrically as much as possible to obtain a uniform load distribution. In the first design attempt, torsion springs are employed but the results were not good. Then the stages of the gearboxes of the first two motors were increased. Together with this change counterweights are used. They are manufactured in slice form from 6 mm. sheet metal by considering addition of loads to the head in the future. In this way, by increasing the number of slices, the static balance will be able to be achieved.

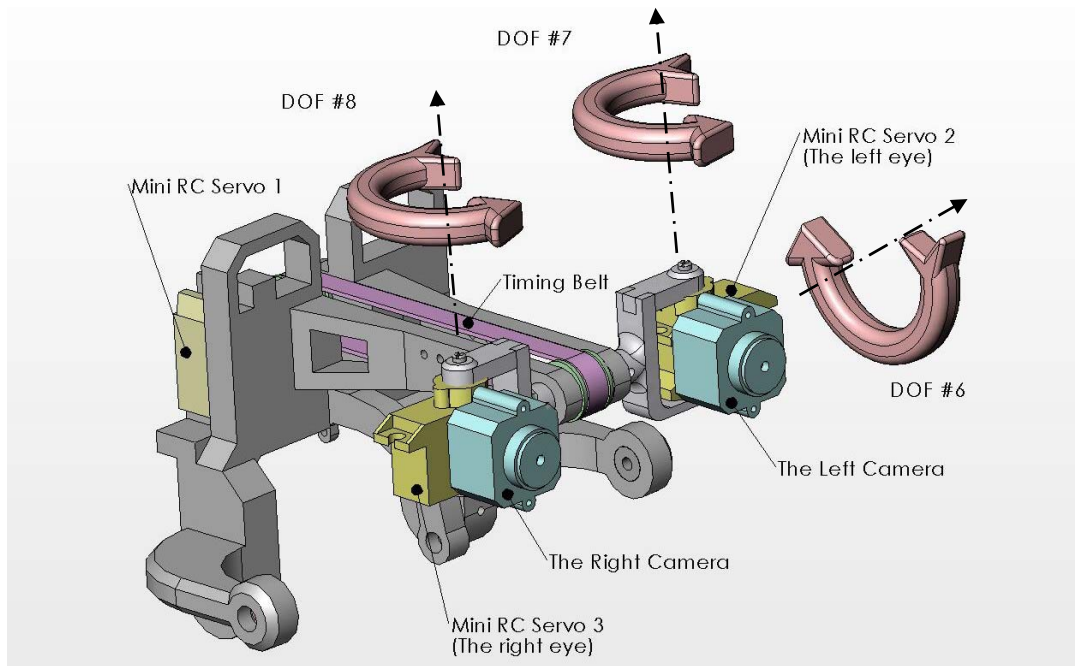


Figure 5.8 3-DOF Eye Mechanism with Two Cameras.

5.4 Summary

In this chapter, the developed mechanisms are presented in detail. Each joint is described with annotated CAD figures.

CHAPTER 6

ELECTRICAL DESIGN

In the design process of a humanoid, not only mechanical design but also electrical design plays an important role. Both mechanical and electrical configurations should be considered at the same time. That is why; we designed and manufactured a basic electronic system in order to test the performance of the developed robot. In this chapter, components of the system will be introduced. These components are designed so that the control system of the robot can be completed in the near future.

The basic electronic subsystems of the robot are shown in Figure 6.1. The custom circuit boards that are used in evaluating the robot's performance are summarized in Table 6.1.

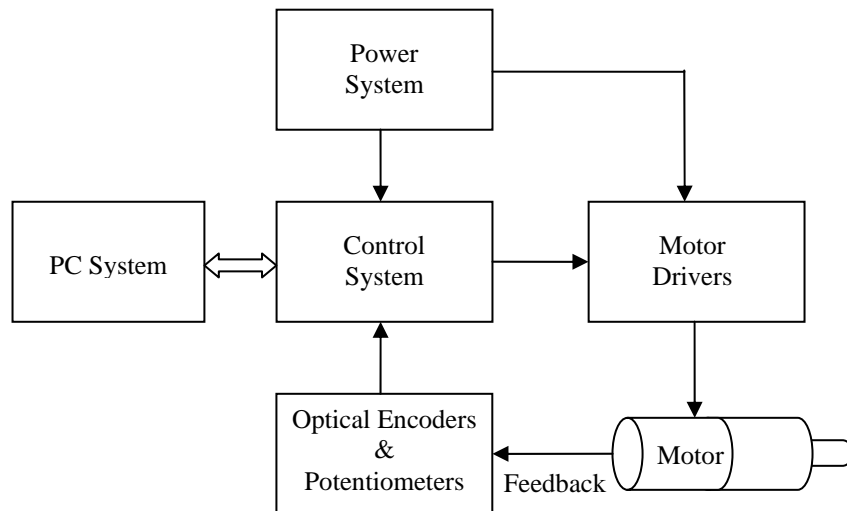


Figure 6.1 Block diagram of the basic electronic system.

Table 6.1 Circuit Boards on the Robot.

	Quantity	Voltage Input [V]
DC Motor Drivers	3	+12
RC Servo Drivers	5	+5
Signal Conditioning Board	1	+5
PIC Based Control Board	1	+12

6.1 Power Supply

All the electronics on the robot receive power from a 30 volt bench supply. In Figure 6.2, the power distribution system is shown.

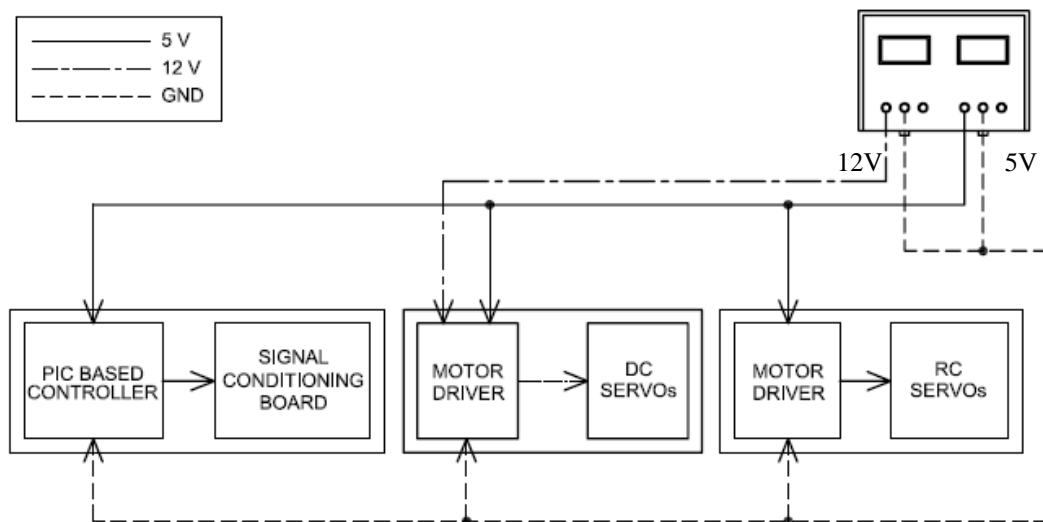


Figure 6.2 Power transfer system.

6.2 Robot Sensors

The robot is equipped with a total of 14 sensors. There are 3 rotary potentiometers that are used to measure positions of the first three joints. For this purpose, generic off-the-shelf analog potentiometers are used. Since each RC servo has its own potentiometers, there is no need to use additional position sensors for them. There are 5 reflective optical sensors that are used to align the joints. In addition, there exist 6 micro switches. They are located such that the joint motion can be ended when it reaches its one of the limits.

When a switch changes its state this generates an interrupt signal and the system rotates the joint back to its original home position.

For the DC servo motors, the original optical shaft encoders are removed and new encoders are manufactured as explained in [79]. The general application circuit for the optical sensor is given in Appendix B. These handmade encoders provide both the velocity and the direction of the movement. Therefore, there are two ways of finding the direction of a joint movement. Although it seems redundant, it gives additional flexibility to control the robot. In the controller design phase of the robot, the most suitable way will be selected to design a robust control system.

The rotary potentiometers are used after a modification. It is preferred to attach the rotary brush of the potentiometer directly to the motor shaft, instead of transferring the motion to the sensor by using a small gear couple. The assembly of the potentiometer and the modification are shown in Figure 6.3.

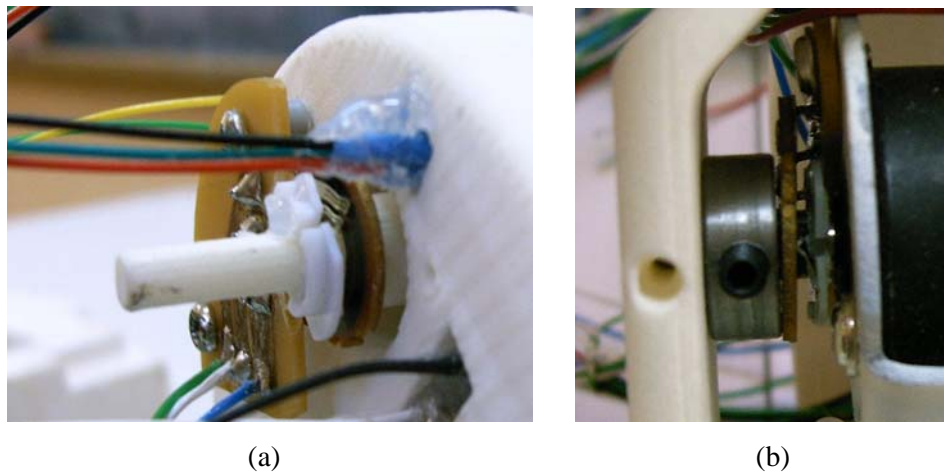


Figure 6.3 Assembly of the Modified Rotary Potentiometers, a)First axis, 2)Second axis.

6.3 Custom Circuit Boards

In the electrical design side of this study, a vast amount of experiment has been conducted. In order to understand the working principles of each of the electronic components and also to drive the actuators properly, we carried out these experiments.

During the work, we focused on creating a development infrastructure to reduce the time spent especially resulted from the repetition of the same steps. With this in mind, we selected Microchip's PIC (Peripheral Interface Controller) series as microcontrollers, which are tiny computers having a processor, memory and input-output ports, because of their important advantageous such as, low cost, easy to put into practice, easy to learn programming and so on.

PIC 16F877 is chosen among the series. It is considered as the most suitable microcontroller for our applications with its 33 input-output ports, large program memory and several internal peripheral features. After deciding on the microcontroller model, we designed and manufactured a board that can allow using all the features of the microcontroller. It became the main controller of the robot's electronic system. Its photograph is shown in Figure 6.4.



Figure 6.4 PIC Based Control Board.

After the main controller, motor drivers are manufactured. By using integrated circuit H bridge drivers we produced three driver modules for the DC servo motors. Each module has the required input output connectors to transfer the power and control signals. The feedback signals from the shaft encoder and potentiometer are also transmitted on this module. As for the RC servo motors, we also produced motor driver circuits however, they are not implemented yet. Since RC servo motors already have control systems within their packages we utilized those systems to drive the RC servos.

Finally, we created a signal conditioning board that includes the necessary circuitries to properly use the optical and mechanical switches. The board is an interface between the components placed on the robot and the controller. The schematics of the boards can be found in Appendix B.

6.4 Programming Using the Robot Head

We used PIC Basic Pro (PBP) compiler from microEngineering Labs, Inc. to program the PIC micro controllers [80]. It is a basic programming language. The compiler converts the program codes written in an editor to PICmicro micro controller's assembly language. The command set of PBP is very similar to BASIC programming language.

There are several PBP codes written to test the system. They are mainly codes that are taking the control signals from the PC system and converting them to driving signals.

At the PC side, we prefer using Microsoft's Visual Basic programming language. We created an interface to control the motors. The details of the communication protocol and instruction set are given in Appendix F.

CHAPTER 7

RESULTS AND CONCLUSION

In this chapter, we will give the results of the experiments that are conducted to evaluate the design whether it meets the design considerations. Finally, there will be a conclusion and discussion on the future work.

7.1 Results

The first objective of the study is to obtain a human-like robotic head structure. The structure should be designed so that a face can be implemented. In Figures 7.1 and 7.2, the overall design is shown. Since the structural parts are designed according to an anthropomorphic model the robot is similar to a human. Although the robot is very mechanical looking for the time being, its outside view still reminds a human head.

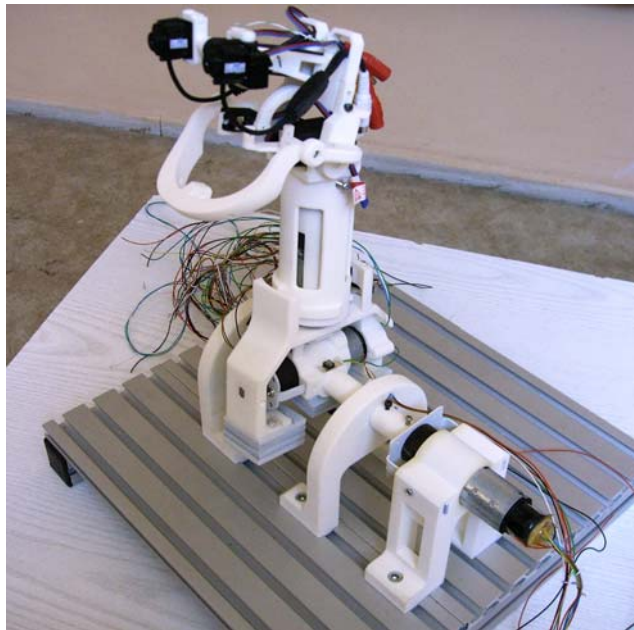


Figure 7.1 An Overview of the Developed Robotic Head.

In Table 7.1, the major head dimensions of a standard man and the manufactured robot are tabulated. The dimensions can also be followed from Figure 7.3. As can be noted, the first four major dimensions of the robotic head are slightly less than the specified values. This way is deliberately preferred in order not to exceed the specified dimensions when the outside of the structure is covered with a skin-like material. On the other hand, the distance between the two eyeballs is adjustable as mentioned in Chapter 5. It can be changed by only replacing the pin, connecting the holder parts, with a longer or shorter one.

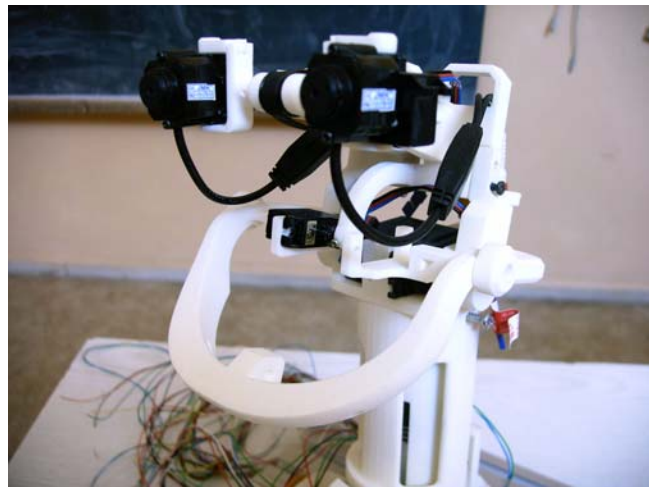


Figure 7.2 A Photo of the Designed Robotic Head.

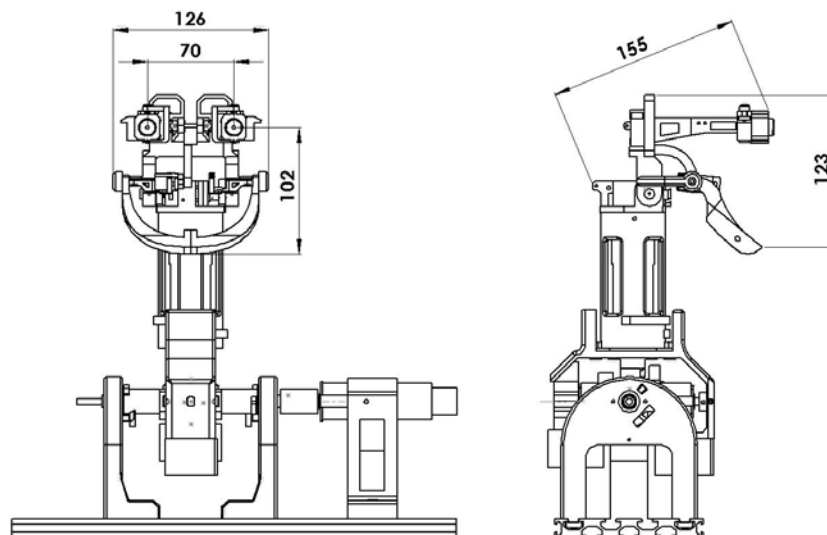


Figure 7.3 Major Dimensions of the Manufactured Robotic Head.

We have designed proper mechanisms in order to replace the anatomical joints with mechanical ones. In Table 7.2, the DOF configuration of the designed robotic head is given. It has the major degrees of freedom of the human head and neck.

Range of motion of each joint is similar to those of humans. The range of movement of the neck and eye's degrees of freedom are given in Table 7.3. There exists only one movement that is not exceeded among the all. It is the neck flexion which performed by the lower pitch joint. However this movement is in fact a combined motion obtained by moving the upper and lower pitch axes simultaneously. Therefore the design has a more flexible neck mechanism that can be exploited for further purposes.

Table 7.1 Major Head Dimensions with Results.

Dimensions	Anthropomorphic Measure	Standard Man [cm]	Developed Head [cm]
	Head Width	15.1	12.6
	Head Length	18.71	15.5
	Head Height	18.72	12.3
	Distance Between Eyes and Jaw	11.63	10.2
	Distance Between Eyes	6.12	7.0

Table 7.2 DOF Configuration.

Mechanical Degrees of Freedom	Part	Axis	Quantity	
	Neck	Upper Pitch		= 4 D.O.F.
		Lower Pitch		
		Yaw		
		Tilt		
	Jaw		= 1 D.O.F.	
Eyes	Yaw x 2		= 3 D.O.F.	
	Pitch			
Total			= 8 D.O.F.	

Table 7.3 Range of Movements of Each Joint.

Joint	Axis	Standard Man [deg]	Developed Head [deg]
Neck	Upper Pitch	±30	±35
	Lower Pitch	±45	±45
	Yaw	±40	±85
	Roll	±24	±38
Jaw		+30	+35
Eyes	Yaw	±25	±45
	Pitch	±20	±40

The developed robotic head weighs around 2.1 kg. The platform profiles, the first motor and its equipment and the two base parts are not included to this value by considering them as belonging to the torso. In Chapter 3, 4 kg is specified as the upper limit of the weight of the design. Having the measured weight, the robot satisfies this design criterion. It has been aimed to develop the lightest design by regarding the future additions to the head such as the ears, lips, eyebrows, eyelids, skin and so on. With this configuration, it is possible to add more features.

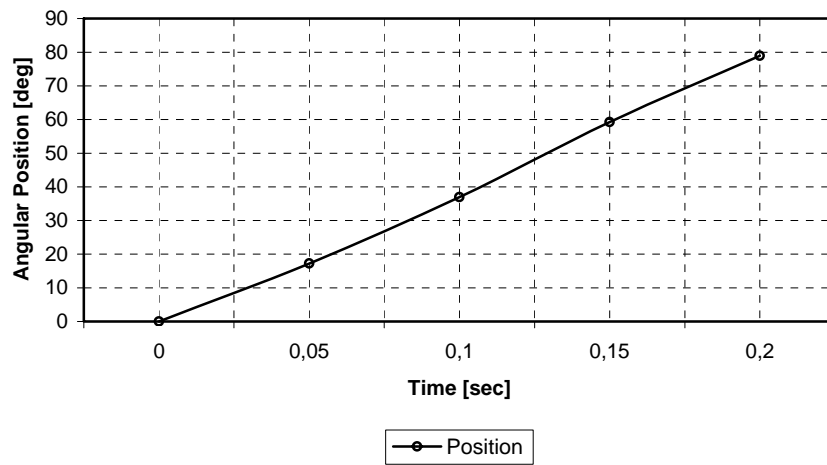
The actuators are the most important components of the robot. Selection of the actuators was, in fact, the first step in the design process. The procedure is done by following the anthropomorphic data and the kinematic model. After the design considerations, we preferred low cost off-the-shelf actuators by regarding our budget. One actuator was placed for each joint axis as planned. It has been achieved to realize human-like motion with the selected motors. The joint torque generated by each actuator is enough to support the mechanical structure. The motor selection calculations are provided in Appendix C together with the specifications of the motors.

The designed robotic head satisfies the joint velocities. We have used two methods to measure the angular velocities of each joint. In the first method, to measure the position of the motor shaft the attached potentiometers are used. Measurements are carried on over a period. Stored position values are then differentiated to obtain the joint velocity. In the second method, the durations of the joint movements are recorded using an external

camera. And then the movement amplitudes in each time interval which is found from the frame rate are evaluated. The results are given in Figure 7.4 and 7.5 for the right eye horizontal and vertical movements and for all the neck movements, respectively.

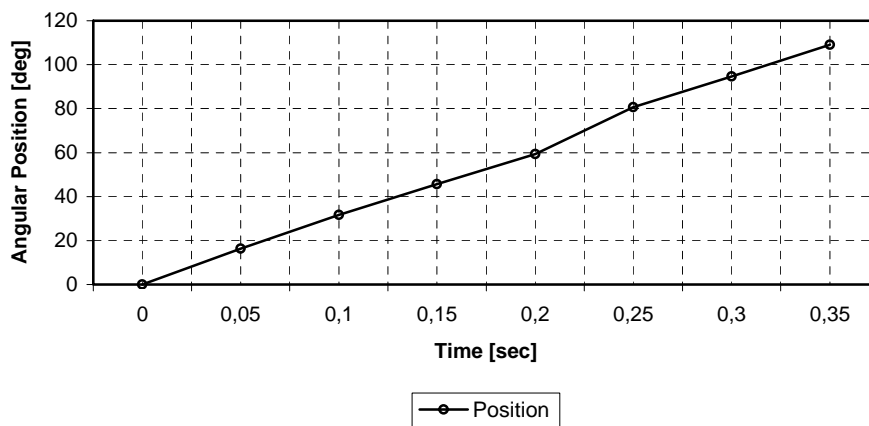
Peak velocities are reported to exceed 500 [deg/sec] for saccades. That is the designed robot can perform rapid saccade like eye movements. The aimed maximum speed for the neck movements is 100 [deg/sec]. As can be seen from Figure 7.5 a to d, up to 250 [deg/sec] can be achieved with the designed mechanisms for each neck axis.

Right Eye Yaw Motion



(a)

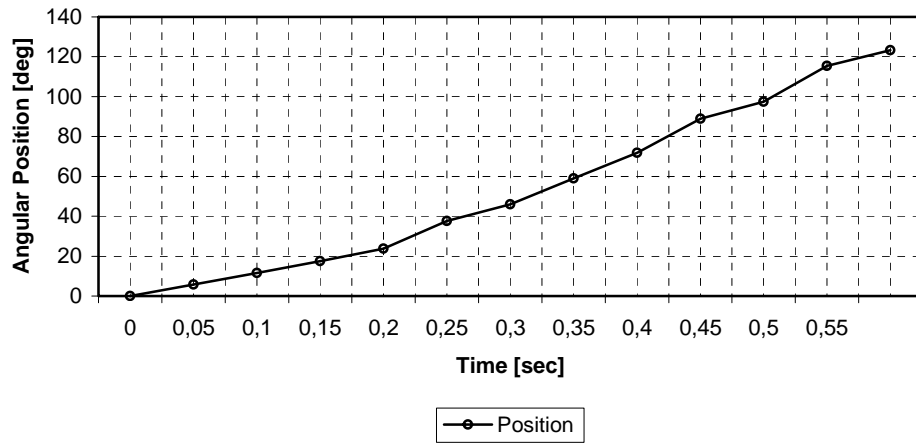
Both Eyes Tilt Motion



(b)

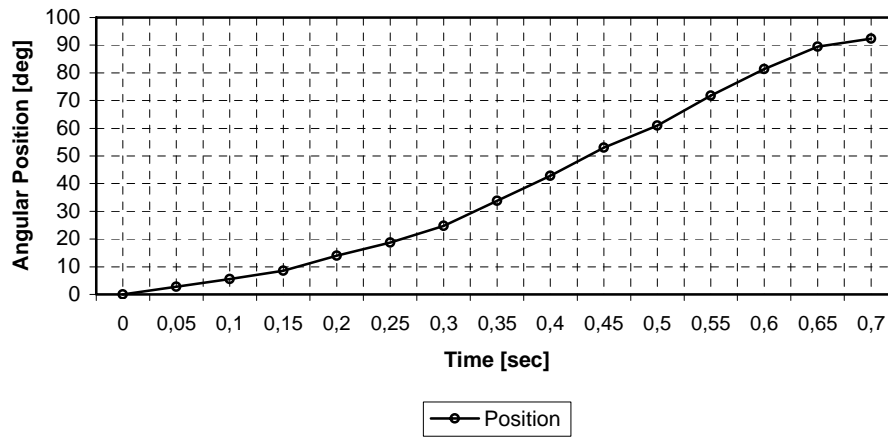
Figure 7.4 Average time elapsed vs. amplitude of motion for all movements of the right eye.

Neck Lower Pitch (Tilt Motion)



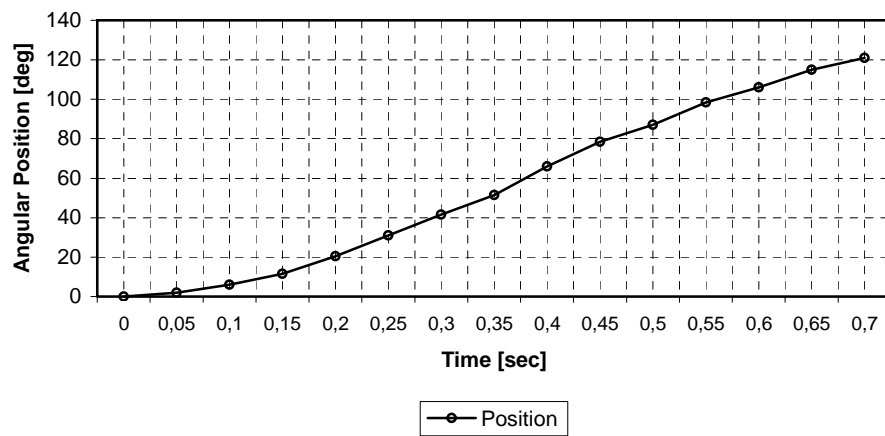
(a)

Neck Roll Motion



(b)

Neck Yaw Motion



(c)

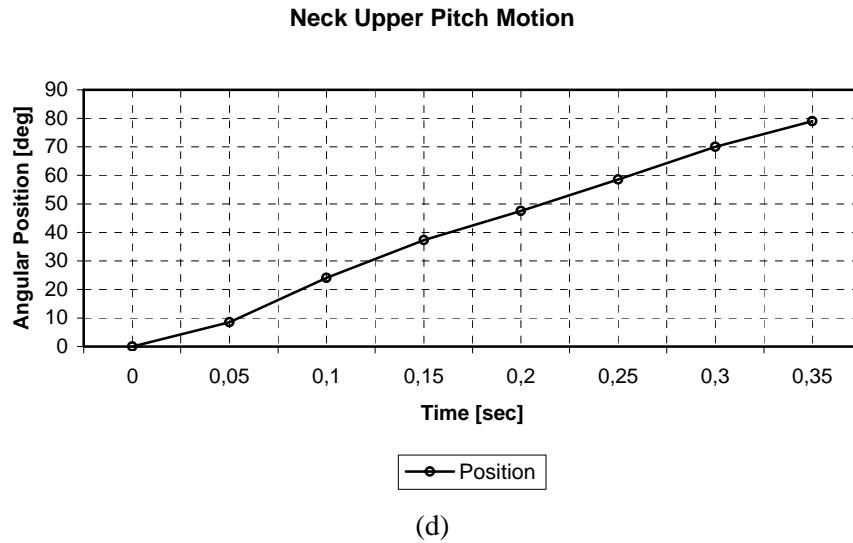


Figure 7.5 Average time elapsed vs. amplitude of motion for all movements of the neck. a and d are for vertical movements, b is for roll and finally c is for yaw movements.

7.2 Conclusion and Future Work

In this thesis study, we presented the design and manufacturing steps of our robotic head platform, which is to be used in human-robot interaction research. The current design has 8 mechanical degrees of freedom in total. The neck region consists of a 4-DOF mechanism. The eyes mechanism has 3 DOF forming a vision system with two cameras placed like the eyeballs. The head also has a 1-DOF lower jaw mechanism. In the construction of the robotic head, off-the-shelf components are preferred. The ranges of motion of each joint are similar to those of humans, hence kinematic constrains extracted from anthropomorphic data are achieved. The actuators are selected to satisfy dynamic constrains.

The rapid prototyping is used as the main manufacturing process. It allows designing complicated parts and even mechanisms as a whole. The process is faster than the traditional techniques.

The research and development of this humanoid robotic head will be an ongoing project. The immediate future work is to implement all of the underlying control and sensory systems. The sensory systems mainly include the vision system.

In the future, we are also planning to adopt a human-like face to the robot and investigate the response of people to different appearances. Tests will be conducted by increasing the number of features on the head face such as eyebrows, lips, ears etc. New degrees of freedom will be implemented at the end of these tests if necessary. The addition of a face will enable the robot to exhibit much mimics, and hence a richer set of emotions will be conveyed to people.

REFERENCES

- [1] Engelberger, J. F., "Robotics in Practice: Management and Application of Industrial Robots", Kluwer Academic Publishers Group, 1980.
- [2] Brooks, R. A., Breazeal, C., Marjanović, M., Scassellati, B., Williamson, M. M., "The Cog Project: Building a Humanoid Robot", MIT Artificial Intelligence Lab., 1999.
- [3] Wikipedia, The Free Encyclopedia, "Autism", <http://en.wikipedia.org/wiki/Autism>, Last Access Date: 10.08.2007.
- [4] Kozima, H., Nakagawa, C., Kawai, N., Kosugi, D., Yano, Y., "A Humanoid In Company With Children", 4th IEEE/RAS International Conference on Humanoid Robots, Santa Monica, LA, USA, 2004.
- [5] Pongas, D., Guenter, F., Gulgnard, A., Billard, A. G., "Development of A Miniature Pair of Eyes with Camera for the Humanoid Robot Robota", 4th IEEE/RAS International Conference on Humanoid Robots, Santa Monica, LA, USA, 2004.
- [6] National Institute of Information and Communications Technology, Infanoid Project, <http://www.infanoid.com/index-eng.html>, Last Access Date: 10.08.2007.
- [7] EPFL, Learning Algorithms and Systems Laboratory, "Robota Pictures and Videos", http://lasa.epfl.ch/research/toys/robota/photos_videos/index.php, Last Access Date: 10.08.2007.
- [8] Matarić, M. J., "Getting Humanoids to Move and Imitate", IEEE Intelligent Systems, July/August 2000.
- [9] CMU/Pitt, "Nursebot Project", <http://www.cs.cmu.edu/~nursebot/web/scope.html>, Last Access Date: 10.08.2007.
- [10] Pollack, M.E., Brown, L., Colbry, D., Orosz, C., Peintner, B., Ramakrishnan, S., Engberg, S., Matthews, J.T., Dunbar-Jacob, J., McCarthy, C.E., Thrun, S., Montemerlo, M., Pineau, J., Roy, N., "Pearl: A Mobile Assistant For Elderly", AAAI The Eighteenth National Conference on Artificial Intelligence, 2002.
- [11] Roy, N., Baltus, G., Fox, D., Gemperle, F., Goetz, J., Hirsch, T., Margaritis, D., Montemerlo, M., Pineau, J., Schulte, J., Thrun, S., "Towards Personal Service Robots for The Elderly", Workshop on Interactive Robotics and Entertainment (WIRE), 2000.
- [12] CMU/Pitt, "Nursebot Project", <http://www.cs.cmu.edu/~nursebot/web/images7.html>, Last Access Date: 10.08.2007.

- [13] Bischoff, R., “HERMES – A Humanoid Mobile Manipulator for Service Tasks”, International Conference on Field and Service Robots (FSR), Canberra, 1997.
- [14] Intelligent Robots Laboratory, “Humanoid Service Robot HERMES”, <http://www.unibw.de/robotics/robots/hermes>, Last Access Date: 10.08.2007.
- [15] Sakagami, Y., Watanebe, R., Aoyama, C., Matsunaga, S., Higaki, N., Fujimura, K., “The Intelligent ASIMO: System Overview and Integration”, Proceedings of the 2002 IEEE/RSJ International Conference on Intelligent Robots and Systems EPFL, Lausanne, Switzerland, 2002.
- [16] Hirai, K., Hirose, M., Haikawa, Y., Takenaka, T., “The Development of Honda Humanoid Robot”, Proceedings of the 1998 IEEE International Conference on Robotics and Automation, Leuven, Belgium, 1998.
- [17] Honda, Honda Worldwide, “ASIMO”, <http://world.honda.com/ASIMO/new/>, Last Access Date: 10.08.2007.
- [18] Kaneko, K., Kanehiro, F., Kajita, S., Yokoyama, K., Akachi, K., Kawasaki, T., Ota, S., Isozumi, T., “Design of Prototype Humanoid Robotics Platform for HRP”, Proceedings of the 2002 IEEE/RSJ International Conference on Intelligent Robots and Systems EPFL, Lausanne, Switzerland, 2002.
- [19] Diftler, M.A., Culbert, C. J., Ambrose, R.O., Platt, R., Bluethmann, W. J., “Evolution of the NASA/DARPA Robonaut Control System”, Proceedings of the 2003 IEEE International Conference on Robotics and Automation, Taipei, Taiwan, 2003.
- [20] NASA Johnson Space Center, “Robonaut”, <http://robonaut.jsc.nasa.gov/>, Last Access Date: 10.08.2007.
- [21] Kawada Industries, Inc., Humanoid Robot HRP-2 “Promet”, http://www.kawada.co.jp/global/ams/hrp_2.html, Last Access Date: 10.08.2007.
- [22] AIST: AIST Today 2003-No.8, “A Tele-Operated Humanoid Robot Drives a Backhoe in the Open Air!”, http://www.aist.go.jp/aist_e/aist_today/2003_08/hot_line/hot_line_19.html, Last Access Date: 10.08.2007.
- [23] Humanoid Robotics at USC_Humanoid Heads, MAVERic, http://www-humanoids.usc.edu/HH_summary.html, Last Access Date: 10.08.2007.
- [24] Vijakumar, S., Conradt, J., Shibata, T., Schaal, S., “Overt Visual Attention for a Humanoid Robot”, Proceedings of the 2001 IEEE/RSJ International Conference on Intelligent Robots and Systems, Hawaii, USA, 2001.
- [25] Heralic, A., “Design and Control of the Prototype Humanoid Robot HR-2”, Complex Adaptive Systems, Chalmers University of Technology, Sweden, <http://www.etek.chalmers.se/~almir/>, Last Access Date: 10.08.2007.

- [26] Nagakubo, A., Kuniyoshi, Y., Cheng, G., “Development of a High-Performance Upper-Body Humanoid System,” Proceedings of the 2000 IEEE/RSJ International Conference on Intelligent Robots and Systems, Takamatsu, Japan, 2000.
- [27] Robosapiens – “ETL Humanoid”, <http://robosapiens.mit.edu/etl.htm>, Last Access Date: 10.08.2007.
- [28] Park, W., Kim, J., Park, S., Oh, J., “Development of Humanoid Robot Platform KHR-2 (KAIST Humanoid Robot-2)”, 4th IEEE/RAS International Conference on Humanoid Robots, Santa Monica, LA, USA, 2004.
- [29] Han, J.D., Zeng, S.Q., Tham, K.Y., Badgero, M., Weng, J.Y., “DAV: A Humanoid Robot Platform for Autonomous Mental Development”, Proceedings of the 2nd International Conference on Development and Learning, Cambridge, Massachusetts USA, 2002.
- [30] Nishiwaki, K., Sugihara, T., Kagami, S., Kanehiro, F., Inaba, M., Inoue, H., “Design and Development of Research Platform for Perception-Action Integration in Humanoid Robot: H6”, Proceedings of the 2000 IEEE/RSJ International Conference on Intelligent Robots and Systems, Takamatsu, Japan, 2000.
- [31] JSK Laboratory, “Humanoid Robot H6 Homepage”, <http://www.jsk.t.u-tokyo.ac.jp/research/h6/>, Last Access Date: 10.08.2007.
- [32] UNECE United Nations Economic Commission for Europe, IFR Statistical Department, ECE/STAT/05/P03, Geneva, 11 Oct. 2005.
- [33] Wisse, M., “Three Additions to Passive Dynamic Walking: Actuation, An Upper Body, and 3D Stability”, 4th IEEE/RAS International Conference on Humanoid Robots, Santa Monica, LA, USA, 2004.
- [34] Hashimoto, S., Narita, S., Kasahara, H., Shirai, K., Kobayashi, T., Takanishi, A., Sugano, S., Yamaguchi, J., Sawada, H., Takanobu, H., Shibuya, K., Morita, T., Kurata, T., Onoe, N., Ouchi, K., Noguchi, T., Niwa, Y., Nagayama, S., Tabayashi, H., Matsui, I., Obata, M., Matsuzaki, H., Murasugi A., Kobayashi, T., Haruyama, S., Okada, T., Hidaki, Y., Taguchi, Y., Hoashi, K., Morikawa, E., Iwano, Y., Araki, D., Suzuki, J., Yokoyama, M., Dawa, I., Nishino, D., Inoue, S., Hirano, T., Soga, E., Gen, S., Yanada, T., Kato, K., Sakamoto, S., Ishii, Y., Matsuo, S., Yamamoto, Y., Sato, K., Hagiwara, T., Ueda, T., Honda, N., Hashimoto, K., Hanamoto, T., Kayaba, S., Kojima, T., Iwata, H., Kubodera, H., Matsuki, R., Nakajima, T., Nitto, K., Yamamoto, D., Kamizaki, Y., Nagaike, S., Kunitake, Y., Morita, S., “Humanoid Robots in Waseda University – Hadaly-2 and WABIAN”, Autonomous Robots, 12, 25-38, 2002.
- [35] Lopes, M., Beira, R., Praça, M., Santos-Victor, J., “An Anthropomorphic robot torso for imitation: design and experiments”, Proceedings of the 2004 IEEE/RSJ International Conference on Intelligent Robots and Systems, Sendai, Japan, 2004.
- [36] Adams, B., Breazeal, C., Brooks, R.A., Scassellati, B., “Humanoid Robots: A New Kind of Tool”, IEEE Intelligent Systems, July/August 2000.

- [37] Morita, T., Iwata, H., Sugano, S., “Development of Human Symbiotic Robot: WENDY”, Proceedings of the 1999 IEEE International Conference on Robotics and Automation, Detroit, USA, 1999.
- [38] Weiss K., Woern, H., “Development of a Modular Anthropomorphic Robot Hand Using Servo Hydraulic Actuators”, 4th IEEE/RAS International Conference on Humanoid Robots, Santa Monica, LA, USA, 2004.
- [39] Bhattacharya, S., “New robot face smiles and sneers”, <http://www.newscientist.com/article.ns?id=dn3398>, Last Access Date: 10.08.2007.
- [40] Fong, T., Nourbakhsh, I., Dautenhahn, K., “A Survey of Socially Interactive Robots: Concepts, Design, and Applications”, Technical Report CMU-RI-TR-02-29, 2002.
- [41] DiSalvo, C.F., Gemperle, F., Forlizzi, J., Kiesler, S., “All Robots Are Not Created Equal: The Design and Perception of Humanoid Robot Heads”, Human Computer Interaction Institute and School of Design, Carnegie Mellon University, 2002.
- [42] Bischoff, R., Graefe, V., “Dependable Multimodal Communication and Interaction with Robotic Assistants”, 11th IEEE International Workshop on Robot and Human Interactive Communication, Berlin, 2002.
- [43] Breazeal, C., Edsinger, A., Fitzpatrick, P., Scassellati, B., “Active Vision for Sociable Robots”, IEEE Transactions on Man, Cybernetics and Systems, Vol. 31, Issue.5, 443-453, 2002.
- [44] Oxford Advanced Learner’s Dictionary, Oxford University Press, 6th Ed., 2000.
- [45] Random House Webster’s Electronic Dictionary and Thesaurus.
- [46] Wikipedia, The Free Encyclopedia, “Humanoid Robot”, http://en.wikipedia.org/wiki/Humanoid_robot, Last Access Date: 10.08.2007.
- [47] INL Idaho National Laboratory, Adaptive Robotics, <http://www.inl.gov/adaptiverobotics/humanoidrobotics/index.shtml>, Last Access Date: 10.08.2007.
- [48] McNicol, T., “The rise of the machines”, <http://search.japantimes.co.jp/cgi-bin/fl20031125zg.html>, Last Access Date: 10.08.2007.
- [49] Wikipedia, The Free Encyclopedia, “Humanoid Robot”, http://en.wikipedia.org/wiki/Uncanny_Valley, Last Access Date: 10.08.2007.
- [50] AIST: AIST Today 2002-No.5, “Laboring Humanoid Robot”, http://www.aist.go.jp/aist_e/aist_today/2002_05/hot_line/hot_line_21.html, Last Access Date: 10.08.2007.
- [51] MIT AI Laboratory, “COG Project Overview”, <http://www.ai.mit.edu/projects/humanoid-robotics-group/cog/hardware.html>, Last Access Date: 10.08.2007.

- [52] Jung, Y., Lee, K. M., “Effects of Physical Embodiment on Social Presence of Social Robots”, 7th Annual International Workshop on Presence, Valencia, Spain, 2004.
- [53] MIT AI Laboratory, “Kismet Overview”, <http://www.ai.mit.edu/projects/sociable/overview.html>, Last Access Date: 10.08.2007.
- [54] Kim, H., York, G., Burton, G., Murphy-Chutorian, E., Triesch, J., “Design of an anthropomorphic robot head for studying autonomous development and learning”, International Conference on Robotic and Automation (ICRA), New Orleans, LA, USA, 2004.
- [55] Kim, H., Lau, B. and Triesch, J., “Adaptive Object Tracking with an Anthropomorphic Robot Head”, International Conference on the Simulation of Adaptive Behaviors (SAB’04), Los Angeles, CA, USA, 2004.
- [56] Takanishi, A. Matsuno, T., Kato, I., “Development of an Anthropomorphic Head-Eye Robot with Two Eyes – Coordinated Head-Eye Motion and Pursuing Motion in the Depth Direction”, IEEE/RSJ International Conference on Intelligent Robots and Systems, Grenoble, France, 1997.
- [57] Waseda University, “Head Robot Team, Emotion Expression Humanoid”, <http://www.takanishi.mech.waseda.ac.jp/research/we/we-4rII/index.htm>, Last Access Date: 10.08.2007.
- [58] Kayış, B., “Türk Erkek Toplumunun Antropometrik Ölçülerinin Belirlenmesi”, TÜBİTAK, YAE, Ankara, 1989.
- [59] King, A.I., Viano, D.C., “Mechanics of the Head/Neck”, The Biomedical Engineering Handbook: Second Edition. Edited By Joseph D. Bronzino. Boca Raton: CRC Press LLC, 2000.
- [60] Purves, D., Augustine, G.J., Fitzpatrick, D., Katz, L. C., LaMantia, A.S., McNamara, J.O., “Neuroscience”, Sianuer Associates, 1997.
- [61] RHS Carpenter, “Eye Movements, Oculomotor System”, “<http://www.cai.cam.ac.uk/people/rhsc/oculo.html>”, Last Access Date: 10.08.2007.
- [62] Leigh, R.J., Zee, D.S., “The Neurology of Eye Movements”, Oxford University Press, 1999.
- [63] Optican, L.M., Zee, D.S., Chu, F.C., “Adaptive Response to Ocular Muscle Weakness in Human Pursuit and Saccadic Eye Movements”, Journal of Neurophysiology, Vol.54, No.1, July 1985.
- [64] Morningstar, M.W., Pettibon, B.R., Schlappi, H., Schlappi, M., Ireland, T.V., “Reflex control of the spine and posture: a review of the literature from a chiropractic perspective”, Chiropractic & Osteopathy, doi: 10.1186/1746-1340-13-16, 2005.

- [65] NASA, Man-Systems Integration Standards, <http://msis.jsc.nasa.gov/images/Section03/Image64.gif>, Last Access Date: 10.08.2007.
- [66] LoPresti, E. F., Brienza, D. M., Angelo, J., Gilbertson, L., “Neck Range of Motion and Use of Computer Head Controls”, Vol. 40 No. 3, Pages 199 — 212, May/June 2003.
- [67] Ergonomics and Design, “A Reference Guide”, Compiled and Written by S. Openshaw, E. T. Allsteel, Allsteel, www.allsteeloffice.com/ergo, Last Access Date: 21.07.2007.
- [68] Albers, A., Brudniok, S., Burger, W., “Design and Development Process of A Humanoid Robot Upper Body Through Experimentation”, Proceedings of the 2004 IEEE Conference on Humanoid Robots, Santa Monica, USA, 2004.
- [69] Thalmann, D., “Human Modeling and Animation”, http://vrlab.epfl.ch/Publications/pdf/Thalmann_EG_93.pdf, (13.08.2007).
- [70] Karolinska Institutet, “Anatomy and Histology”, <http://www.ama-assn.org/ama1/pub/upload/images/446/skeletonatlas.gif>, Last Access Date: 13.08.2007.
- [71] Monheit, G., Badler, N. I., “A kinematic Model of The Human Spine and Torso”, IEEE, Computer Graphics and Applications, Vol.11, Issue.2, 29-38, March 1991.
- [72] Farrell, K., “Kinematic Human Modeling and Simulation Using Optimization-Based Posture Prediction”, MSc. Thesis, the University of Iowa, December 2005.
- [73] Ahn, H. S., “A Virtual Model of the Human Cervical Spine for Physics-based Simulation and Applications”, Phd Dissertation, The University of Memphis, May 2005.
- [74] Peterson, B.W., Choi, H., Hain, T., Keshner, E., Peng, G.C.Y., “Dynamic and Kinematic Strategies for Head Movement Control”, Annals of the New York Academy of Sciences, Vol.942, 381-393, October 2001.
- [75] Balkan, T., Özgören, M.K., Arikan, M.A.S., Baykurt, H.M., “A method of inverse kinematic solution including singular and multiple configuration for a class of manipulators”, Mechanism and Machine Theory Vol.35, 1221-1237, 2000.
- [76] Özgören, M.K., “Application of Exponential Rotation Matrices to the Kinematic Analysis of Manipulators”, in Proceedings, Seventh World Congress on the Theory of Machines and Mechanisms, Seville, Spain, 1987.
- [77] Özgören, M.K., “Position and Velocity Related Singularity Analysis of Manipulators”, in Proceedings, Ninth World Congress on the Theory of Machines and Mechanisms, Milan, Italy, 1995.
- [78] Özgören, M.K., “Topological analysis of 6-joint serial manipulators and their inverse kinematics solutions”, Mechanism and Machine Theory Vol.37, 511-547, (2002).

- [79] Anderson D. P., "Home-Brew Shaft Encoders", http://www.geology.smu.edu/~dpa-www/robo/Encoder/pitt_html/encoders.html, Last Access Date: 23.07.2007
- [80] PicBasic Pro Compiler, microEngineering Labs, Inc., www.melabs.com, 2002, Last Access Date: 23.07.2007.
- [81] Madsen, J.D., PIC-Programmer 2 for PIC16C84 etc., <http://www.jdm.homepage.dk/newpics.htm>, Last Access Date: 23.07.2007.
- [82] Anderson, D.P., Home-Brew Shaft Encoders, Home-Brew Shaft Encoders for the Pittman GM8712 Gearhead Motor, http://www.geology.smu.edu/~dpa-www/robo/Encoder/pitt_html/encoders.html, Last Access Date: 23.07.2007.

APPENDIX A

TECHNICAL DRAWINGS

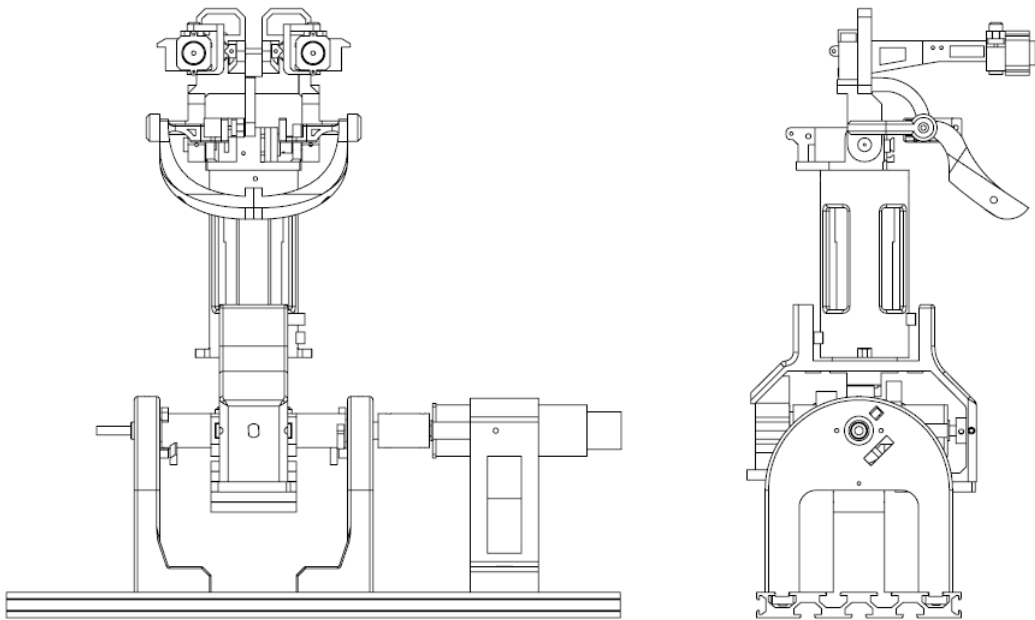


Figure A.1 The Front and Left Side Views of The Assembly

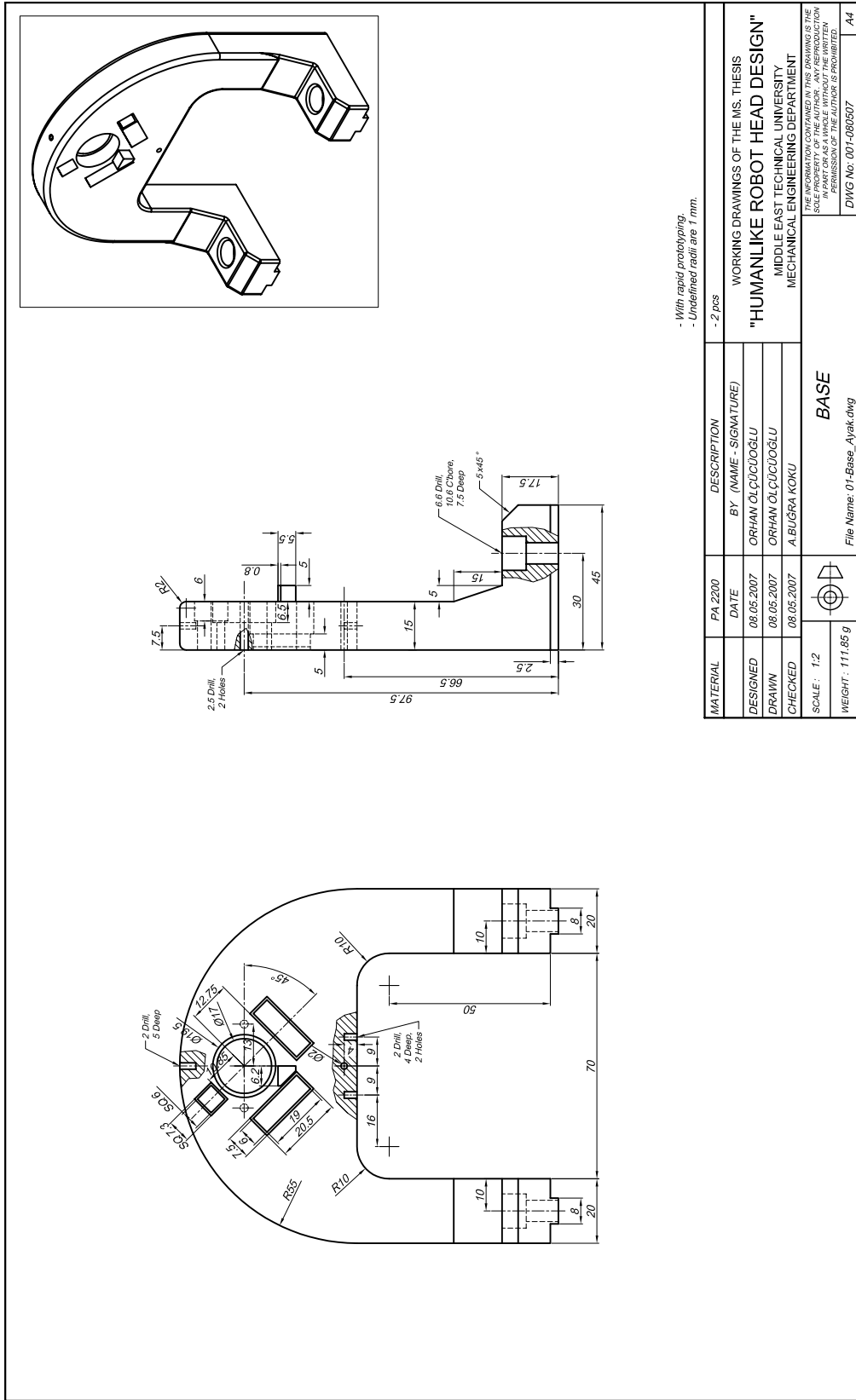


Figure A.2 Technical Drawing of Base

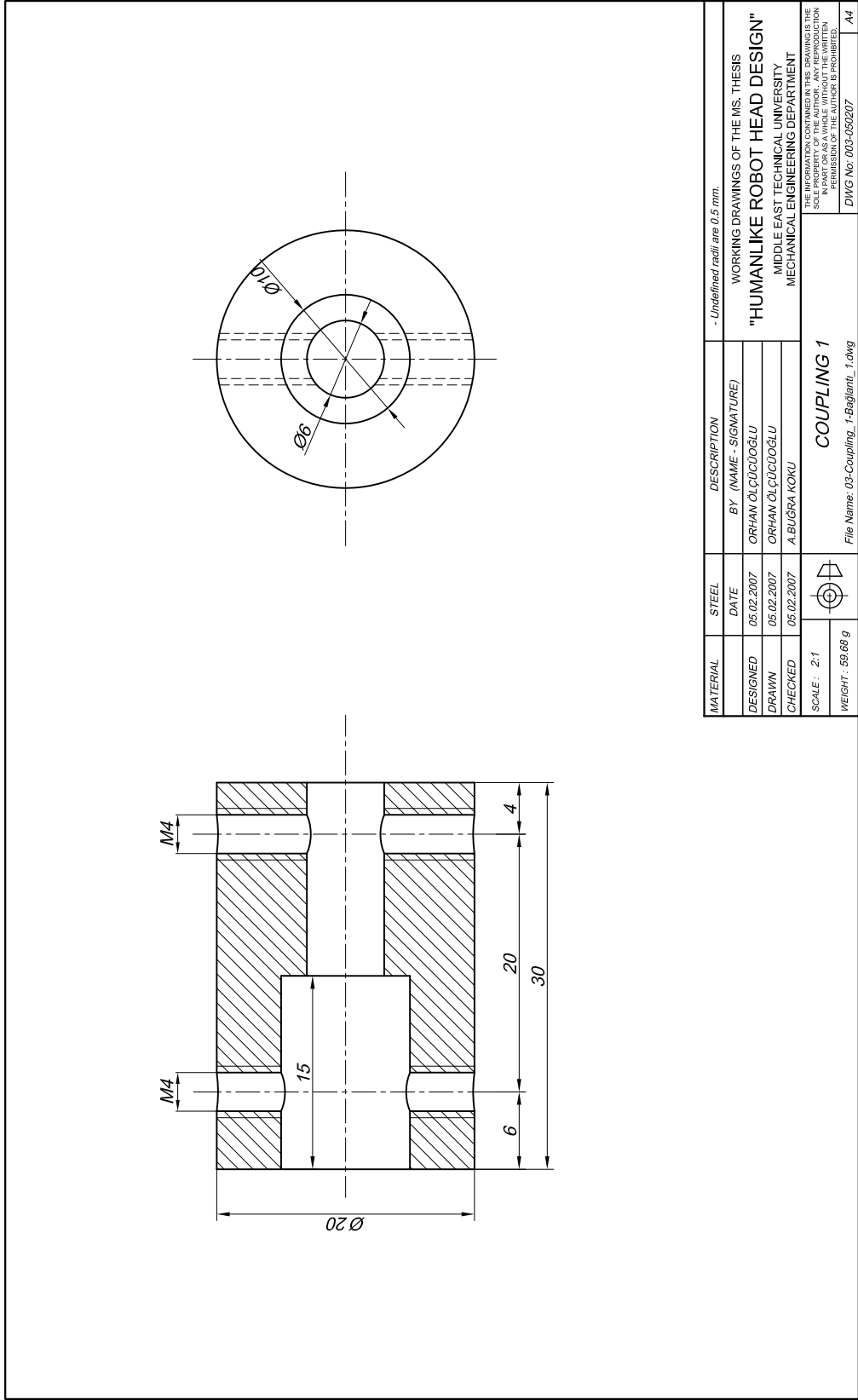


Figure A.4 Technical Drawing of Coupling 1

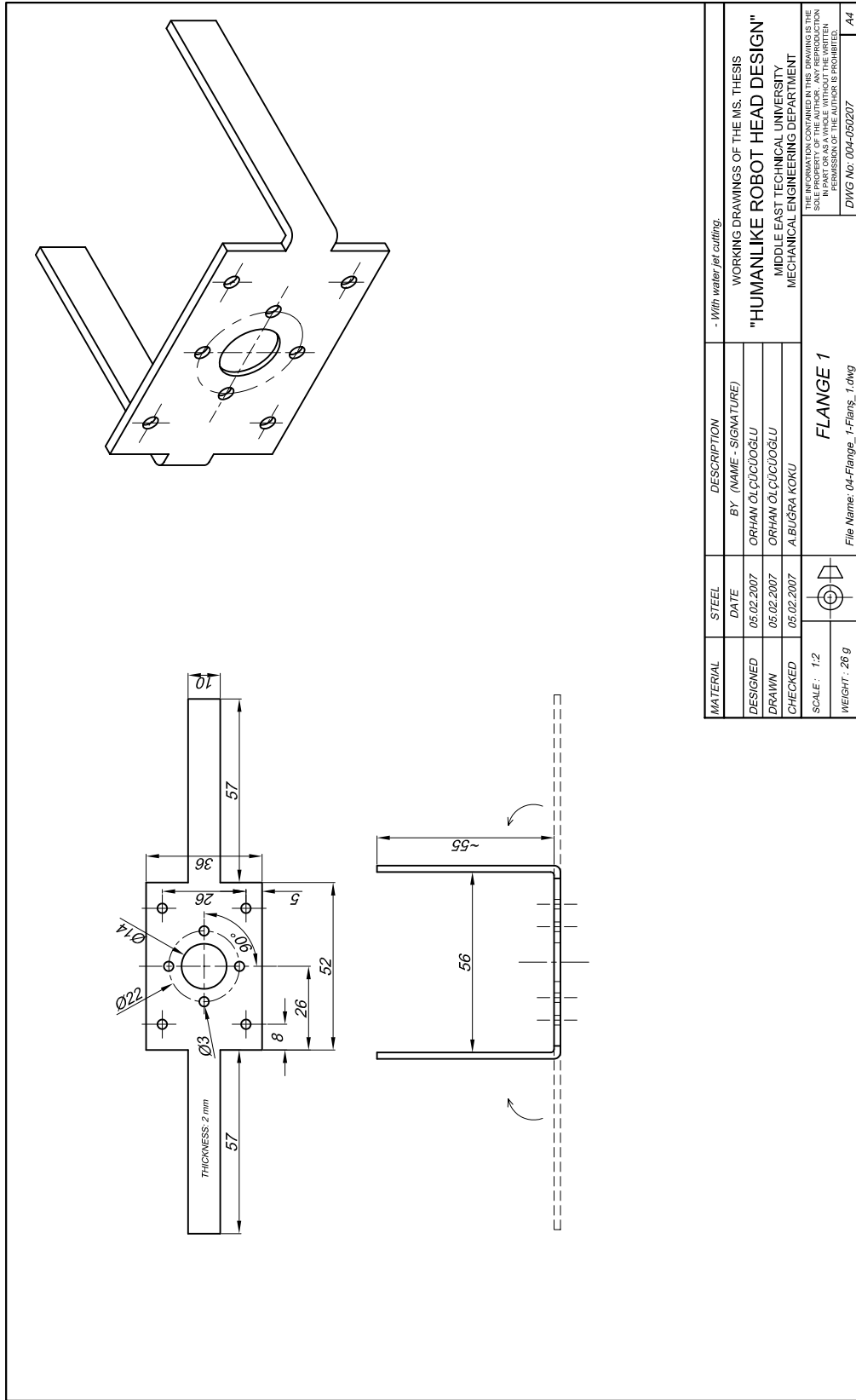


Figure A.5 Technical Drawing of Flange 1

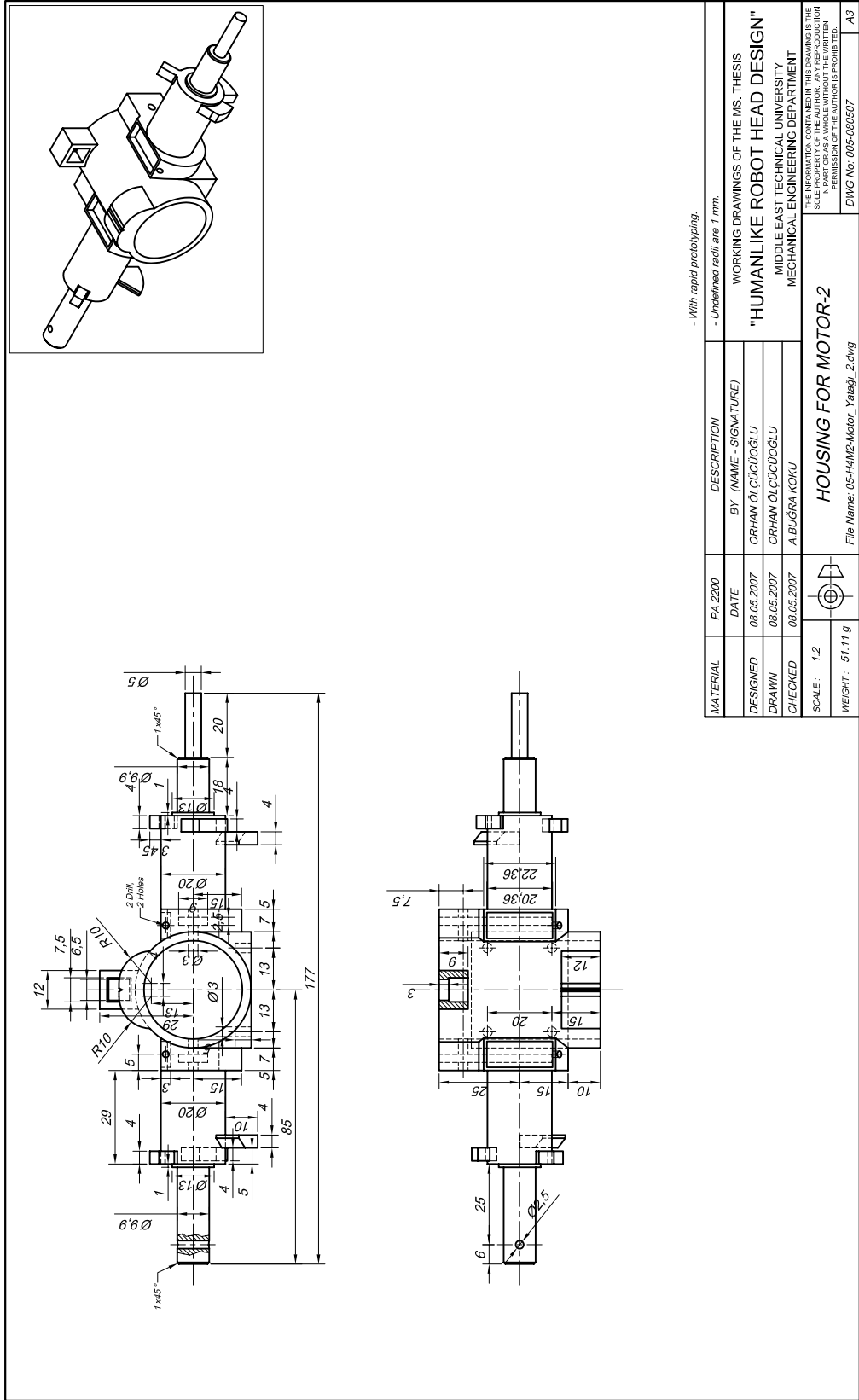


Figure A.6 Technical Drawing of H4M2

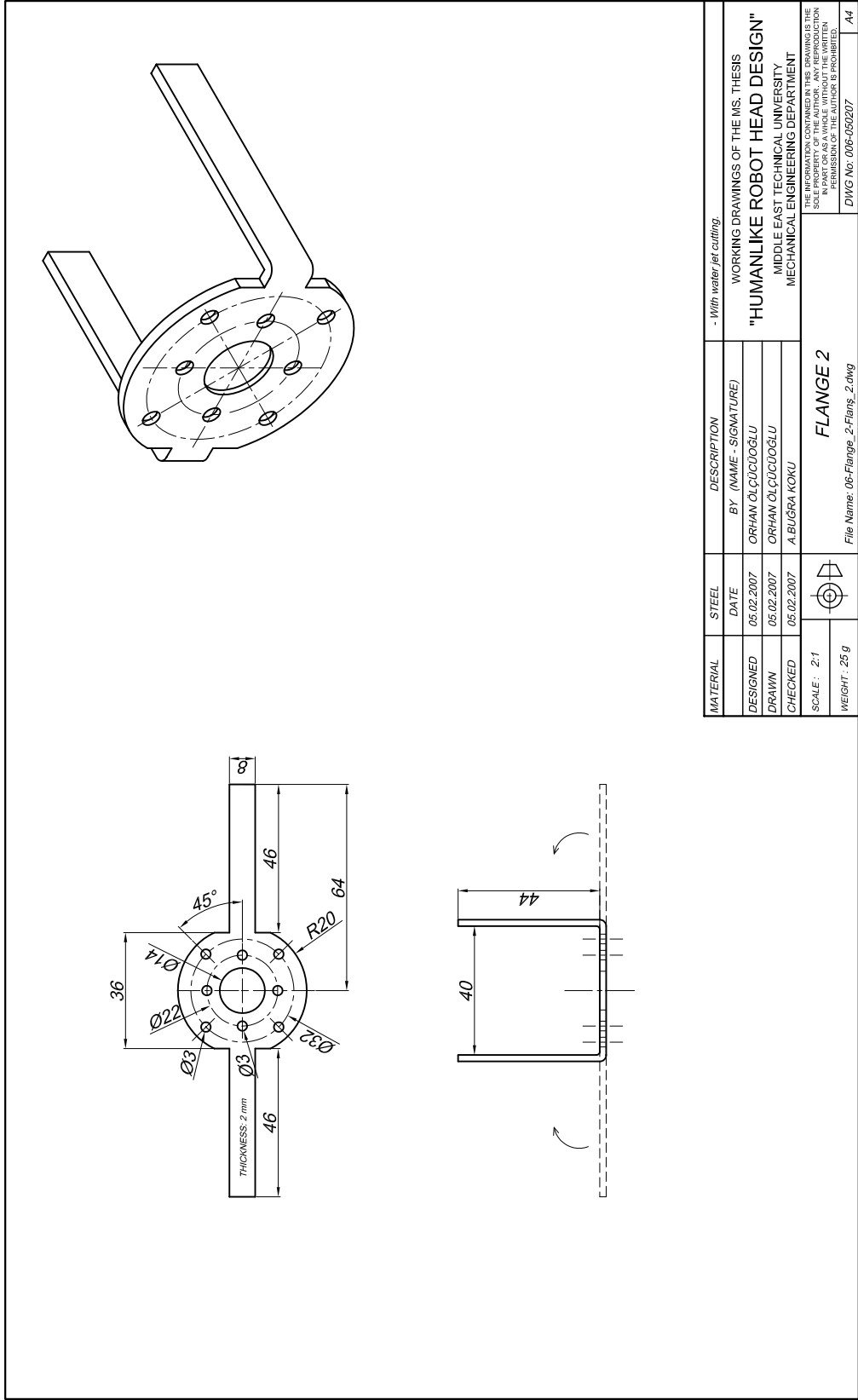


Figure A.7 Technical Drawing of Flange 2

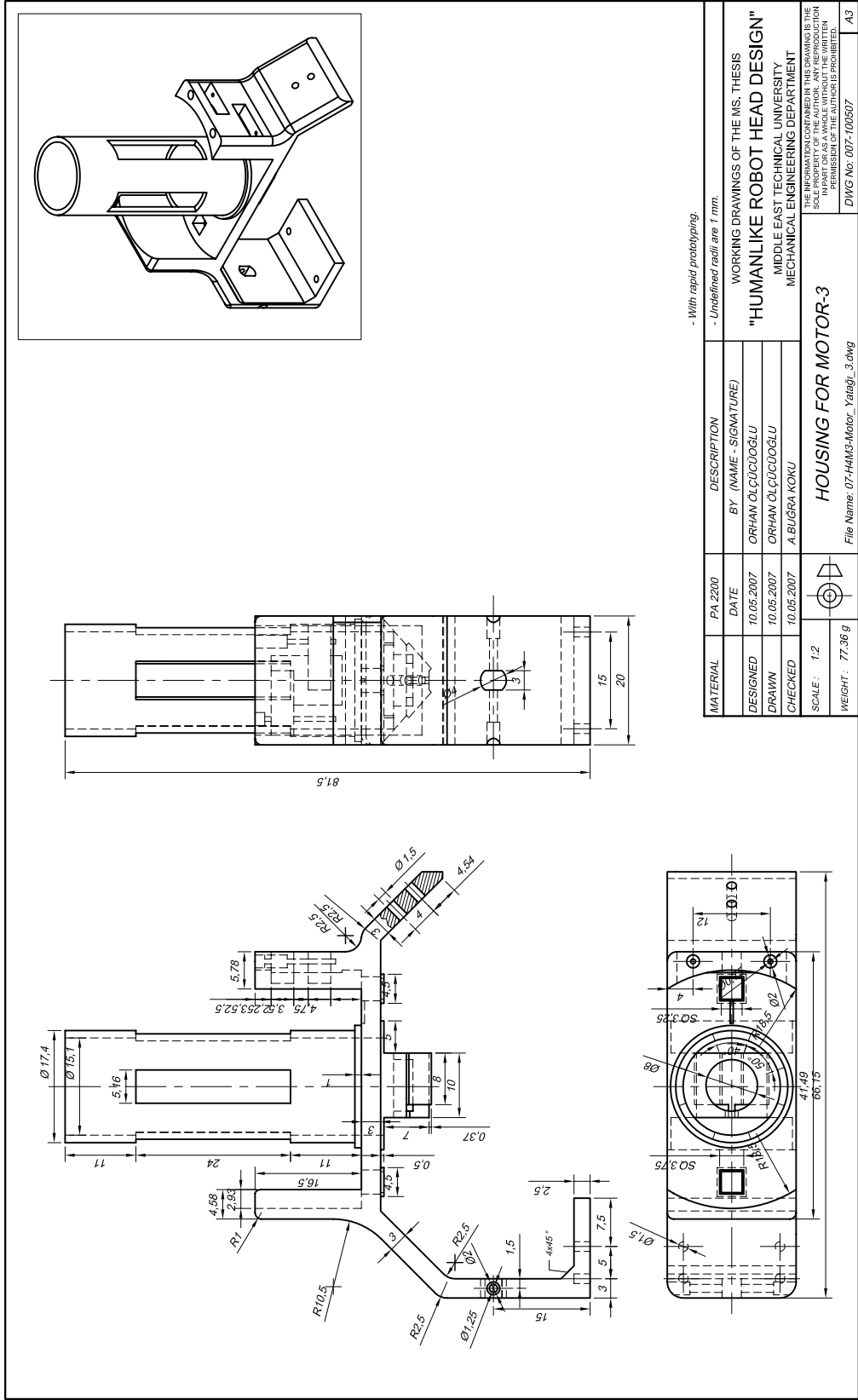


Figure A.8 Technical Drawing of H4M3

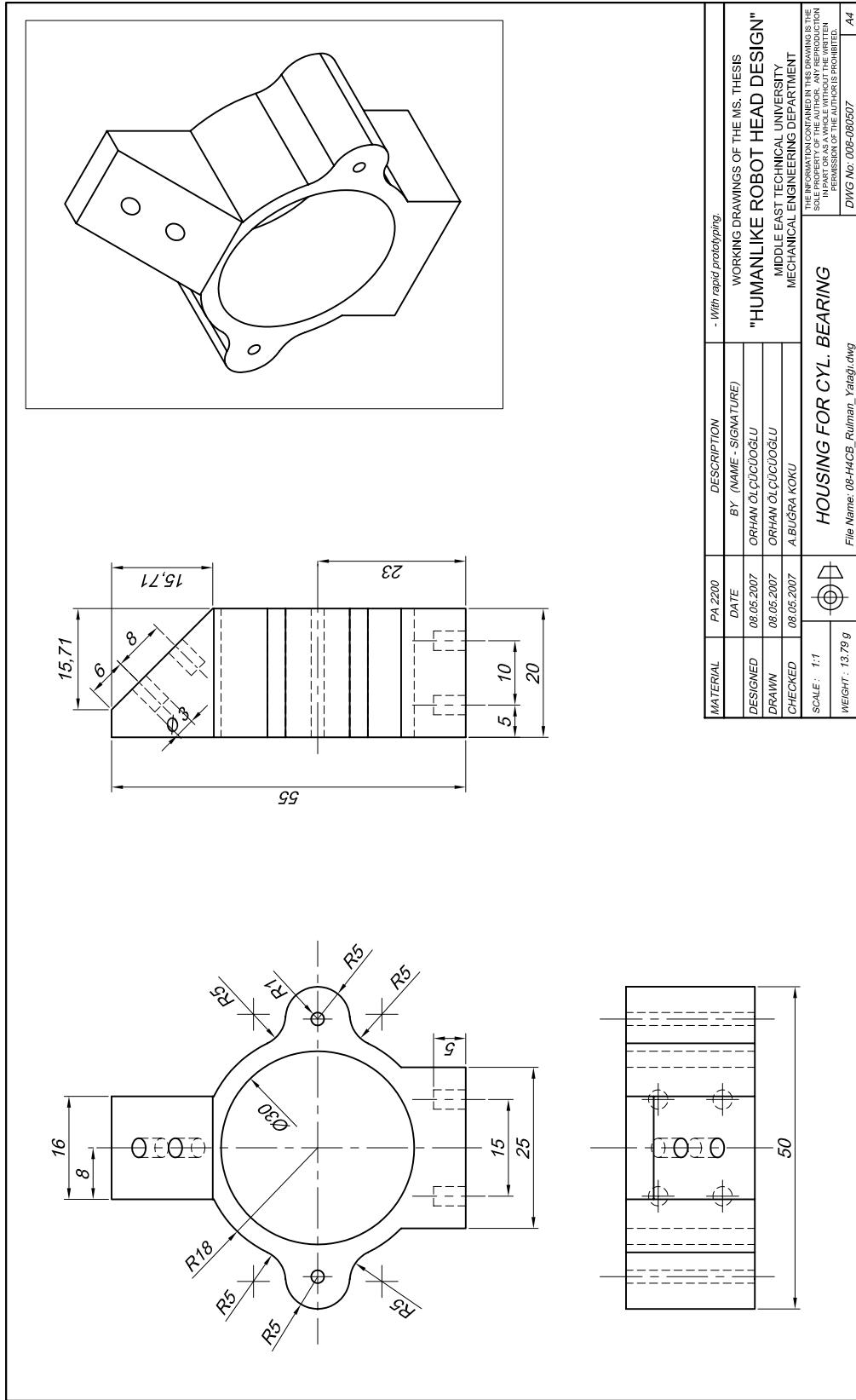


Figure A9 Technical Drawing of H4CB

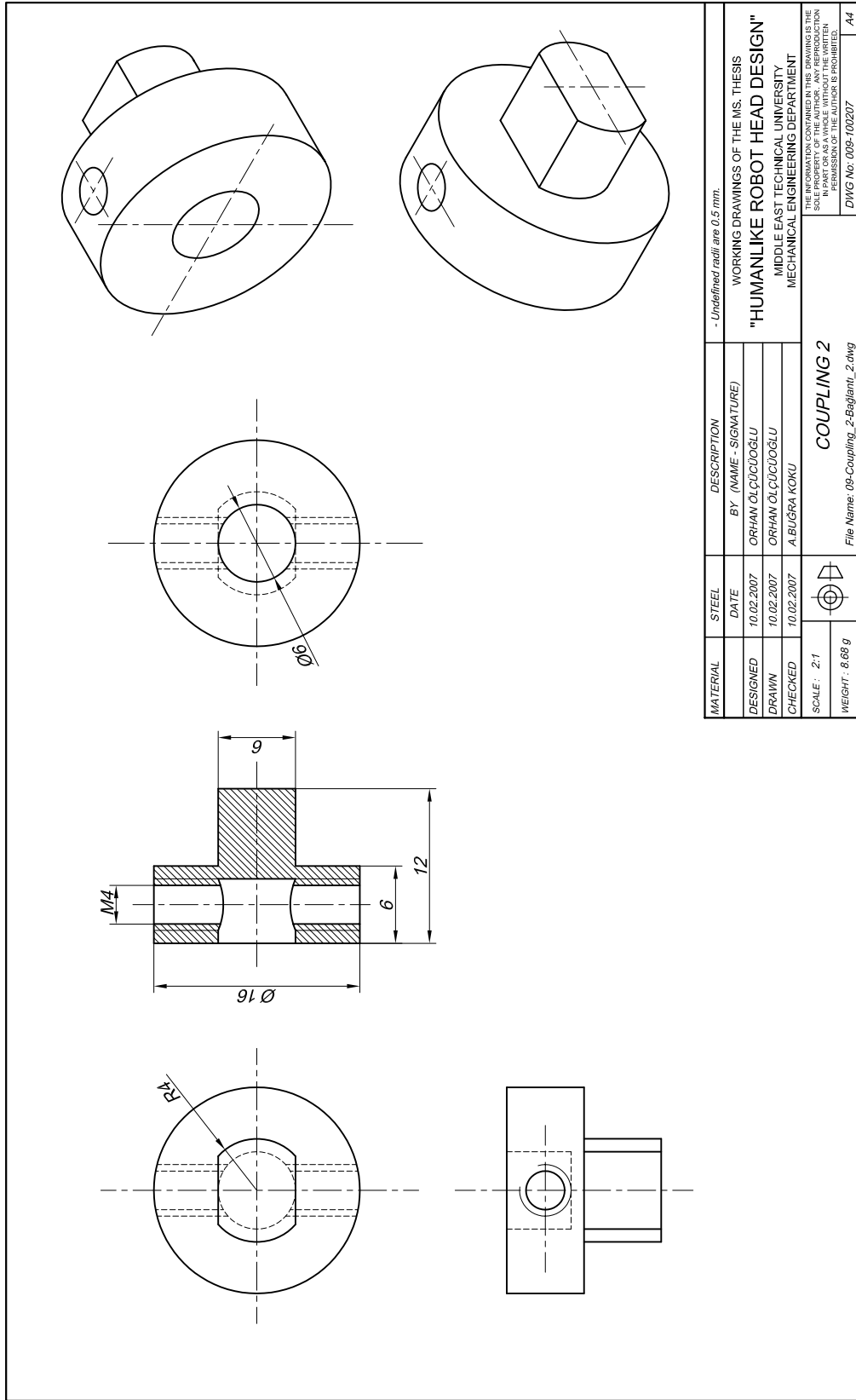


Figure A.10 Technical Drawing of Coupling 2

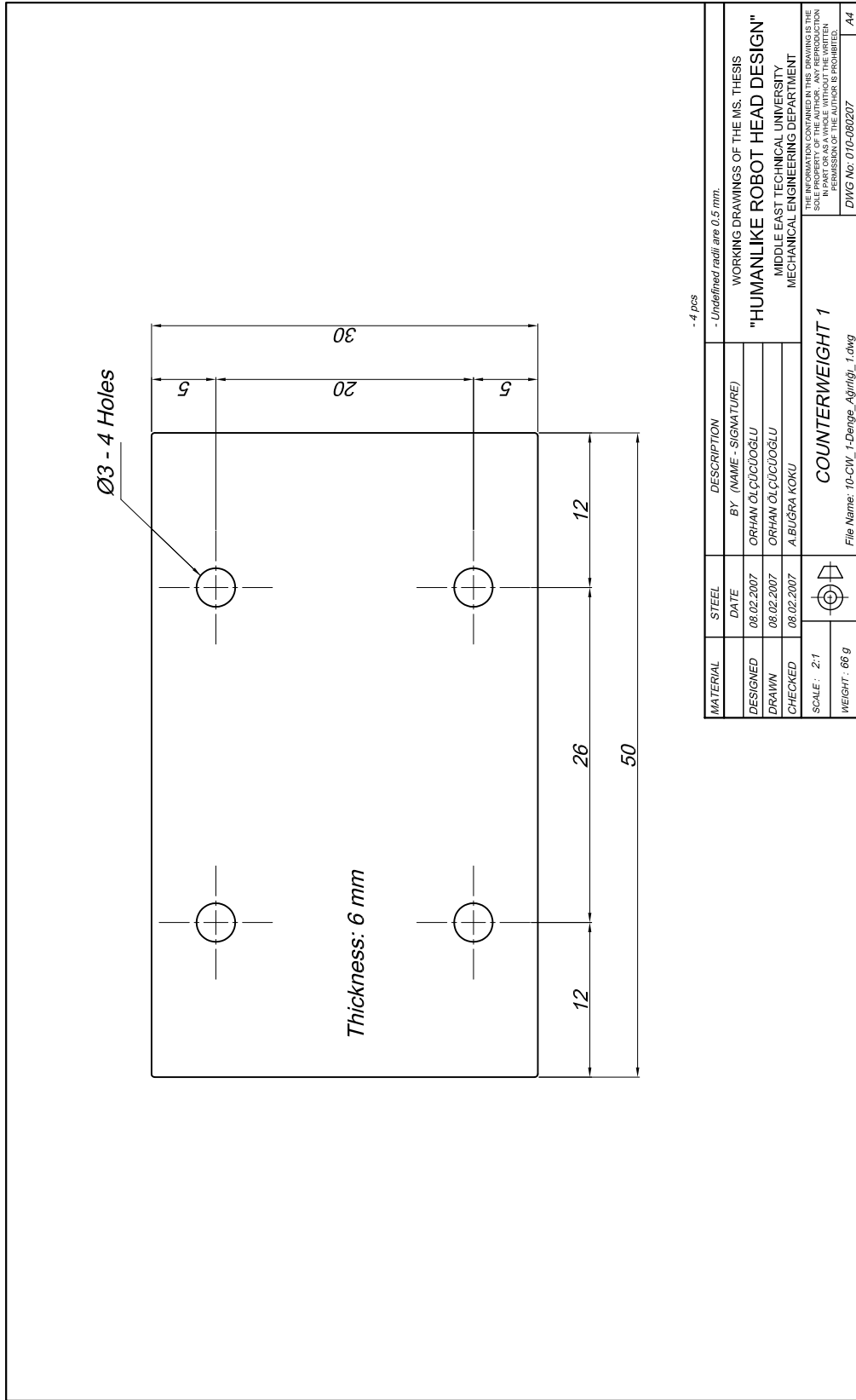


Figure A.11 Technical Drawing of Counterweight 1

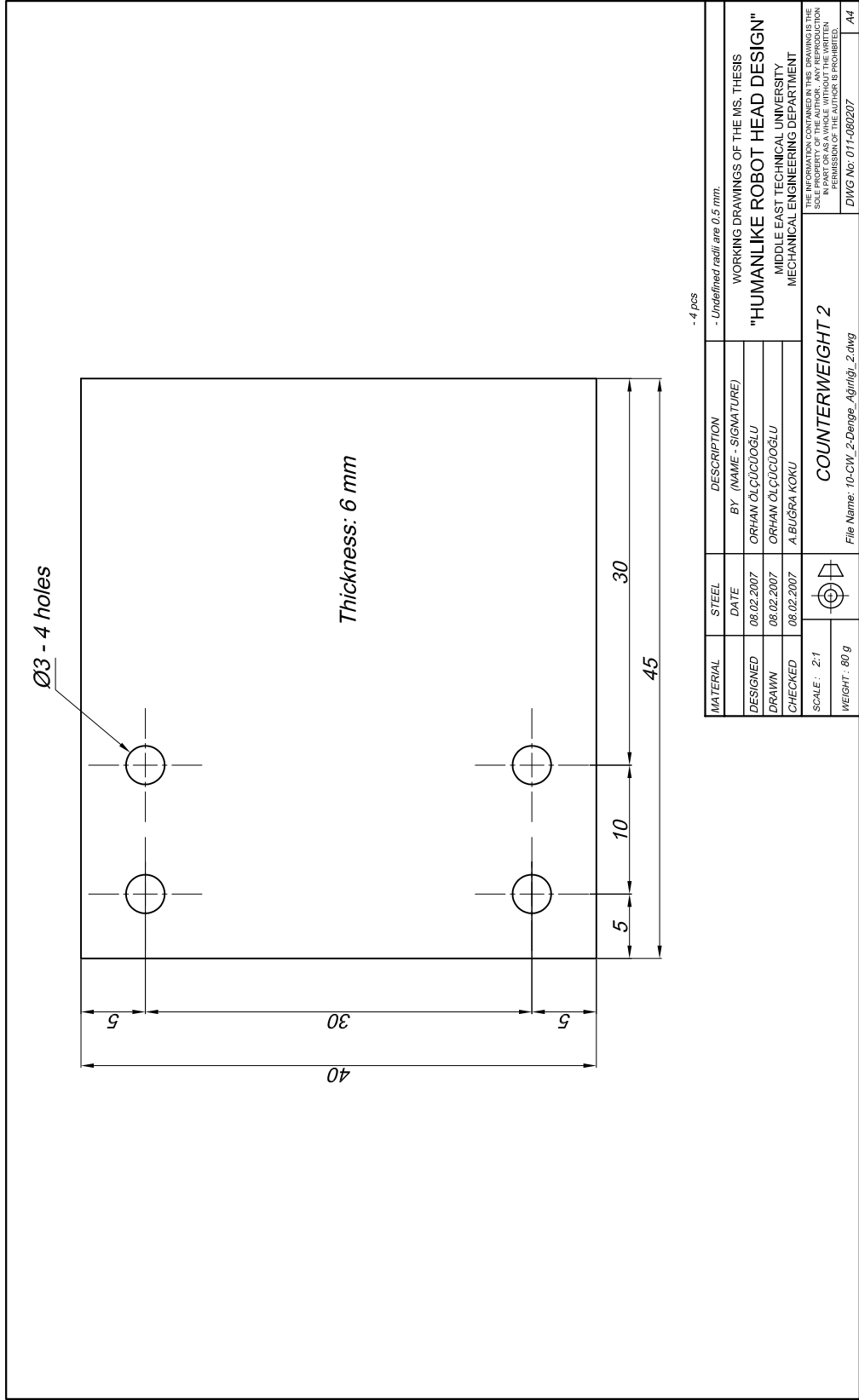


Figure A.12 Technical Drawing of Counterweight 2

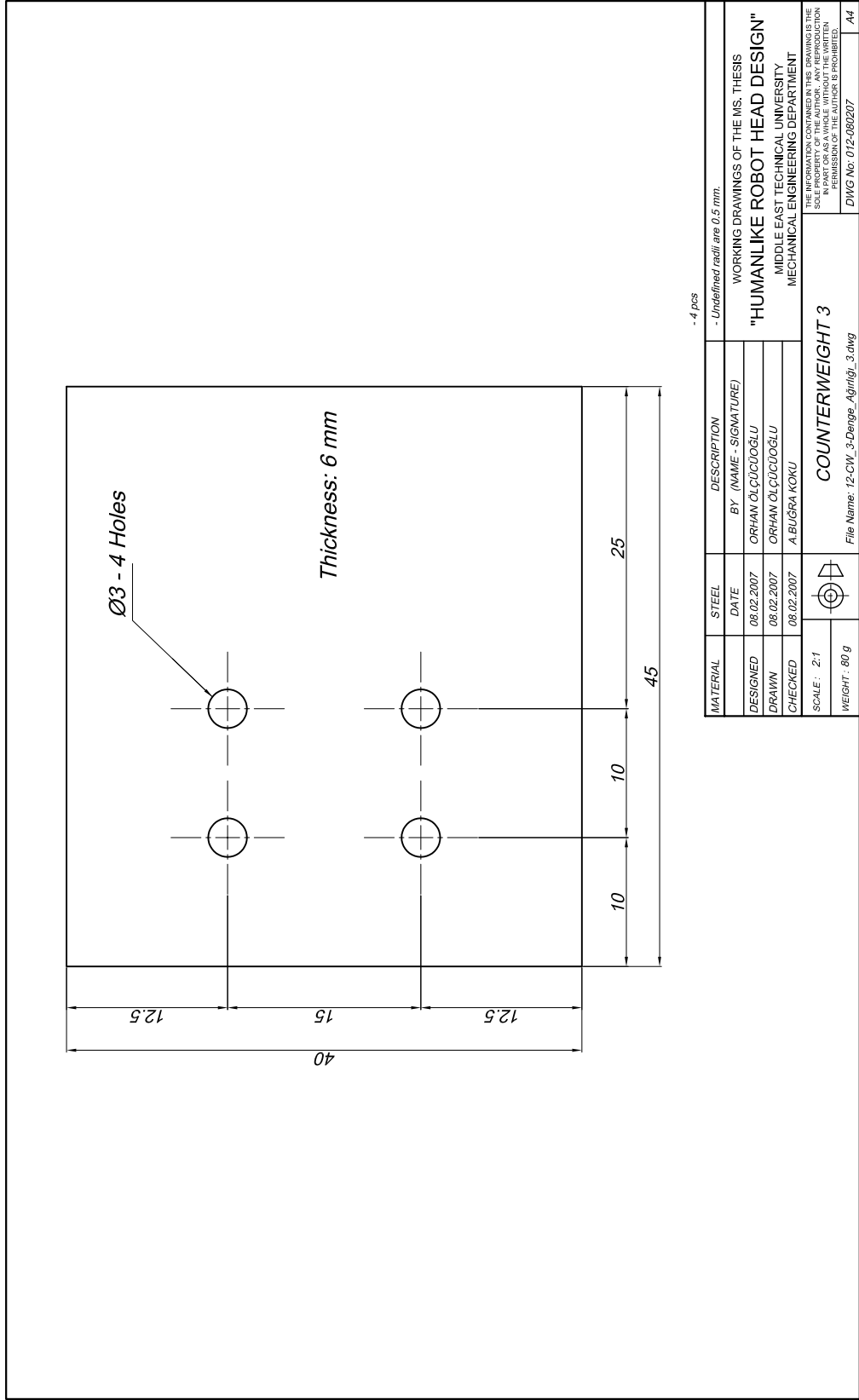


Figure A.13 Technical Drawing of Counterweight 3

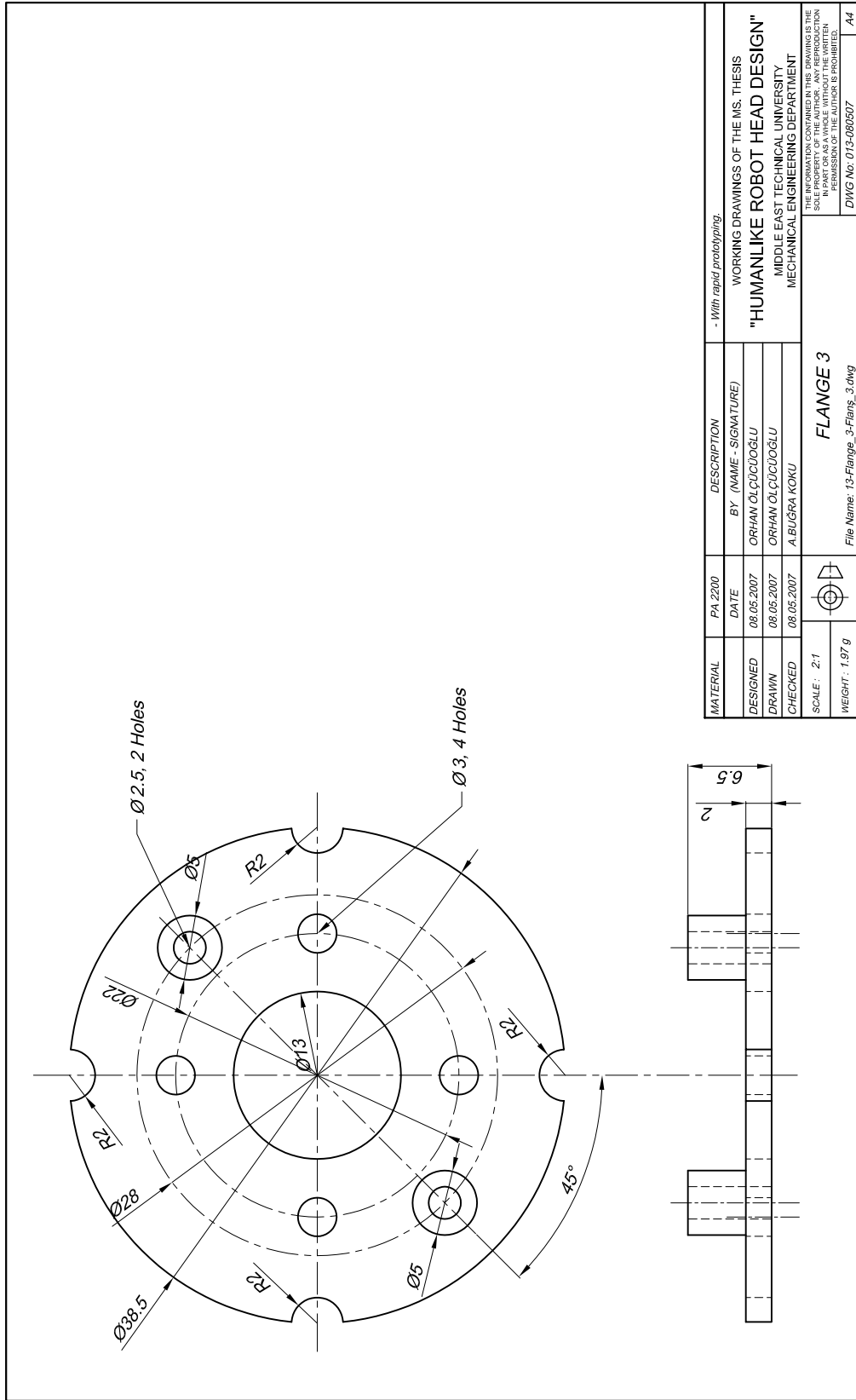


Figure A.14 Technical Drawing of Flange 3

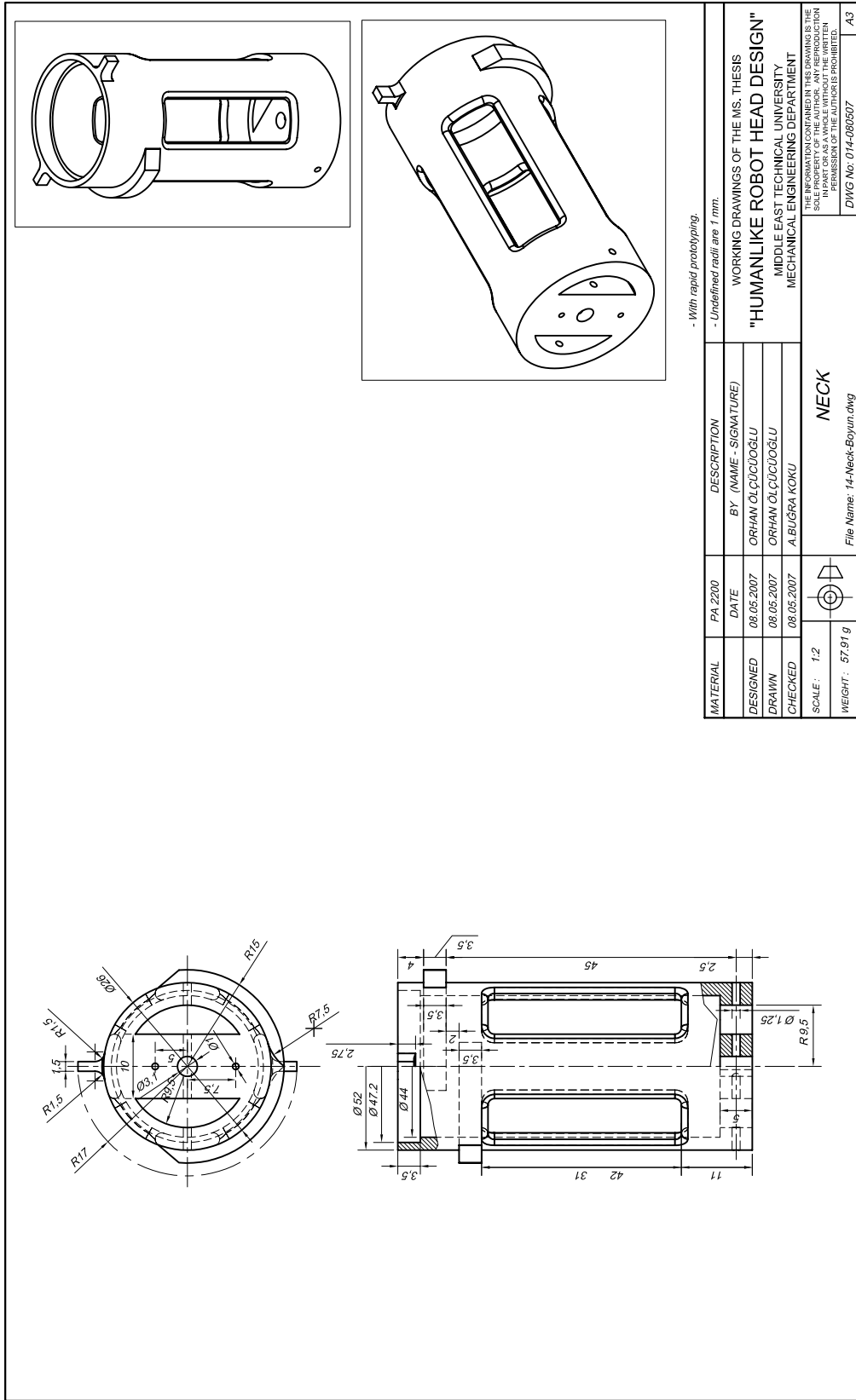


Figure A.15 Technical Drawing of Neck

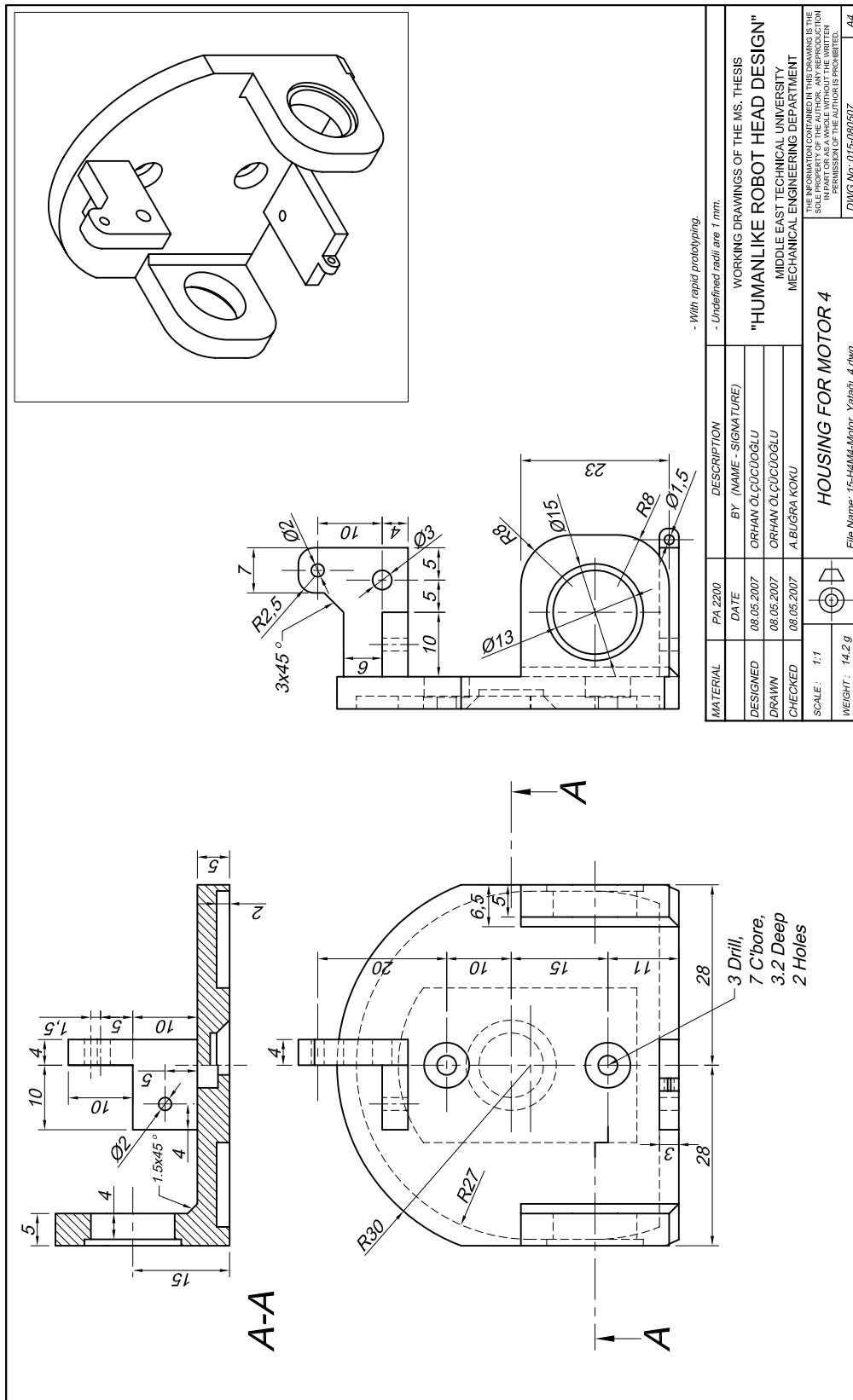


Figure A.16 Technical Drawing of H4M4

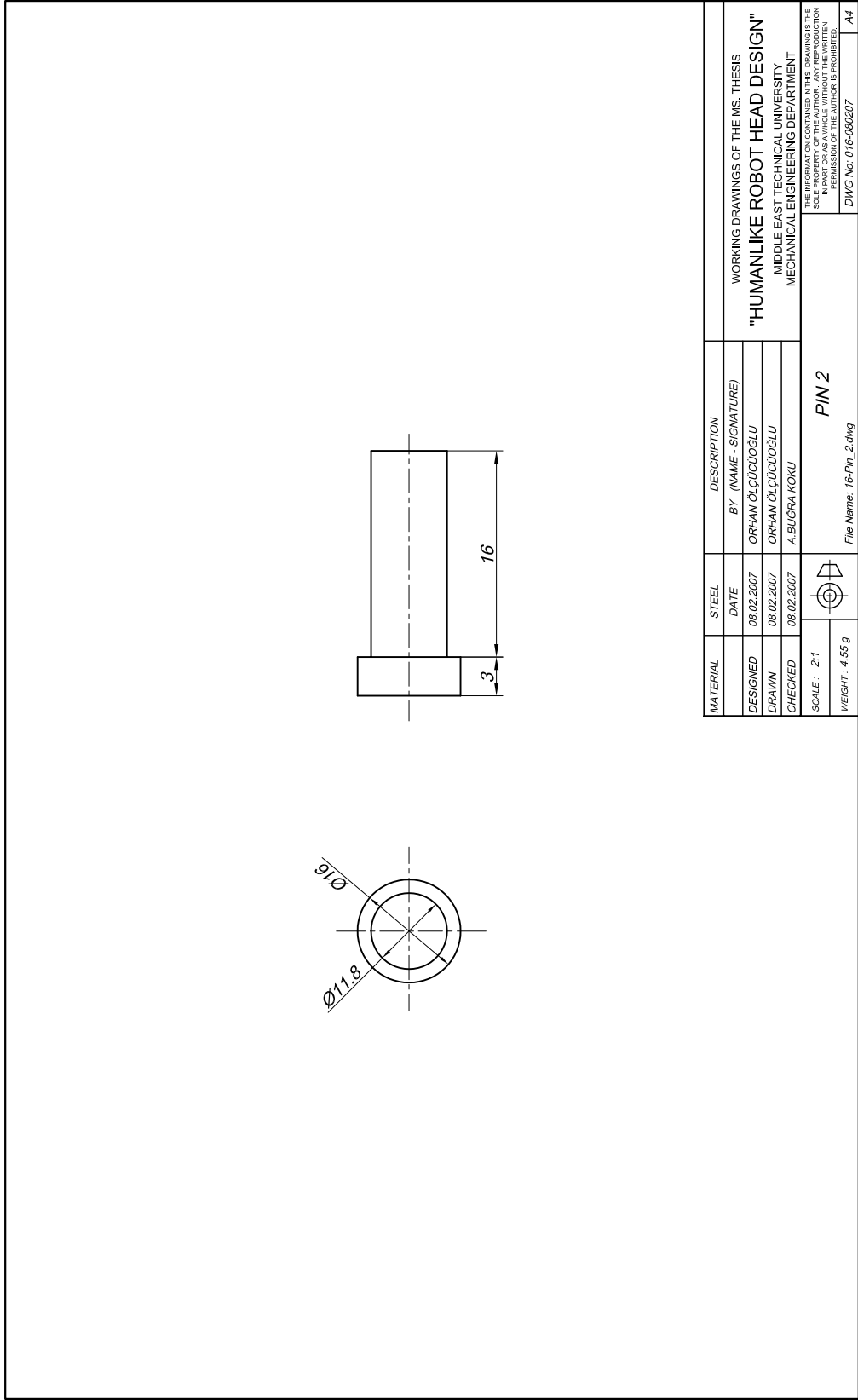


Figure A.17 Technical Drawing of Pin 2

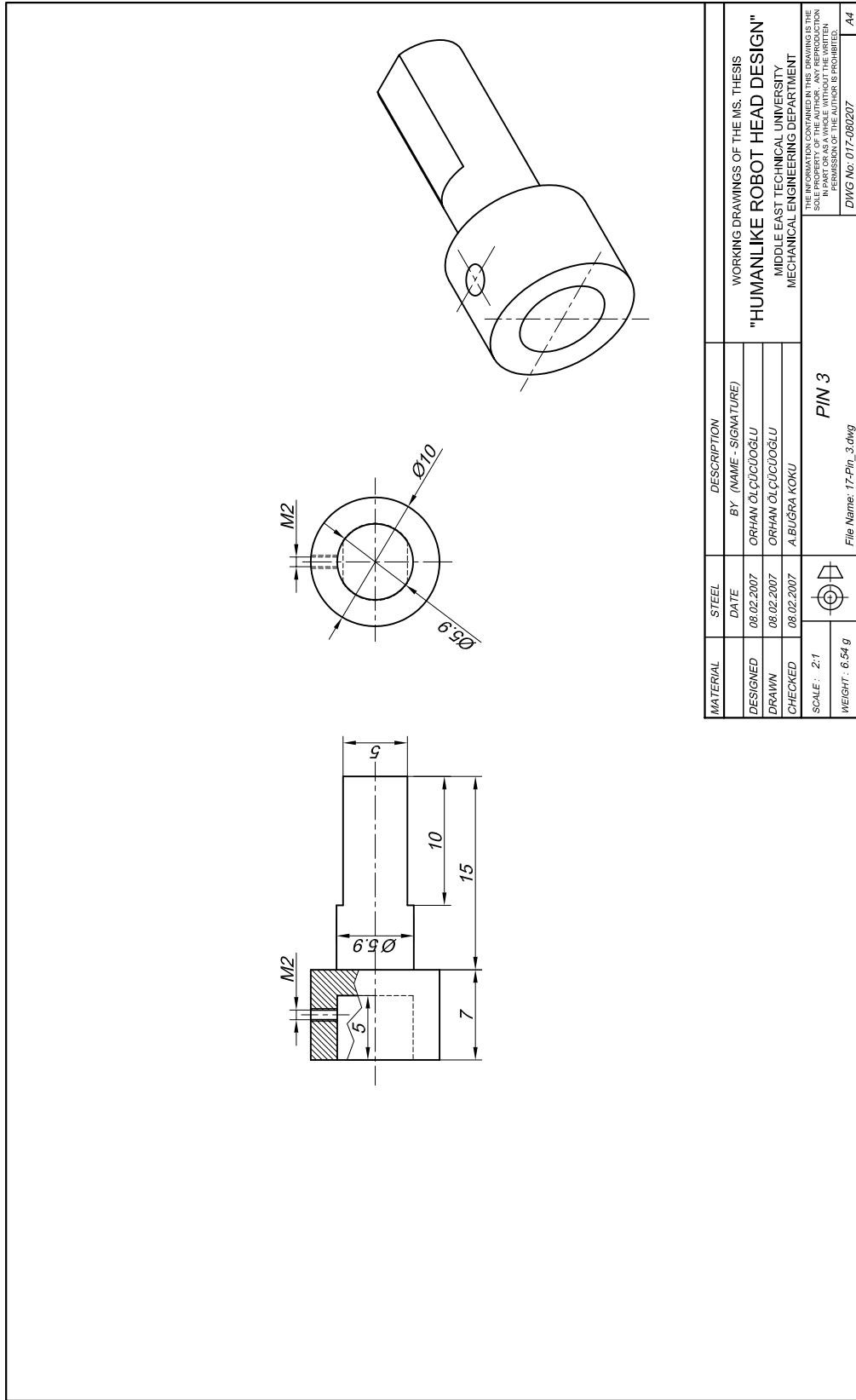


Figure A.18 Technical Drawing of Pin 3

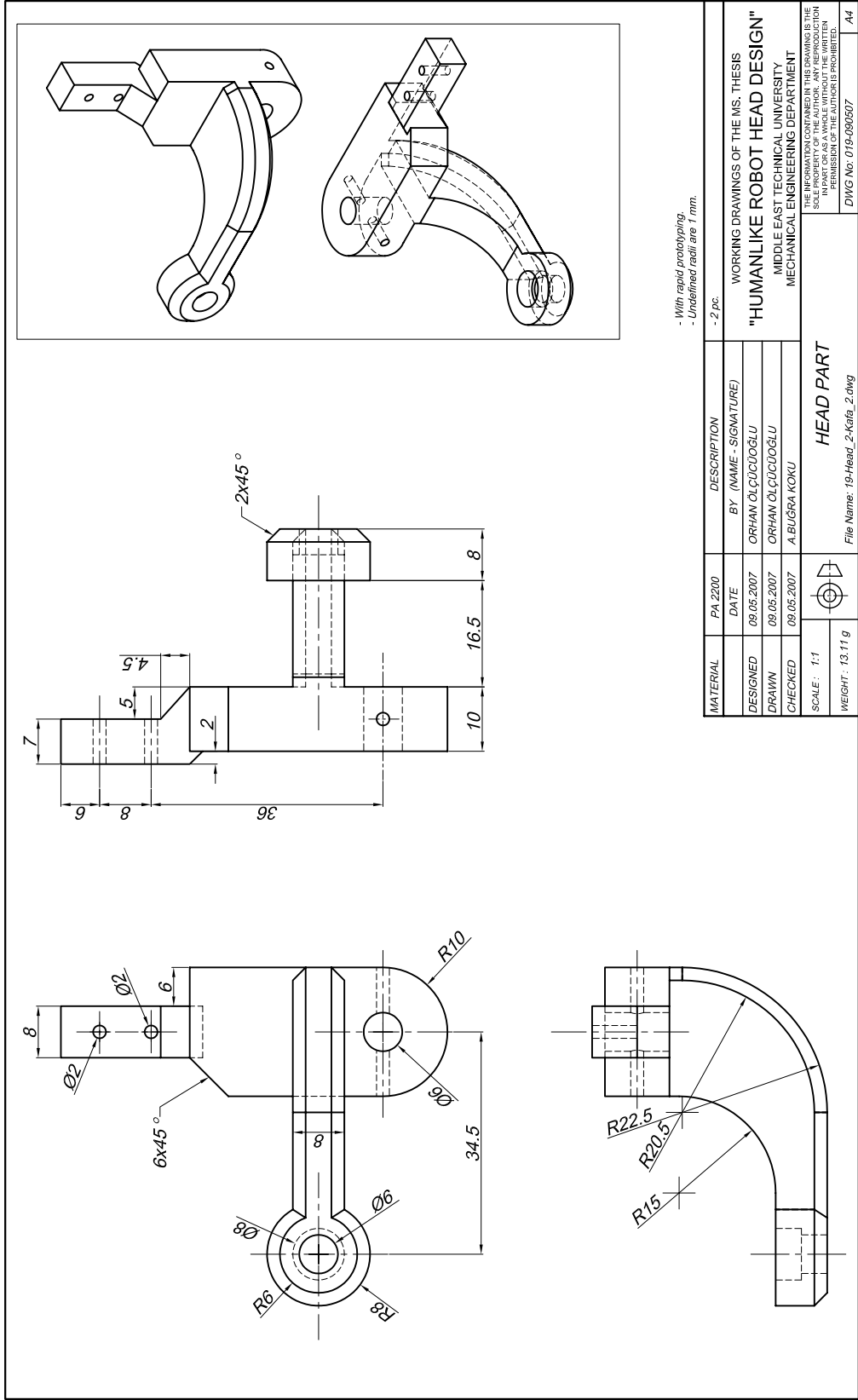


Figure A.20 Technical Drawing of Head 2

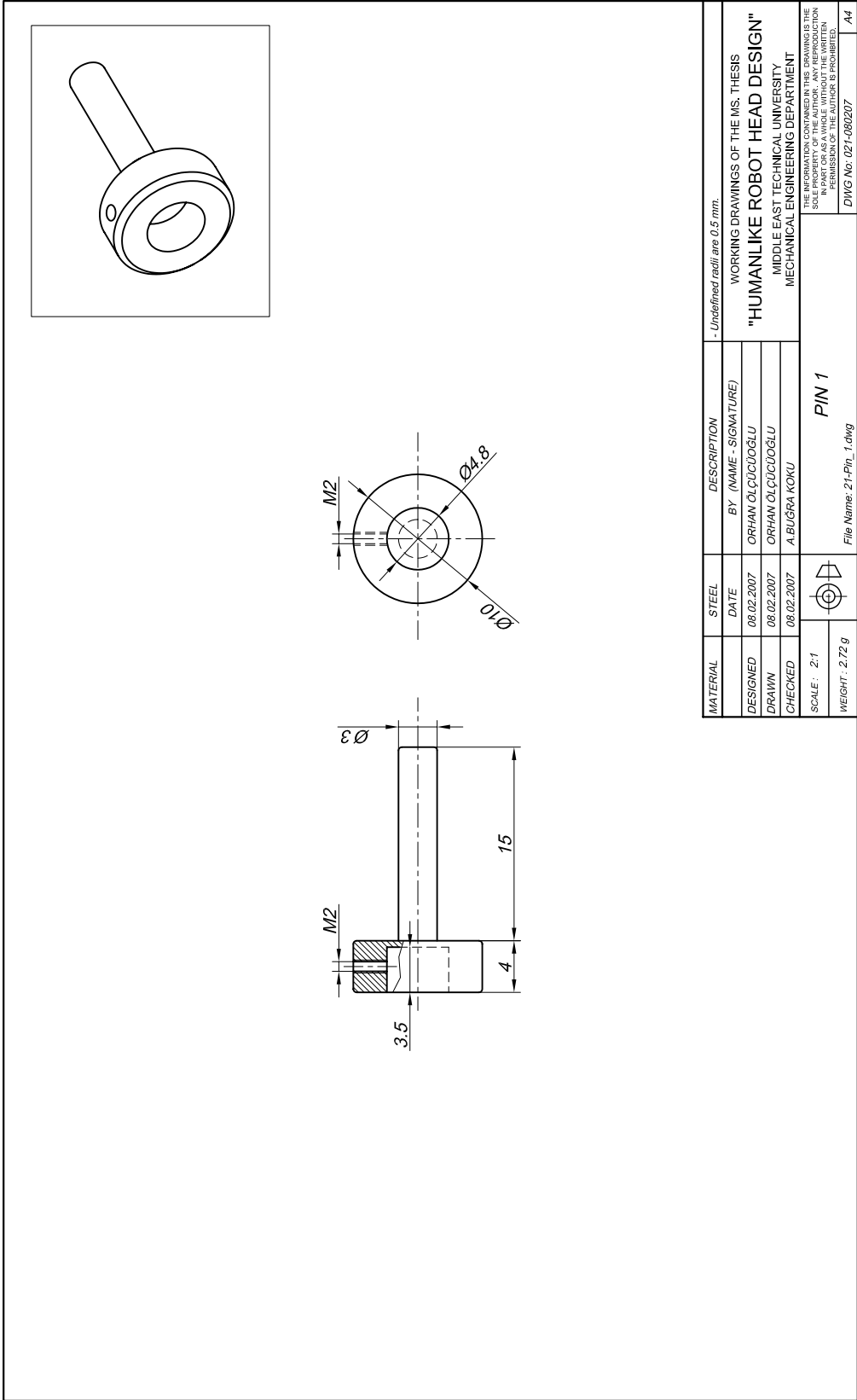
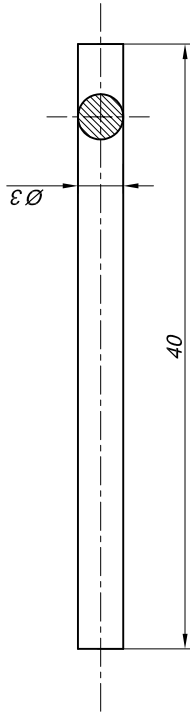


Figure A.22 Technical Drawing of Pin 1




MATERIAL	STEEL	DESCRIPTION
DATE	15.07.2007	BY (NAME - SIGNATURE) ORHAN ÖLÇÜCÜOĞLU
DESIGNED	15.07.2007	ORHAN ÖLÇÜCÜOĞLU
DRAWN	15.07.2007	ORHAN ÖLÇÜCÜOĞLU
CHECKED	15.07.2007	A.BUGRA KOKU
SCALE : 2:1		
WEIGHT : 2,20 g.		
		 CAMERA SHAFT File Name: 22-CameraShaft-Kamera_Milli.dwg
		WORKING DRAWINGS OF THE MS. THESIS "HUMANLIKE ROBOT HEAD DESIGN" MIDDLE EAST TECHNICAL UNIVERSITY MECHANICAL ENGINEERING DEPARTMENT <small>THE INFORMATION CONTAINED IN THIS DRAWING IS THE SOLE PROPERTY OF THE AUTHOR. ANY REPRODUCTION OR TRANSMISSION IN ANY FORM OR BY ANY MEANS WITHOUT THE WRITTEN PERMISSION OF THE AUTHOR IS PROHIBITED.</small>
		DWG No: 1022-160707
		A4

Figure A.23 Technical Drawing of Shaft

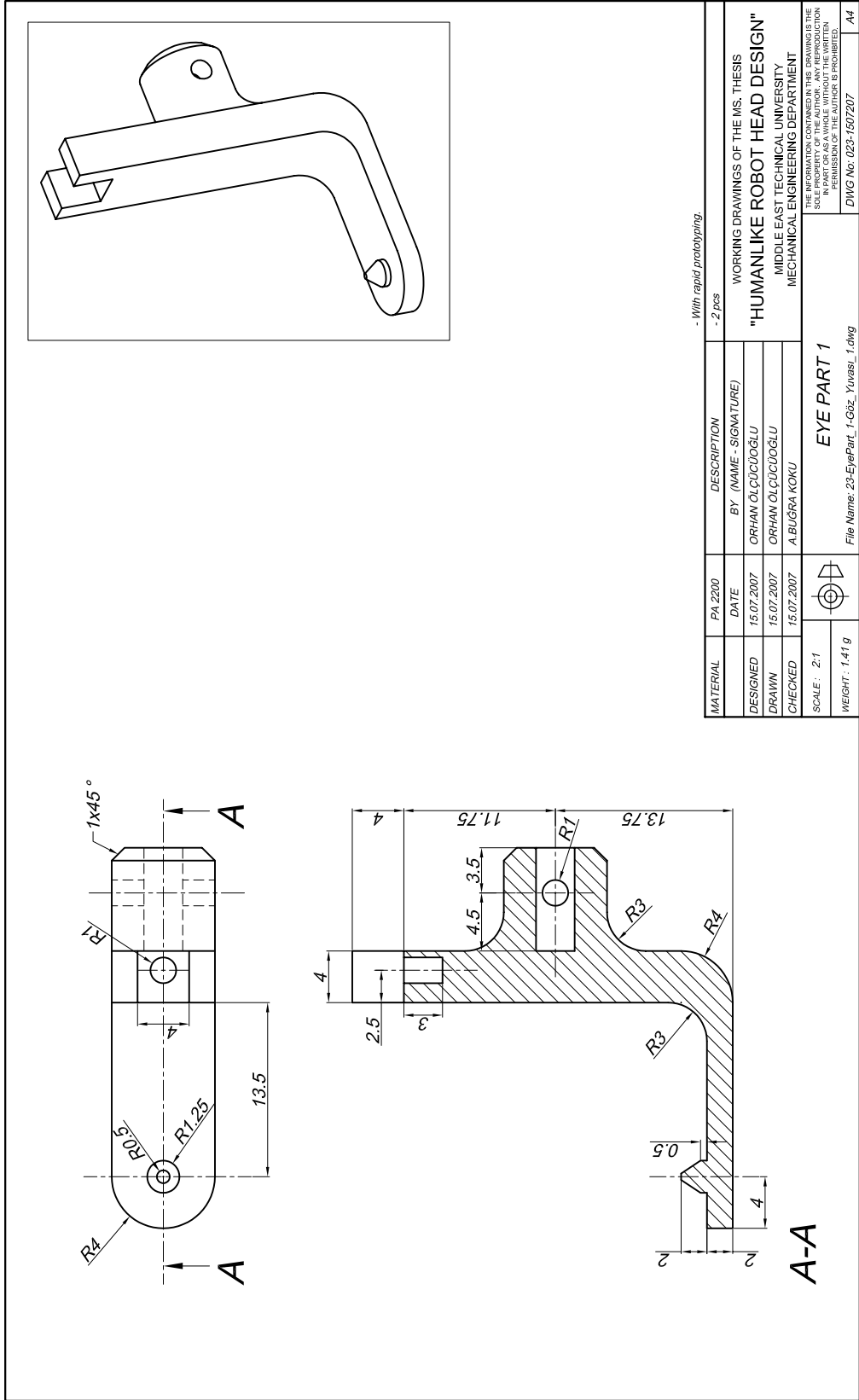


Figure A.24 Technical Drawing of Camera Part 1

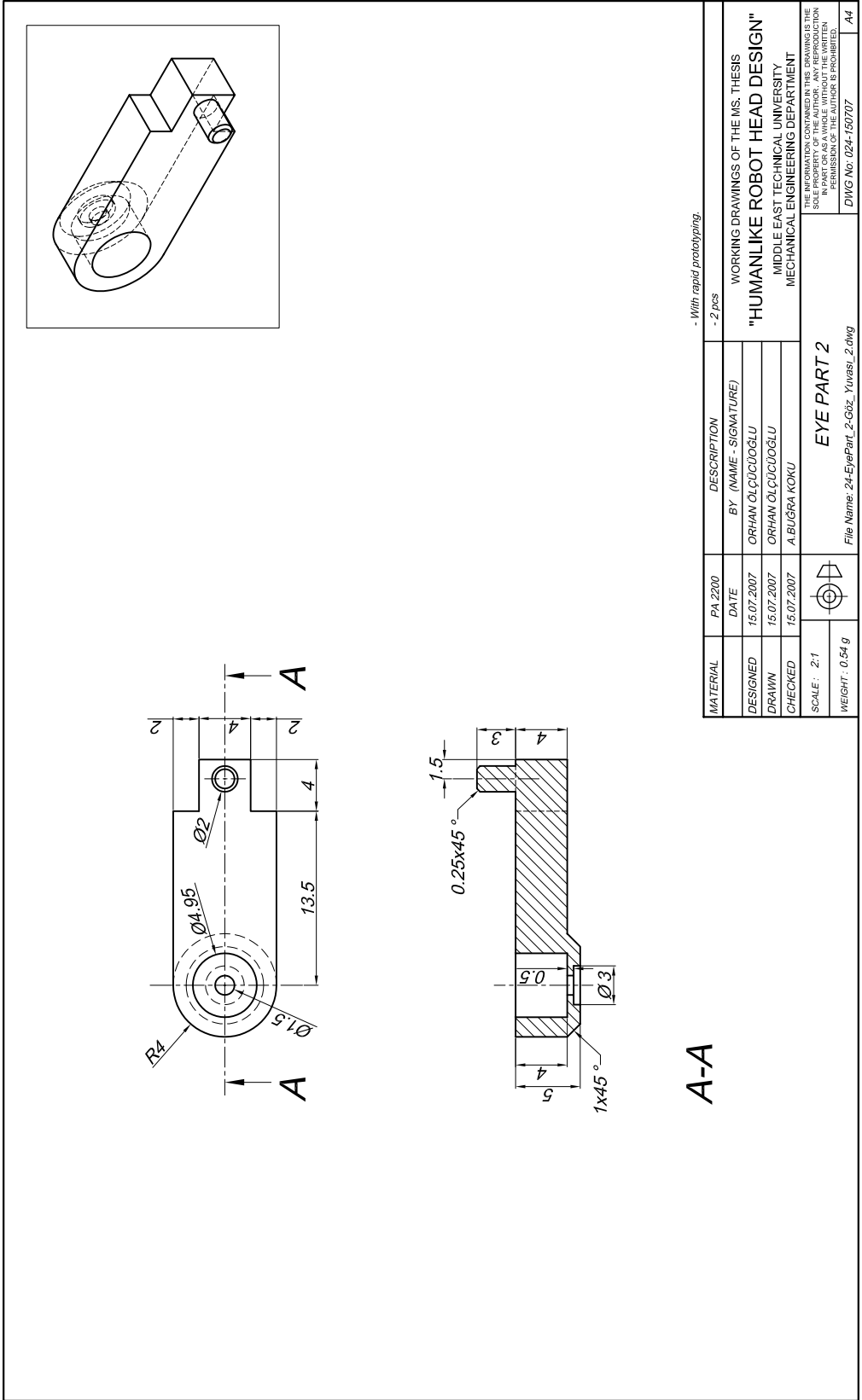


Figure A.25 Technical Drawing of Camera Part 2

APPENDIX B

CIRCUIT SCHEMATICS

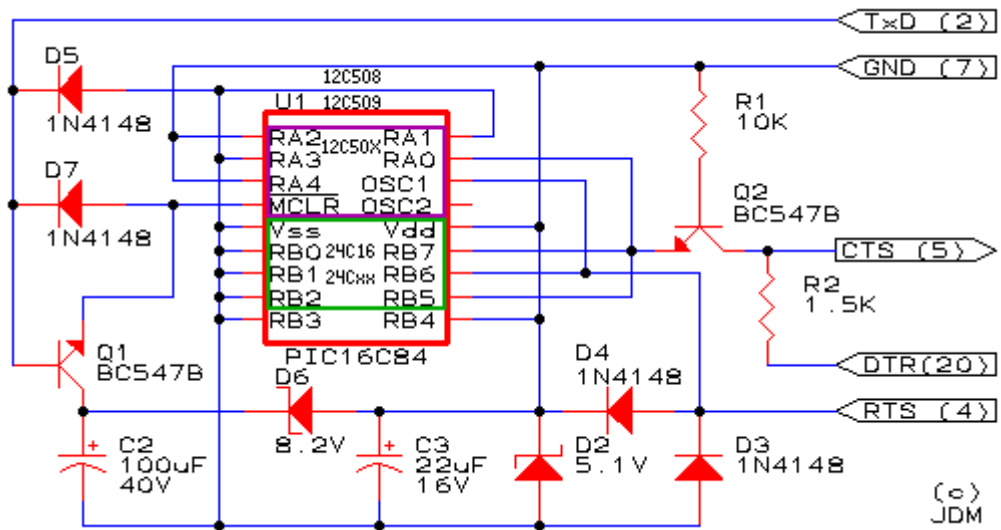


Figure B.1 JDM2 - Microchip PIC Programmer Circuit Schematic [81].

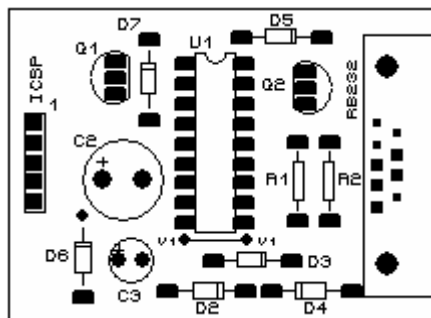
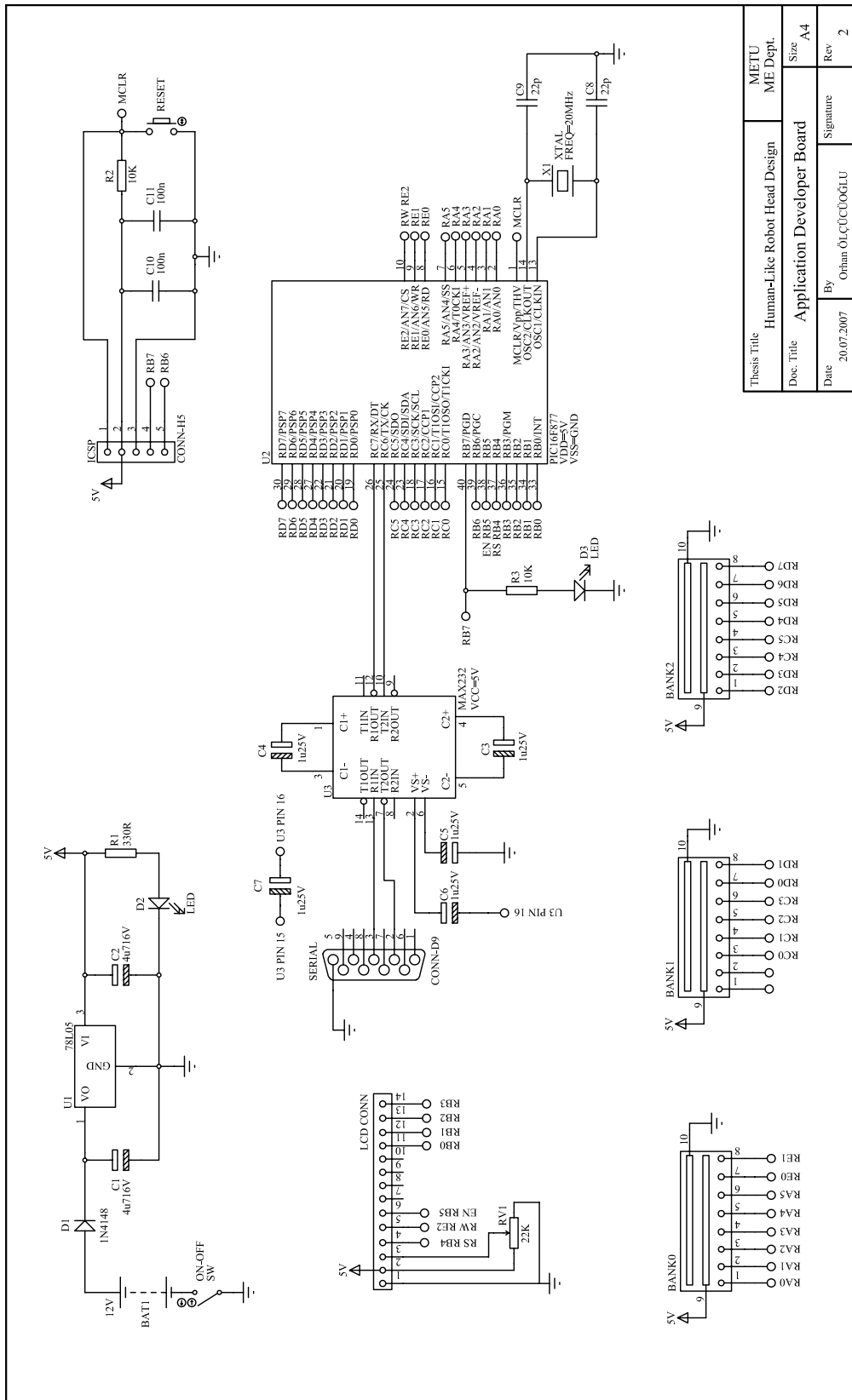


Figure B.2 PCB Layout of JDM2 Programmer – Component Side



Thesis Title	Human-Like Robot Head Design	METU
Doc. Title	Application Developer Board	ME Dept.
Date	20.07.2007	Size
By	Orhan ÖLÇÜOĞLU	Signature
		Rev
		2

Figure B.3 Schematics of Microchip PIC Based Application Developer Board

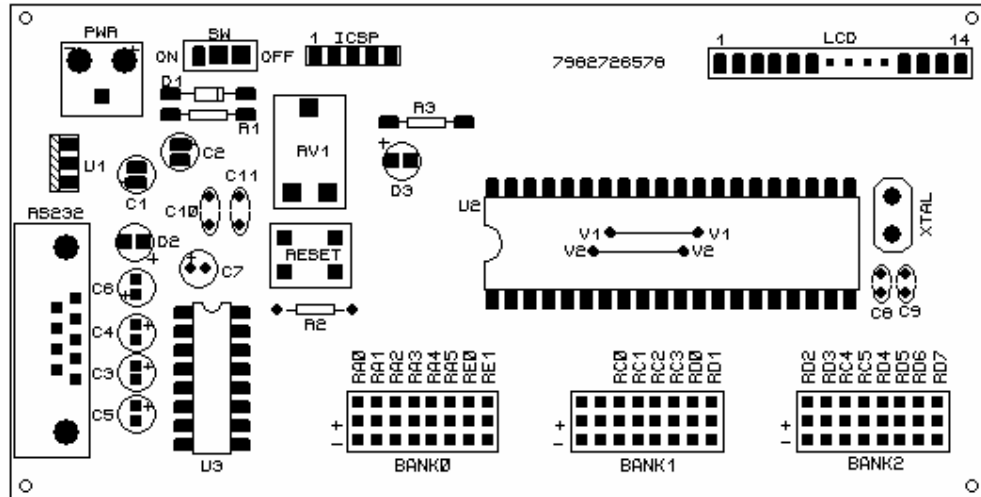


Figure B.4 PCB Layout of Application Developer Board – Component Side

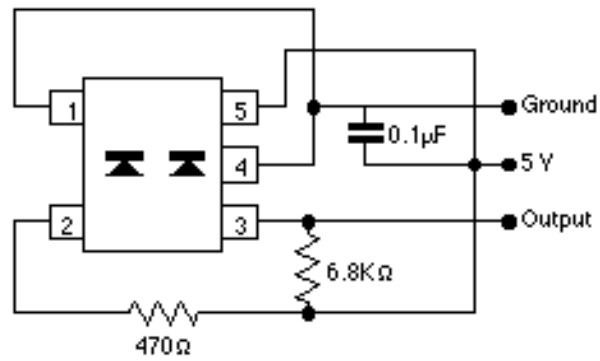


Figure B.5 Schematic of Application Circuit for Hamamatsu P5587 [82].

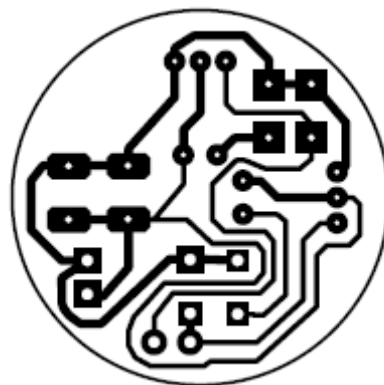
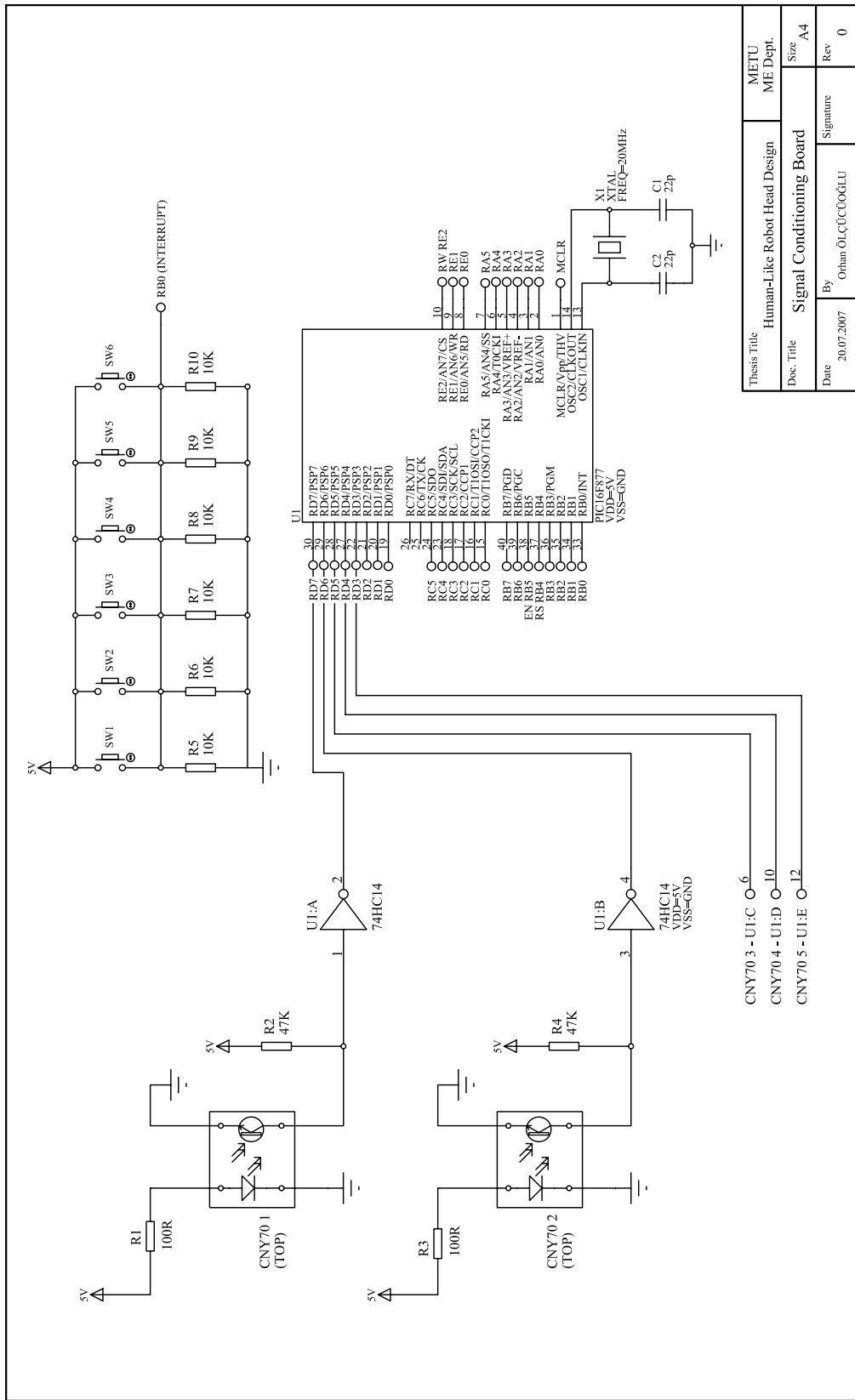


Figure B.6 PCB Layout of Shaft Encoder – Bottom Copper Side



Thesis Title		Human-Like Robot Head Design		METU	
Doc. Title		Signal Conditioning Board		ME Dept.	
Date	20.07.2007	By	Orhan ÖLÇÜCÜOĞLU	Signature	
				Size	A4
				Rev	0

Figure B.8 Schematic of Signal Conditioning Board

APPENDIX C

ACTUATOR SPECIFICATIONS

In this appendix, firstly, specifications of the actuators that are used in the robot are given. Then, actuator selection calculations are provided.

C.1 Airtronics-SANWA HYPER ERG-VB High Torque Servo



Figure C.1 RC Servo Motor Model Used to Actuate the Fourth Axis of the Robot.

Table C.1 Technical Specifications of RC₁ - SANWA HYPER ERG-VB.

Weight	60	[g]
Dimensions	39 x 20 x 37.4	[mm]
Volts	4.8/6.0	[V]
Torque	13	[kg.cm]
Speed	0.13/0.10	[sec] / 60 [deg]
Gear	Plastic and Metal	

C.2 Airtronics-SANWA SX 091 Micro Servo



Figure C.2 RC Servo Motor Model Used to Actuate All the Axes in the Eye and Jaw Mechanisms.

Table C.2 Technical Specifications of RC₂ - SANWA SX 091.

Weight	9	[g]
Dimensions	23.2 x 11.2 x 22	[mm]
Volts	4.8/6.0	[V]
Torque	1.3	[kg.cm]
Speed	0.12	[sec] / 60 [deg]
Gear	Plastic	

C.3 Dunker Motoren GR 30.2 DC Motor - 6 W

We have used the same DC motor with two different gear heads. The first two neck axes are actuated by the combination of the motor and the 3-stage gearbox. In the neck yaw motion a 2-stage gearbox is preferred

C.3.1 DunkerMotoren PLG 30 Planetary Gearbox

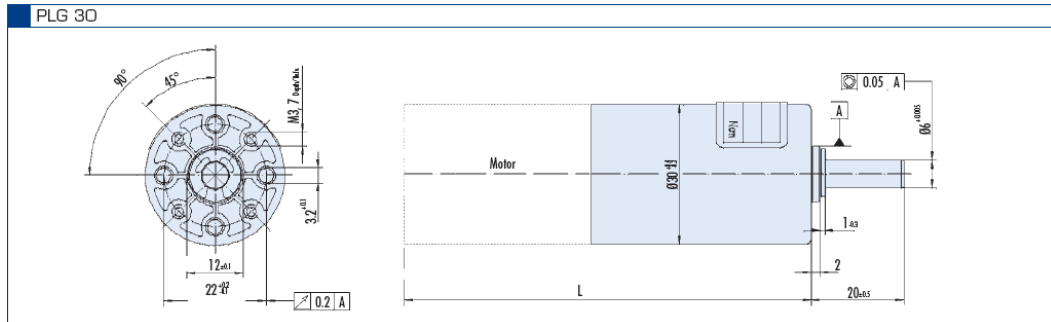


Figure C.4 Dimensions of DunkerMotoren PLG 30 Planetary Gearbox (in mm).

Table C.4 Technical Specifications of DunkerMotoren PLG 30 Planetary Gearbox

	DC ₂	DC ₁	
Number of Stages	2	3	
Reduction Ratio	36	91.12	
Continuous Torque	80	180	[N.cm]
Efficiency	0.81	0.73	
Weight of Gearbox	0.08	0.09	[kg]
Axial Load	10	10	[N]
Radial Load	24	24	[N]
Motor & Gearbox Combination Length (L)	78	88	[mm]

C.4 Actuator Selection Calculations

Three different motors are used in the robot. The required data for the calculations are collected in Table C.5.

Table C.5 Data Used in the Calculations for Each Joint Axis.

#	Motor Type	Joint Variable	Axis	Total Weight of the Load [g]	Mass Moment of Inertia [g.cm ²]	Specified Max. Speed [deg/sec]
1	DC ₁	θ_1	Neck's Lower Pitch	1756.62	187452	100
2	DC ₁	θ_2	Neck's Roll	1364.63	141592	100
3	DC ₂	θ_3	Neck's Yaw	339.85	16819	100
4	RC ₁	θ_4	Neck's Upper Pitch	206.02	12265	100
5	RC ₂	θ_5	Eyes' Pitch	87.86	154	500
6	RC ₂	θ_6	Right Eye's Yaw	35	76	500
7	RC ₂	θ_7	Left Eye's Yaw	35	76	500
8	RC ₂	θ_8	Jaw's Pitch	38.73	722	500

The continuous torque that can be obtained from each motor shaft is as follows:

For the RC Servo motors, the torque values are directly taken from their specification tables (Table C.1 and Table C.2).

$$T_{RC_1} = 13 [kg.cm] = 1.275 [N.m] \quad (C.1)$$

$$T_{RC_2} = 1.3 [kg.cm] = 0.1275 [N.m] \quad (C.2)$$

As for the DC Motors, the torque of the motor shaft to the gear output can be found by using the following equation.

$$T = M_{\max.\text{cont.}} \cdot i \cdot \eta \quad (\text{C.3})$$

where

i the reduction ratio and

η is the efficiency of the gear head.

Therefore

$$T_{DC_1} = M_{\max.\text{cont.}} \cdot i_1 \cdot \eta_1 = 0.01 [N.m] \cdot (162) \cdot (0.73) = 1.1826 [N.m] \quad (\text{C.4})$$

$$T_{DC_2} = M_{\max.\text{cont.}} \cdot i_2 \cdot \eta_2 = 0.01 [N.m] \cdot (36) \cdot (0.81) = 0.2916 [N.m] \quad (\text{C.5})$$

These found values are the torques that should not be exceeded for a safe operation. That is, the torque requirements must be below these values.

For each joint axis, maximum inertia and speed values can be seen in Table C.5. For each motor type, we take the maximum inertia and speed from the table to determine the necessary torque requirement.

The maximum inertia of the load to be accelerated by the first actuator type is found as $J_{L_1} = 187452$ [gr.cm²]. The maximum speed is also given as $\alpha_{1\max} = 100$ [deg/sec]. Therefore, to calculate the necessary torque that must be transferred by the actuator output shaft can be computed as

$$M_{\alpha_1} = J_{L_1} \alpha_{1\max} = 0.0187452 [\text{kg.m}^2] \cdot 100 [\text{deg/sec}] \cdot \frac{\pi}{180}$$

$$M_{\alpha_1} = 0.0327 [N.m] \quad (\text{C.6})$$

Similarly, the other torques can be determined as follows.

$$M_{\alpha_2} = J_{L_2} \alpha_{2\max} = 0.0141592 [\text{kg.m}^2] \cdot 100[\text{deg/sec}] \cdot \frac{\pi}{180}$$

$$M_{\alpha_2} = 0.0246 [N.m] \quad (\text{C.7})$$

$$M_{\alpha_3} = J_{L_3} \alpha_{3\max} = 0.0016819 [\text{kg.m}^2] \cdot 100[\text{deg/sec}] \cdot \frac{\pi}{180}$$

$$M_{\alpha_3} = 0.00292 [N.m] \quad (\text{C.8})$$

$$M_{\alpha_4} = J_{L_4} \alpha_{4\max} = 0.0012265 [\text{kg.m}^2] \cdot 500[\text{deg/sec}] \cdot \frac{\pi}{180}$$

$$M_{\alpha_4} = 0.0106 [N.m] \quad (\text{C.9})$$

$$M_{\alpha_{5678\max}} = J_{L_{5678\max}} \alpha_{5678\max} = (7.22) \cdot 10^{-5} [\text{kg.m}^2] \cdot 500[\text{deg/sec}] \cdot \frac{\pi}{180}$$

$$M_{\alpha_{5678\max}} = (6.29) \cdot 10^{-4} [N.m] \quad (\text{C.10})$$

$$T_{DC_1} > M_{\alpha_1} \quad (\text{C.11})$$

$$T_{DC_1} > M_{\alpha_2} \quad (\text{C.12})$$

$$T_{DC_2} > M_{\alpha_3} \quad (\text{C.13})$$

$$T_{RC_1} > M_{\alpha_4} \quad (\text{C.14})$$

$$T_{RC_2} > M_{\alpha_{5678\max}} \quad (\text{C.15})$$

Thus the selected actuators satisfy the torque requirements for all the movements.

APPENDIX D

SPECIFICATIONS OF RAPID PROTOTYPING MACHINE



Figure D.1 Machine Type: EOS EOSINT P380

Table D.1 Technical Specifications

Build Volume :	X axis : 340 mm Y axis : 340 mm Z axis : 620 mm
Process Step :	0.15 mm \pm 0.05 mm
Laser Power :	50 W (max.)
Materials :	Fine Polyamide PA 2200

Fine Polyamide PA 2200

Table D.2 Material Properties

Average particle size	Laser	60	μm
Bulk density	ASTM D4164	0.44	g/cm ³
Density of lasersintered part	ASTM D792	0.95	g/cm ³
Moisture Absorption 23°C	ASTM D570	0.41	%

Table D.3 Mechanical Properties

Tensile Modulus	ASTM D638	1700	MPa
Tensile strength	ASTM D638	45	MPa
Elongation at break	ASTM D638	15	%
Flexural Modulus	ASTM D790	1300	MPa
Izod . Impact Strength	ASTM 256	440	J/m
Izod . Notched Impact	ASTM 256	220	J/m

APPENDIX E

CMOS CAMERA SPECIFICATIONS

Table E.1 JMK JK-007A Micro Wired Pinhole Color Audio Camera

Video Camera Parts:	1/3CMOS, 1/4 Image Sensors
System:	PAL/CCIR NTSC/EIA
Scanning Frequency:	PAL/CCIR: 50Hz, NTSC/EIA: 60Hz
Effective Pixel:	PAL: 628 x 582, NTSC: 510 x 492
Image Area:	PAL: 5.78 x 4.19mm, NTSC: 4.69 x 3.45mm
Minimum Illumination:	3 lux
Horizontal Definition:	380 Lines
Transmission Signal:	Audio, Video
Sensitivity:	+18 DB – AGC ON / OFF
Voltage:	6V DC, 12V DC
Current:	200 mA
Power Consumption:	200 mW

Table E.2 JMK WS-309AS Micro Wired Pinhole Color Audio Wireless Camera

Video Camera Parts:	1/3CMOS, 1/4 Image Sensors
System:	PAL/CCIR NTSC/EIA
Scanning Frequency:	PAL/CCIR: 50Hz, NTSC/EIA: 60Hz
Effective Pixel:	PAL: 628 x 582, NTSC: 510 x 492
Image Area:	PAL: 5.78 x 4.19mm, NTSC: 4.69 x 3.45mm
Minimum Illumination:	3 lux
Horizontal Definition:	380 Lines
Transmission Signal:	Audio, Video
Sensitivity:	+18 DB – AGL ON / OFF
Voltage:	6V DC, 9V DC
Current:	300 mA
Power Consumption:	640 mW
Output Electrical Level:	50mW
Output Frequency:	1.2G/2.4G
Linear Transmission Distance:	50-100 m.

APPENDIX F

COMMUNICATION PROTOCOL

In this appendix, the instruction set that is used to send the test signals from the PC system to the microcontroller board is given. The system has no data flow from the microcontroller side to the PC side yet.

There are mainly two programs written to control the robot. The first one is written in PicBasic Pro Compiler for the microcontrollers. It only receives the signals from the PC system to drive the motors. The second program is written in Visual Basic. The program allows selecting each actuator to individually drive. These two programs communicate via RS232 serial connection protocol. The microcontroller PIC 16F877 has a hardware USART (Universal Synchronous Asynchronous Receiver Transmitter). We use this peripheral feature of the microcontroller to establish a serial connection. The serial data is in 8N1 format, that is, 8 data bits, no parity bit and 1 stop bit. The selected baud rate is 9600 bps.

In Figure F.1, the signal flow is basically illustrated. The signal has mainly four divisions. First of all, a single byte “a” character is sent to start the communication between the PC and the controller. The controller does not generate a pulse of any type until this character is received. Then Motor ID is sent. Each actuator is given an ID number. Since we used two different types of actuator the necessary signals that are required to drive them are different. According to the ID received, the program jumps to the related loop. After Motor ID, Motor Position and Motor Velocity values are received and the appropriate driving signal is generated. Motor Velocity values are ignored if a RC Servo is to be actuated. In Table F.1, motor ID’s of each actuators and microcontroller connection ports are given. For test purposes, two different microcontrollers were used. Ports that are given in the table can be followed from the schematics seen in appendix B.

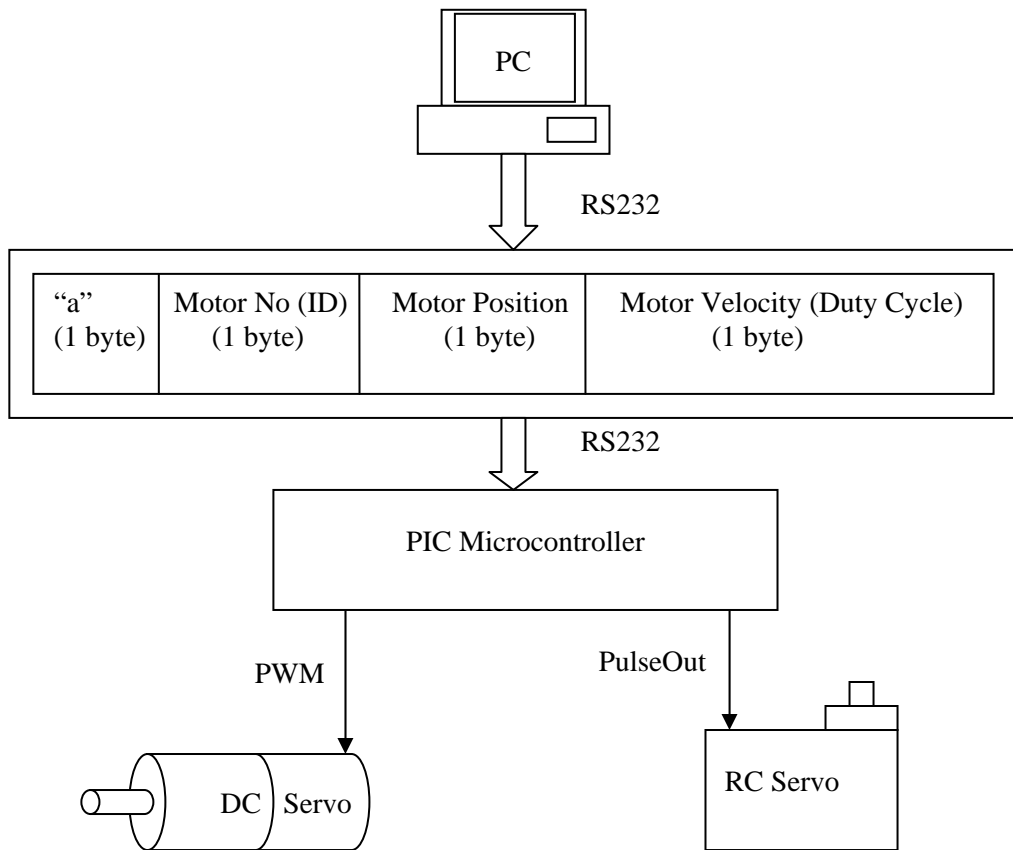


Figure F.1 General Data Flow and Instruction Set.

Table F.1 Motor ID Numbers and Microcontroller Pin Connections

#	Motor ID	Motor Definition	Related PIC Resource
1	1	Neck's Lower Pitch	PIC #1 - Port D.5 - Port D.6
2	2	Neck's Roll	PIC #1 - Port D.2 - Port D.3
3	3	Neck's Yaw	PIC #1 - Port B.6 - Port B.7
4	4	Neck's Upper Pitch	PIC #2 - Port D.3
5	5	Eyes' Pitch	PIC #2 - Port D.4
6	6	Right Eye's Yaw	PIC #2 - Port D.5
7	7	Left Eye's Yaw	PIC #2 - Port C.4
8	8	Jaw's Pitch	PIC #2 - Port C.5